ALFRED-WEGENER-INSTITUT
HELMHOLTZ-ZENTRUM FÜR POLAR- UND MEERESFORSCHUNG

723
2018

Berichte
zur Polar- und Meeresforschung

Reports on Polar and Marine Research

The Expedition PS114 of the Research Vessel POLARSTERN to the Fram Strait in 2018

Edited by

Wilken-Jon von Appen

with contributions of the participants

HELMHOLTZ GEMEINSCHAFT

Die Berichte zur Polar- und Meeresforschung werden vom Alfred-Wegener-Institut, Helmholtz-Zentrum für Polar- und Meeresforschung (AWI) in Bremerhaven, Deutschland, in Fortsetzung der vormaligen Berichte zur Polarforschung herausgegeben. Sie erscheinen in unregelmäßiger Abfolge.

Die Berichte zur Polar- und Meeresforschung enthalten Darstellungen und Ergebnisse der vom AWI selbst oder mit seiner Unterstützung durchgeführten Forschungsarbeiten in den Polargebieten und in den Meeren.

Die Publikationen umfassen Expeditionsberichte der vom AWI betriebenen Schiffe, Flugzeuge und Stationen, Forschungsergebnisse (inkl. Dissertationen) des Instituts und des Archivs für deutsche Polarforschung, sowie Abstracts und Proceedings von nationalen und internationalen Tagungen und Workshops des AWI.

Die Beiträge geben nicht notwendigerweise die Auffassung des AWI wider.

Herausgeber
Dr. Horst Bornemann

Redaktionelle Bearbeitung und Layout
Birgit Reimann

Alfred-Wegener-Institut
Helmholtz-Zentrum für Polar- und Meeresforschung
Am Handelshafen 12
27570 Bremerhaven
Germany

www.awi.de
www.reports.awi.de

Der Erstautor bzw. herausgebende Autor eines Bandes der Berichte zur Polar- und Meeresforschung versichert, dass er über alle Rechte am Werk verfügt und überträgt sämtliche Rechte auch im Namen seiner Koautoren an das AWI. Ein einfaches Nutzungsrecht verbleibt, wenn nicht anders angegeben, beim Autor (bei den Autoren). Das AWI beansprucht die Publikation der eingereichten Manuskripte über sein Repositorium ePIC (electronic Publication Information Center, s. Innenseite am Rückdeckel) mit optionalem print-on-demand.

The Reports on Polar and Marine Research are issued by the Alfred Wegener Institute, Helmholtz Centre for Polar and Marine Research (AWI) in Bremerhaven, Germany, succeeding the former Reports on Polar Research. They are published at irregular intervals.

The Reports on Polar and Marine Research contain presentations and results of research activities in polar regions and in the seas either carried out by the AWI or with its support.

Publications comprise expedition reports of the ships, aircrafts, and stations operated by the AWI, research results (incl. dissertations) of the Institute and the Archiv für deutsche Polarforschung, as well as abstracts and proceedings of national and international conferences and workshops of the AWI.

The papers contained in the Reports do not necessarily reflect the opinion of the AWI.

Editor
Dr. Horst Bornemann

Editorial editing and layout
Birgit Reimann

Alfred-Wegener-Institut
Helmholtz-Zentrum für Polar- und Meeresforschung
Am Handelshafen 12
27570 Bremerhaven
Germany

www.awi.de
www.reports.awi.de

The first or editing author of an issue of Reports on Polar and Marine Research ensures that he possesses all rights of the opus, and transfers all rights to the AWI, including those associated with the co-authors. The non-exclusive right of use (einfaches Nutzungsrecht) remains with the author unless stated otherwise. The AWI reserves the right to publish the submitted articles in its repository ePIC (electronic Publication Information Center, see inside page of verso) with the option to "print-on-demand".

Titel: Ein Schlauchboot fährt zwischen Eisschollen in der Fram-Straße (Foto: Lennard Frommhold, AWI)

Cover: A zodiac navigates between ice floes in Fram Strait (Photo: Lennard Frommhold, AWI)

The Expedition PS114 of the Research Vessel POLARSTERN to the Fram Strait in 2018

Edited by
Wilken-Jon von Appen
with contributions of the participants

Please cite or link this publication using the identifiers

http://hdl.handle.net/10013/epic.6eb7513b-9577-4c77-834c-054f6150b6b3 and https://doi.org/10.2312/BzPM_0723_2018

ISSN 1866-3192

PS114
FRAM2018

10 July 2018 - 3 August 2018

Bremerhaven - Tromsø

Chief Scientist
Wilken-Jon von Appen

Coordinator
Rainer Knust

Contents

1. ÜBERBLICK UND FAHRTVERLAUF

Wilken-Jon von Appen
Alfred-Wegener-Institut

Am 10. Juli lief *Polarstern* von Bremerhaven aus und die Expedition PS114 begann. Der Transit ins Arbeitsgebiet dauerte 5 Tage. Am 16. Juli erreichte *Polarstern* das Arbeitsgebiet: die Fram-Straße zwischen Spitzbergen und Grönland (Abb. 1.1).

Die Reise war um 19 Verankerungsaufnahmen und 8 Verankerungsauslegungen herum strukturiert, die mit der Helmholtz Infrastruktur Initiative FRAM in Verbindung stehen. Die Expedition bearbeitete das Arbeitsgebiet von Ost nach West, um Verankerungen zu warten, die Bestandteil sind von (i) Langzeitbeobachtungen der Temperatur und des Transports im West-Spitzbergen Strom, (ii) Langzeitbeobachtungen der Stoffflüsse ins Sediment an der Meereiskante, (iii) einer Prozessstudie, die die Primärproduktion in der euphotischen Zone an der Eiskante zum Ziel hat, (iv) einer Prozessstudie, um die saisonalen Eigenschaften der Rezirkulation in der Fram-Straße einzugrenzen und (v) einer Prozessstudie, um die saisonalen Strömungen von warmem Atlantikwasser auf dem Ostrgrönlandschelf und unter den 79N-Gletscher einzugrenzen.

An den meisten Tagen im Arbeitsgebiet fanden während der Tagesstunden Verankerungs-aufnahmen oder Verankerungsauslegungen statt. In den Nachtstunden fanden stationsbasierte Messungen, u.a. mit der CTD-Rosette, dem Multinetz, dem LOKI, dem kameragesteuerten Mehrkernsammler und dem Ozeanbodenbeobachtungssystem statt. Diese Instrumente maßen verschiedene hydrographische und biologische Parameter und sammelten Wasser-, Exemplar- und Sedimentproben für biologische und chemische Analysen. Hydrographische Parameter und Strömungs-Eigenschaften wurden ebenfalls mit *En-route*-Systemen gemessen und biologische und chemische Proben in regelmäßigen Intervallen aus den Seewassersystemen von *Polarstern* entnommen. Parameter, die untersucht wurden, waren u.a. (i) Phytoplankton, Zooplankton und Bakterienhäufigkeit, Artenverteilung, und molekulare und genetische Variabilität, (ii) Primärproduktion, (iii) epibenthische Megafauna, (iv) gelöste und partikuläre inorganische und organische Nährstoffe und Kohlenstoff und (v) die Transportwege und Emissionen von Spurengasen N_2O, CH_4, DMS und CO. Mit Hilfe von Inkubationsexperimenten wurden die Transportraten der Spurengase unter sich ändernden Antriebsszenarien abgeschätzt.

Während des Transits und im Arbeitsgebiet wurden Luftproben für die Analyse neuartiger organischer Schadstoffen genommen. Im westlichen, meereisbedeckten Teil des Arbeitsgebiets, wurden Schneeproben von Eisschollen mit dem Schlauchboot, dem Mummy Chair (Personenkorb) und dem Helikopter für die Analyse neuartiger organischer Schadstoffe gesammelt.

Fahrtverlauf im Detail: Am 16. Juli wurden 3 Verankerungen an der HAUSGARTEN Zentralstation HG-4 aufgenommen, gefolgt von einer vollen biologischen Station mit 4 CTDs (tief, flach, 2 Wasser-nahmen für Inkubationen), Mulitnetz, LOKI, TVMUC während der Nacht. Am 17. Juli wurden 3 Verankerungen an der HAUSGARTEN Zentralstation ausgelegt ,gefolgt von Stationsmessungen an der HG-S3 Station in der Nacht. Am 18. Juli wurden 2 Verankerungen an der F4 Station auf der westlichen Seite des West Spitzbergen Stroms aufgenommen,

gefolgt von Stationsarbeiten (inklusive Wassernahmen für Inkubationen) an F4 und einem niedrig aufgelösten CTD Schnitt über den West Spitzbergen Strom. Am 19. Juli wurden 3 Verankerungen an der F4 Station ausgebracht gefolgt von einem Transit zum Nullmeridian und dem Anfang eines CTD Schnitts entlang des Nullmeridians. Am 20. Juli wurden die Verankerungen R1 und R2 auf dem Nullmeridian bei 78°10'N bzw. 78°50'N geborgen in Verbindung mit LOKI und tiefen CTD Profilen an den Verankerungspositionen. Am 21. Juli wurde zum ersten Mal Meereis erreicht, als Verankerung R3 auf dem Nullmeridian bei 79°30'N geborgen wurde. Nachfolgend fand ein Transit zur HAUSGARTEN Nord Gegend in der Nacht statt mit CTD, TVMUC und einem OFOS Profil bei HG-N5. Am 22. Juli wurde bei HG-N4 eine Verankerung geborgen und ausgelegt, später in der Nacht CTD und TVMUC und danach CTD und TVMUC bei HG-N3. Am 23. Juli wurde die Arbeit bei HG-N3 mit einem OFOS Profil beendet und ein Transit nach Norden in dichtes Packeis begonnen. In den frühen Morgenstunden des 24. Juli wurde die nördlichste Station der Reise bei 81°10'N erreicht mit einer Fortführung des CTD Schnittes entlang des Nullmeridians.

Während des Tages musste das Schiff auf günstige Eisbedingungen warten, um Verankerung R5 auf dem Nullmeridian bei 80°50'N zu bergen; Wasser für Inkubationen wurde aufgenommen. Am 25. Juli wurden ebenso schwierige Eisbedingungen während der Bergung von Verankerung R4 bei 80°10'N angetroffen. Der CTD Schnitt mit LOKI und tiefen CTDs an den Verankerungspositionen konnte dann in der Nacht mit einer fehlenden CTD Station beendet werden. Am 26. Juli wurde eine Verankerung bei HG-EG4 geborgen, anschließend wurden Schneeprobennahme per Schlauchboot und Stationsarbeiten plus OFOS Profil durchgeführt. In der Nacht wurde nur ein TVMUC bei HG-EG2 eingesetzt (HG-EG3 musste übersprungen werden). Am 27. Juli wurde eine Verankerung bei HG-EG1 ausgebracht, zusammen mit einer großen Station inklusive Wasserentnahme für Inkubationen und Schneeprobennahme vom Mummy Chair aus. Satellitendaten zeigten, dass die Festeissituation in der Nähe des 79Nord Gletschers sehr ungünstig war. Trotzdem wurde entschieden, ein eingeschränktes Programm in der Gegend zu versuchen, was zu einem Transit zur grönländischen Küste in der Nacht führte. Der 28. Juli begann mit dichtem Nebel, aber dieser lichtete sich und Satellitendaten zeigten, dass eine große Scholle von ehemals Festeis sich gerade weit genug bewegt hatte, um die Aufnahmen einer Verankerung im Westwind-Trog bei 79°40'N zu möglichen. Aufgrund günstiger Flugbedingungen am Nachmittag konnten Schneeproben per Helikopter gesammelt werden. Die weitere Eiserkundung zeigte, dass die Aufnahme von 3 Verankerungen möglich sein würde. Diese Verankerungen konnten während des Nachmittages und Abend erfolgreich geborgen werden.

Im Anschluss erfolgten Stationsarbeiten in der Wassersäule. Die Eiserkundung zeigte allerdings auch, dass Verankerung 79N2 nur einen Kilometer von der Gletscherkalbungskante des 79Nord Gletschers 20 km entfernt im Festeis lag. Daraufhin wurde entschieden, nicht unverhältnismäßig viel Schiffszeit für eine mögliche Aufnahme und Wiederauslage der Verankerung zu investieren. Während des 29. Juli erfolgte eine Transitfahrt während derer auch eine Schneeprobennahme vom Mummy Chair aus stattfand.

Am 30. Juli wurden 3 Verankerungen am Ausgang des Norske Trogs entlang 10°W aufgenommen. Anschließend wurde ein CTD-Schnitt vom Küstenschelf in die Grönlandsee hinein durchgeführt. Am 31. Juli wurde die letzte Verankerung von PS114 auf dem Kontinentalhang geborgen und der CTD-Schnitt abgeschlossen, bevor die wissenschaftlichen Arbeiten der Expedition PS114 mit einer tiefen CTD in der Grönlandsee beendet wurden.

Nach einem 3-tägigen Transit endete die *Polarstern*-Expedition PS114 am 3. August 2018 in Tromsø.

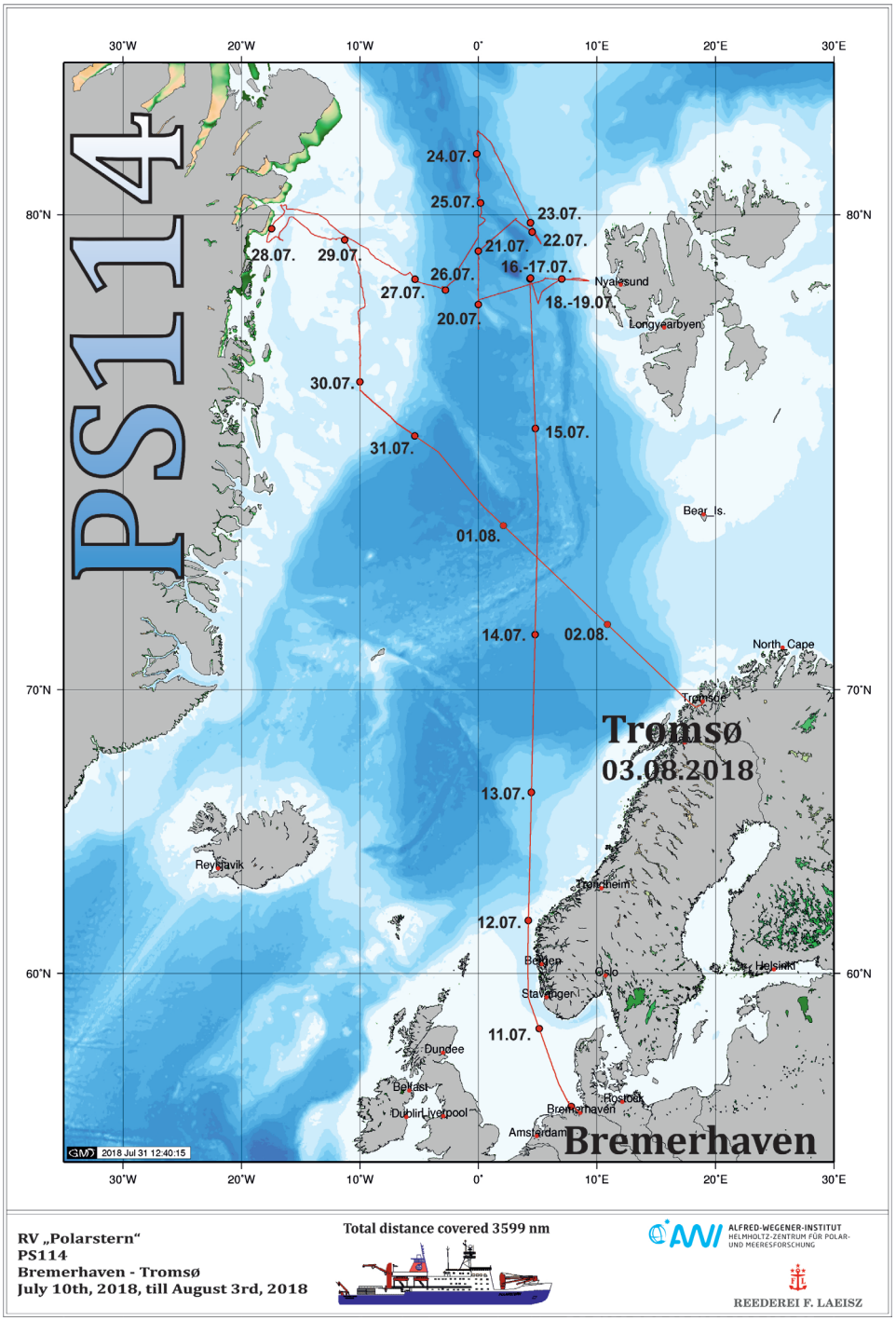

Abb. 1.1 Fahrtverlauf der PS114 von Bremerhaven nach Tromsø. Siehe https://doi.pangaea.de/10.1594/PANGAEA.893556 für eine Darstellung des master tracks in Verbindung mit der Stationsliste für PS114.

Fig. 1.1 Cruise track of PS114 from Bremerhaven to Tromsø. See https://doi.pangaea.de/10.1594/PANGAEA.893556 to display the master track in conjunction with the list of stations for PS114.

SUMMARY AND ITINERARY

Polarstern left Bremerhaven on July 10 starting expedition PS114. The transit to the working area took 5 days. On July 16, *Polarstern* arrived in the working area: Fram Strait between Svalbard and Greenland (Fig. 1.1).

The cruise was structured around 19 mooring recoveries and 8 mooring deployments associated with the Helmholtz Infrastructure Initiative FRAM. The cruise progressed from east to west across the working area to service moorings that are part of (i) long-term observations of the West Spitsbergen Current temperature and transport, (ii) long-term observations for sedimentary fluxes to the sea-floor, (iii) a process study aiming at primary production in the euphotic zone at the ice-edge, (iv) a process study to constrain the seasonal properties of the recirculation in Fram Strait, and (v) a process study to constrain the seasonal flow patterns of warm Atlantic Water on the East Greenland shelf and underneath the 79 North Glacier.

On most days in the working area, mooring recoveries or deployments took place during day time ship working hours. During night hours station-based sampling took place including the deployment of the CTD rosette, multinet, LOKI, *in-situ* particle camera, TV multi-corer, and ocean floor observation system. These instruments measured various hydrographic and biological parameters and retrieved water, specimen, and sediment samples for biological and chemical analyses. Hydrographic and current properties were also monitored with underway systems and biological and chemical samples were taken at regular intervals from sea-water intakes of *Polarstern*. Properties that were investigated included (i) phytoplankton, zooplankton, and bacteria abundance, species distribution, and molecular and genetic variability, (ii) primary production, (iii) epibenthic megafauna, (iv) dissolved and particulate inorganic and organic nutrients and carbon, and (v) pathways and emissions of trace gases N_2O, CH_4, DMS, and CO. Incubations assessed rates of trace gas exchanges under varying forcing.

During the transit and in the working area, air samples were collected for analyses of emerging organic contaminants. In the western part of the working area, where sea-ice was present, snow samples were retrieved from ice floes by using a zodiac, the mummy chair, and the helicopter for analyses of emerging organic contaminants.

Itinerary in detail, on July 16 three moorings were recovered at the HAUSGARTEN Central Station (HG4) followed by full a biological station with 4 CTDs (deep, shallow, 2 water collections for incubations), multinet, LOKI, TVMUC during the night. On July 17 three moorings were deployed at the HAUSGARTEN Central Station followed by station sampling at the HG-S3 station during the night. On July 18, two moorings were recovered at the F4 station on the western side of the West Spitsbergen Current. Afterwards station sampling (including water for

incubations) at F4 and a low resolution CTD section across the West Spitsbergen Current was performed. On July 19, three moorings were deployed at the F4 station. Then a transit followed to the prime meridian and the beginning of a CTD section along the prime meridian. On July 20 moorings R1 and R2 on the prime meridian at 78°10'N respectively 78°50'N were recovered combined with LOKI and deep CTD casts at the mooring locations. On July 21 sea-ice was encountered for the first time as mooring R3 on the prime meridian at 79°30'N was recovered followed by a transit to the HAUSGARTEN North area during the night and CTD, TVMUC, and an OFOS transect at HG-N5. On July 22, a mooring was recovered and deployed at HG-N4 followed by CTD and TVMUC and then CTD and TVMUC at HG-N3 during the night.

On July 23, the work at HG-N3 was finished with an OFOS transect and then a transit north into heavy pack ice started. During the early hours of July 24, the northern most location of the cruise at 81°10'N was reached with a continuation of the CTD section along the prime meridian. Throughout the day, the ship had to wait for favorable ice conditions in order to recover mooring R5 on the prime meridian at 80°50'N; also water for incubations was collected. On July 25 similarly challenging ice conditions were encountered during the recovery of mooring R4 at 80°10'N. The CTD section with LOKI and deep CTDs at the moorings along the prime meridian was then concluded overnight with one station missing. On July 26, a mooring at HG-EG4 was recovered followed by snow collection by zodiac and station sampling plus OFOS transect.

During the night a TVMUC only at HG-EG2 (HG-EG3 had to be skipped) was collected. On July 27 a mooring was deployed at HG-EG1 together with large station sampling including water for incubations and snow recovery by mummy chair. Satellite products indicated that the fast ice situation in the vicinity of the 79North Glacier was extremely unfavourable. Regardless, it was decided to attempt a minimal programme there resulting in a transit to the Greenland coast overnight. July 28 started with heavy fog, but the fog lifted and satellite products indicated that a big ice floe of previous fast ice had moved just enough to probably make mooring recoveries in Westwind Trough at approximately 79°40'N possible. With flight conditions in the afternoon snow could be recovered by helicopter and ice reconnaissance showed that three moorings could be recovered, which was done during the afternoon and evening followed by water column station work. The ice reconnaissance, however, also indicated that mooring 79N2 1 km from the calving front of the 79North Glacier was 20 km into fast ice resulting in the decision to not invest a disproportionate amount of ship time to possibly recover and redeploy it.

The whole day of July 29 was used by performing a transit including snow recovery by mummy chair. On July 30 three moorings at the mouth of Norske Trough along 10°W were recovered followed by a CTD section across the shelfbreak into the Greenland Sea. On July 31 the final mooring of PS114 on the continental slope was recovered and the CTD section was finished before the scientific work of PS114 was concluded by a deep CTD in the Greenland Sea.

After a 3-day transit, *Polarstern* expedition PS114 ended in Tromsø on August 3, 2018.

2. WEATHER CONDITIONS DURING PS114 AND ADDITIONAL RADIOSOUNDINGS DURING THE SPECIAL OBSERVING PERIOD OF THE YEAR OF POLAR PREDICTION (YOPP)

Harald Rentsch, Christian Rohleder DWD
H. Schmithüsen (AWI, not on board)

On Tuesday morning, July 10, 2018, 10:00 a.m., *Polarstern* left Bremerhaven (53.6°N, 8.6°E) for the expedition PS114 to steam first to the research area west of the Svalbard (HAUSGARTEN: ~79°N, ~2-6°E). Later on, research was done in Fram Street and nearby the 79N-glacier. The end of the research-cruise was in Tromsø (Norway) on 3 August 2018.

Transit Bremerhaven – Hausgarten (07/10/2018 – 07/16/2018):

For the first part of the expedition the ship steamed over North Sea to the first main working area HAUSGARTEN per transit of nearly 6 days duration. Under influence of a ridge of the Azores high fair weather and northerly winds of 5 Beaufort (Bft) were noted, and after 13 July westerly to southerly winds of force 4 Bft dominated.

During this period the ridge provided a calmed sea (below 2 m) and a comfortable, seasickness-free journey. Low pressure and its fronts caused rain, drizzle and fog-patches, which prevailed during the last two days of transit. From 14 to 15 of July winds of around 5 Bft from Northeast to North were measured, the swell never exceeded 1 m.

Hausgarten / Fram Strait (07/16/2018 – 07/20/2018):

By mostly moderate visibility and a nearly calmed sea (0.5 to 1 m) first moorings were recovered on July 16. During several days the influence of weak ridges of high and a small pressure gradient produced calmed weather, but foggy- and low cloud-conditions in the working area. Air temperatures between 0°C and -1°C, and low clouds below 500 ft were measured, caused by a temperature inversion. Thus, mostly insufficient flight-meteorological conditions were present between HAUSGARTEN and Fram Strait.

On 19 July an approaching low from the Greenland Sea brought moister and warmer air, together with some rain; the wind reached on average 6 Bft. The wind-sea reached 2 m at times. But, the research programme was not significantly restricted by these wave conditions.

Fram Strait / Eastern Greenland / Tromsø (07/20/2018 - 08/03/2018)

From July 20 onward the northeasterly winds abated significantly to below 4 Bft, sea and swell decreased also to values below 2 m in ice-free areas. At a ship's course along the Greenwich meridian first ice floes were reached nearby 79°N, and the swell calmed down rapidly. Lows, which mostly were built up in the Greenland Sea, and their warm fronts lead moist air masses northward to the sea-ice covered working areas, where cooling of air took place. That is why inversions of temperature and fog were produced continually over melting ice floes. Besides,

there were long lasting rainfalls (e.g. 23 July), but also freezing precipitation was observed north of 80°N. There, temperatures fluctuated until 22 July around 0°C.

The significant wave heights reached in ice-free areas 1.5 m to 2 m, the direction of swell varied between southeasterly and northeasterly, all in dependence of the position of *Polarstern* to the centers of the approaching lows.

Between 24 and 26 of July fronts of another northward moving low caused flight conditions below the required values, which were shaped by low clouds and freezing precipitation. The swell in ice-free areas stayed below 1.5 m, the southerly wind freshened up to nearly 6 Bft. In spite of the long lasting misty and clammy weather situation there were no serious ship-based research failures caused by weather up to this time.

On 28 of July *Polarstern* reached eastern Greenland, a katabatic wind brought dryer air masses from the glaciers of Greenland replacing fog and low clouds by sunshine, and temperatures nearby -2°C was the consequence.

Later, from 30 of July onward, another low and its warm front crossed *Polarstern* northward, causing south-easterly winds up to force 3 Bft. Thus, many clouds came in combination with moist air, rain and partly freezing drizzle were led into the last working area near 77°-78°N, 10°W.

Finally, on 1 August during the transit towards Norway, some rain showers fell and winds up to 5 Bft blew from southeasterly directions, wave heights up to 2 m were observed. One day later, cloudy, partly foggy weather dominated, southwesterly winds up to 3 Bft prevailed. The day-maximum temperatures rose to 13°C and reached around 15°C at the port of Tromsø, which *Polarstern* entered on 3 August in the morning.

YOPP Objectives

The „Year of Polar Prediction“ (YOPP) is one of the key elements of the Polar Prediction Project (PPP, www.polarprediction.net). Its mission is:

Enable a significant improvement in environmental prediction capabilities for the polar regions and beyond, by coordinating a period of intensive observing, modelling, verification, user-engagement and education activities.

Within YOPP there are three “Special Observing Periods” (SOPs) defined:

SOP-NH1:	1	Feb. 2018	–	31 Mar. 2018	in the Arctic
SOP-NH2:	1	Jul. 2018	–	30 Sep. 2018	in the Arctic
SOP-SH:	16	Nov 2018	–	15 Feb 2019	in the Antarctic

To contribute to the special observing efforts of YOPP the radiosounding activity on board *Polarstern* was increased to 4 soundings per day. This follows the internationally compiled science plan of PPP (World Weather Research Programme, 2013) and the recommendations in the implementation plan (World Weather Research Programme, 2016) of the project.

Work at sea

Whenever *Polarstern* was north of 60°N and far enough from the coast to ensure that radio sondes would not drop on land, the routinely launched daily radiosounding were extended by another 3 soundings per day. Together, the soundings covered all synoptic main hours, namely 00, 06, 12 and 18 UTC.

Data management

Data management for the YOPP radiosonding is identical to the routinely performed radiosoundings. Data on board was made available through the DWD staff to any interested scientist. Data will be published on PANGAEA after the cruise. Any scientific publication shall use the data from PANGAEA.

References

World Weather Research Programme (2013) WWRP Polar Prediction Project Science Plan. WWRP/PPP No. 1. World Meteorological Organization, Geneva. http://www.polarprediction.net/fileadmin/user_upload/www.polarprediction.net/Home/Documents/Final_WWRP_PPP_Science_Plan.pdf

World Weather Research Programme (2016) WWRP Polar Prediction Project Implementation Plan for the Year of Polar Prediction (YOPP), Version 2.0. WWRP/PPP No. 4. World Meteorological Organization, Geneva. http://www.polarprediction.net/fileadmin/user_upload/www.polarprediction.net/Home/YOPP/YOPP_Documents/FINAL_WWRP_PPP_YOPP_Plan_28_July_2016_web-1.pdf

3. FLOW OF ATLANTIC WATER IN FRAM STRAIT AND ON THE EAST GREENLAND SHELF

Wilken-Jon von Appen[1], Janin Schaffer[1], Matthias Monsees[1], David Kulmey[1], Jutta Vernaleken[1], Axel Behrendt[1], Zerlina Hofmann[1], Mia Sophie Specht[1], Carl Schmidt[1], Maren Richter[1], not on board: A. Münchow[2], M. Simon[3]

[1]AWI
[2]University of Delaware
[3]Greenland Institute of Natural Resources

Grant no. AWI_PS114_01

Background and objectives

West Spitsbergen Current

This cruise supported a long-term effort to monitor and quantify the variability of oceanic fluxes through the Fram Strait with a particular emphasis on the physical oceanography.

The Arctic Ocean is a semi-enclosed marginal sea with the Bering Strait, the Canadian Arctic Archipelago, and the Barents Sea being three shallow connections to the world oceans. The Fram Strait is the only deep strait (2,700 m), thereby allowing for the exchange of intermediate and deep waters between the Arctic Ocean and the Nordic Seas, which are in turn a marginal sea of the North Atlantic. Atlantic origin water is cooled throughout the cyclonic boundary current circulation in the Nordic Seas and enters the Arctic through the Barents Sea and the eastern Fram Strait. The temperature and other properties of the inflowing warm and salty Atlantic Water change in response to interannual variability (Beszczynska-Möller et al., 2012), to large scale-, multi-year climate patterns, such as the North Atlantic Oscillation, and to global climate change. The sum of these effects can be measured in the Fram Strait before it enters the Arctic Ocean, where it participates in the formation of the halocline north of Svalbard and forms a mid-depth cyclonic boundary current. Cooling, freezing, sea-ice melt, mixing with Pacific origin water, and the addition of large amounts of river runoff in the Arctic modifies the inflowing water (Rudels et al., 2005) before it exits through the western Fram Strait (de Steur et al., 2014). Thus observations of the outflow from the Arctic make it possible to monitor the effects of many processes in the Arctic Ocean.

The complicated topography in the Fram Strait leads to a horizontal splitting of the inflowing branches of Atlantic Water. Additionally, some of the Atlantic Water participates in a westward flow called the recirculation that then turns southward to exit the Fram Strait back to the Nordic Seas. The southward flowing cold and very fresh East Greenland Current is responsible for a large part of the liquid freshwater export from the Arctic and most of the solid freshwater export in the form of sea-ice. This freshwater has the potential to impact convection in the Nordic Seas and the northern North Atlantic and in turn the meridional overturning circulation.

Since 1997, AWI and the Norwegian Polar Institute have maintained a mooring array across the Fram Strait to monitor the fluxes of volume flux, and the temperature and salinity of the flow into and out of the Arctic Ocean through this gateway.

Atlantic Water Recirculation

The recirculation of Atlantic Water (AW) in Fram Strait controls how much of the warm nutrient rich AW flowing northward in the West Spitsbergen Current enters the Arctic Ocean. This determines the oceanic heat input and therefore the extent of the partially ice-free halocline formation area north of Svalbard (Rudels et al., 2005). The inflow also impacts the light and nutrient distribution in the Arctic and therefore habitat distribution and biogeography in the Arctic Ocean (Metfies et al., 2016) as well as their future evolution.

The part of the AW that does not enter the Arctic Ocean follows distinct, but poorly understood, pathways in Fram Strait and is then exported southward in the East Greenland Current. Special to Fram Strait is also that the southward advection of sea-ice and the northward advection of AW balance such that the ice-edge location varies very little. Hence, the region where frontal dynamics associated with the meltwater front at the interface between the two can affect the physics (e.g. von Appen et al., 2018) and biology (e.g. Wulff et al., 2016) is confined to a relatively small area. The Polar Water outflow is also located vertically above the AW. While it remains to be explained how that happens, it is clear that the large stratification associated with that transition leads to a similar situation to the halocline of the Arctic Ocean where the vertical nutrient supply to the shallow euphotic zone is inhibited and the primary production has to adapt accordingly. The meridional extent over which the recirculation takes place has not been constrained. A recent numerical model study (Hattermann et al., 2016) has suggested that there are in fact two branches of the recirculation. A southern branch is thought to be comparatively steady, while a northern branch essentially can be considered as an extended region in which eddies are propagating westwards. The recirculation also likely has a baroclinic geostrophic and a barotropic wind-driven component, but it has only been possible to show that both contribute to the recirculation between 78°50'N and 79°0'N (de Steur et al., 2014). It is also known that the West Spitsbergen Current is unstable at 78°50'N, especially in winter (von Appen et al., 2016), but it is not known whether there is even more eddy generation further north. The large seasonality in the region (e.g. de Steur et al., 2014, von Appen et al., 2016) also mean that an understanding solely based on the summer time situation (calmest season) will inherently be incomplete. The dynamics that lead to the splitting of the AW inflow are essential to other regions of the ocean as well. For example, the Irminger Current splits at Denmark Strait and only some of the warm water flows northward through that strait. The lacking dynamical understanding of the present day recirculation also currently makes it impossible to predict how the recirculation and the processes influenced by it will evolve in the future under changing forcing conditions associated with e.g. climate change.

In order to improve the understanding of the recirculation in Fram Strait, it is crucial to measure several physical and biological parameters over the presumed meridional extension of the recirculation including during the winter months. The temperature and salinity distribution in space and time can be used to track the water of the recirculation and determine its modification and vertical motion reflected in the depth of the temperature maximum. The meridional gradient of the density can be used to elucidate the location of baroclinic geostrophic flows and combination with direct velocity measurements can reveal the full current structure. The short term variability of the currents gives information on the eddy field and its possible contribution to the flow. Vertical velocity shear can highlight the interface between the lighter Polar outflow water and the AW. The horizontal motion of those two layers is likely quite different in some regions and possibly also decoupled from the overlying ice motion. The vertical migration of the interface between the two water masses in response to external factors can be tracked even in the absence of profiling temperature and salinity measurements. The oxygen distribution provides insights on the primary productivity while acoustic backscatter elucidates the presence and migration of zooplankton, which possibly responds to changes in the physical environment.

The ideal location to measure these properties is along the prime meridian (0°EW). This is outside of the West Spitsbergen Current and the East Greenland Current and what happens there is therefore not due to the boundary currents, but rather due to the recirculation. The prime meridian also avoids the 5,500 m deep Molloy Hole whose likely topographic steering would add an additional level of complexity to this already complex question. The prime meridian also cuts across the ice-edge (near 79°N at 0°EW) such that the influence of the recirculation on the ice-edge can be studied there. Additionally, the small amount of data that exist on the meridional structure of the recirculation is located along the prime meridian (Marnela et al., 2013) and it is hence valuable to collect new data at a comparable location. Mooring data will also be used for validation of and assimilation into a numerical model of the region around the Fram Strait.

For these reasons, in 2016 during PS100 five equally spaced moorings have been deployed at the following locations along the prime meridian (0°EW): 78°10'N, 78°50'N, 79°30'N, 80°10'N, and 80°50'N which is in water depths between 2,000 m and 3,000 m. Velocity as well as temperature, salinity, and oxygen were measured in the upper 750 m on the moorings.

East Greenland Shelf Circulation

Mass loss from the Greenland Ice Sheet presently accounts for a third to a quarter of sea-level rise (Milne et al., 2009) and the rate of mass loss is increasing (Velicogna 2009). The dominant mechanism is increased mass discharge along the marine margins where numerous major outlet glaciers have undergone a nearly simultaneous retreat, acceleration and thinning (Rignot and Kanagaratnam 2006; Howat et al., 2008; Stearns and Hamilton 2007; Dietrich et al., 2007). Both data and models indicate that this acceleration was triggered by a change at the tidewater margins of these glaciers (Thomas 2004; Nick et al., 2009; Pritchard et al., 2009), suggesting that the ocean plays a key role in modulating the ice sheet's mass balance (Vieli and Nick 2011; Straneo et al., 2012).

The proposed oceanic trigger is supported by recent studies showing that warm Atlantic waters are present and circulating in Greenland's glacial fjords (Holland et al., 2008; Straneo et al., 2010; Murray et al., 2010; Straneo et al., 2011) and by the observation that these waters were warming and accumulating in the subpolar North Atlantic at the same time as the glaciers started to retreat (e.g. Bersch et al., 2007).

Greenland's glacier acceleration has been concentrated along the southeastern and western margins terminating in the subpolar North Atlantic. Only recently, Helm et al., (2014) observed a general reduction in ice sheet elevation near the margins in the northeast of Greenland. Here, mainly two glaciers Nioghalvfjerdsfjorden glacier and Zachariae Isstrom drain the Northeast Greenland Ice Stream (NEGIS) whose drainage basin contains more than 15 % of the Greenland Ice Sheet area (Rignot and Kanagaratnam 2006). Zachariae Isstrom lost about 5 Gt/yr of its mass since 2003 and was observed to retreat at an accelerated rate since fall 2012, whereas no mass loss but an increased bottom melting was found at Nioghalvfjerdsfjorden glacier (Mouginot et al., 2015). Khan et al. (2014) observed an acceleration of the ice flow of Nioghalvfjerdsfjorden glacier and a sustained dynamic thinning of NEGIS, which they linked to a regional warming. The fact that a warming and thickening of the Atlantic layer has recently been observed in the Nordic Seas (e.g. in Fram Strait; Beszczynska-Möller et al., 2012) raises the question of whether the ocean changes may have triggered the fast retreat of Zachariae Isstrom (as suggested by Mouginot et al., 2015) and will trigger unstable behavior of Nioghalvfjerdsfjorden glacier.

Warm Atlantic water is carried to the North by the North Atlantic Current - Norwegian Atlantic Current - West Spitsbergen Current system. In Fram Strait a sizable fraction of the Atlantic water recirculates to the south on the East Greenland continental slope. Studies on the

eastern Greenland shelf in the 1980s and 1990s found this recirculating Atlantic water (RAW) to penetrate through sea bed troughs onto the East Greenland shelf (e.g. Bourke et al., 1987) below the fresh and cold polar waters (PW).

The Atlantic water mass found on the shelf was described by Bourke et al., (1987) as Atlantic Intermediate Water (AIW) with temperatures ranging between 0°C and 3°C and salinities between 34.5 and 34.9. Budeus et al (1997) found two distinct types of Atlantic waters in the trough system. They found 1°C warm Atlantic waters with salinities of 34.9 to be present throughout the southern Norske Trough, which cooled and freshened towards 79N glacier, and 0.5°C warm Atlantic waters with salinities of 34.8 in the northern Westwind Trough. An anticyclonic surface circulation on the continental shelf following the trough axis was found based on hydrographic observations (Bourke et al., 1987, Schneider and Budeus 1995), moored (Topp and Johnson 1997) and ship based (Johnson and Niebauer 1995) velocity measurements. In addition, Topp and Johnson (1997) proposed an anticyclonic subsurface circulation from moored measurements in Westwind Trough, in contrast to Budeus et al. (1997), who proposed that there is no one-directional flushing of the trough system. In the trough area east of the outlet glaciers, i.e. between Westwind and Norske Trough, Budeus and Schneider (1995) suggested a sill depth of 250 m causing the differences in water properties. This part of the shelf has rarely been studied due to a perennially fast sea ice cover (e.g. Schneider and Budeus 1995; Schneider and Budeus 1997), but is of strong interest when studying warm water pathways towards the outlet glaciers. Between 1979-1999 and 2000-2016, the temperature in the deep part of Norske Trough increased by more than 0.5°C (Schaffer et al., 2017).

A survey of Nioghalvfjerdsfjorden glacier in the mid-1990s led to very high estimates of submarine melt rates (about 40 m/yr locally, with a mean basal melt rate of 8 m/yr), which account for the bulk of the ice shelf mass loss (Mayer et al., 2000). The melting was attributed to the presence of AIW in the 600 m to 800 m deep subglacial cavity as observed in several conductivity, temperature and depth (CTD) profiles collected at the glacier's margins (Thomsen et al., 1997; Mayer et al., 2000). A more recent survey conducted in the summer of 2009 (Straneo et al., 2012) confirmed that the AIW found under the floating ice tongue still contains large amounts of heat to drive melting. Based on three CTD sections taken north of the main glacier front, Wilson and Straneo (2015) discussed that warm AIW cannot enter the cavity through Dijmphna Sund due to a sill of 170 m depth but needs to pass the eastern pinned glacier front. They proposed that the exchange of warm Atlantic waters between the continental shelf and the cavity through Norske Trough occurs on timescales of less than a year. Fast hydraulically controlled flow into the cavity was recently observed to supply warm AIW to the overturning circulation in the cavity (Schaffer 2017).

Nonetheless these implications are not based on sufficient observations towards the east/southeast of Nioghalvfjerdsfjorden glacier, and aspects of a direct pathway of warm AIW from the shelf break, through Norske Trough towards Nioghalvfjerdsfjorden glacier are still missing. For these reasons, in 2016 (during PS100) and in 2017 (during PS109) moorings were deployed in front of Nioghalvfjerdsfjorden glacier and close to the shelf break in Norske Trough measuring temperature, salinity, and velocities in various depths.

Work at sea

Moorings

In summer 2016 moorings were deployed in Fram Strait and on the Northeast Greenland continental shelf (*Polarstern* cruise PS100; moorings from AWI and University of Delaware). From those moorings 13 were recovered successfully on PS114 (Fig. 3.1, Tab. 3.1). One mooring located in front of the calving front of the 79 North Glacier was attempted to recover but could not be reached due to an extensive fast-ice cover. The data return of the recovered

instruments was good with most time series of the planned duration and no major instrument problems detected so far.

Furthermore, two moorings belonging to the physical oceanography section of AWI were deployed in the eastern Fram Strait (Tab. 3.1, Fig. 3.1). An overview of all instruments recovered and deployed during PS114 is given in Tab. 3.2 and 3.3, respectively. The settings of the data recording instruments deployed on PS114 are documented in Tab. 3.5 and 3.6.

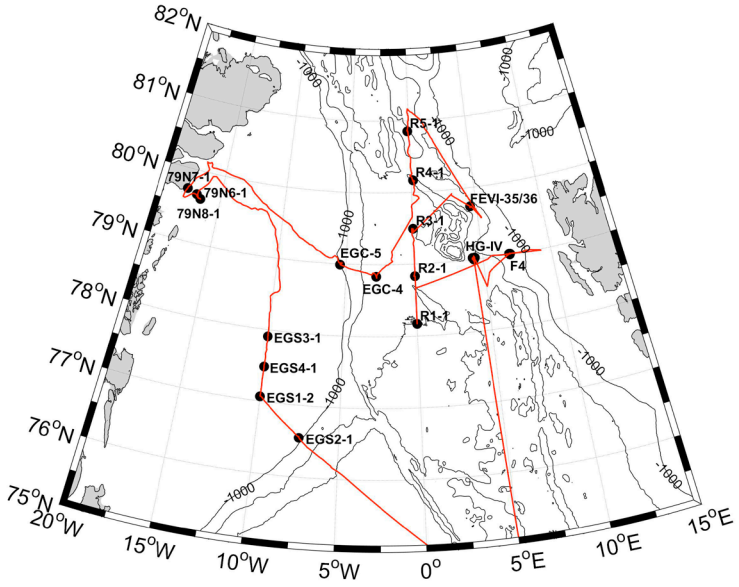

Fig. 3.1: Map of recovered and deployed moorings during PS114

Tab. 3.1: Overview of the mooring actions of the physical oceanography group on PS114 with the latitude, longitude, water depth in meters, station number, and mooring number as well as the action taken

Latitude	Longitude	Depth [m]	Station	Mooring	Status
79° 00.01'N	7° 00.03'E	1217	PS114_011_01	F4-17	recovered
78° 10.21'N	0° 00.04'E	3013	PS114_023_02	R1-1	recovered
78° 50.01'N	0° 00.09'E	2587	PS114_025_01	R2-1	recovered
79° 30.00'N	0° 00.03'N	2778	PS114_029_02	R3-1	recovered
80° 09.75'N	0° 10.19'E	3034	PS114_040_02	R4-1	recovered
80° 51.18'N	0° 07.23'W	3141	PS114_036_01	R5-1	recovered
79° 34.01'N	19° 23.83'W	476		79N2-2	under ice
79° 40.15'N	16° 53.36'W	256	PS115_048_01	79N6-1	recovered
79° 43.23'N	17° 40.40'W	401	PS115_047_01	79N7-1	recovered
79° 37.15'N	16° 32.61'W	287	PS114_049_01	79N8-1	recovered
77° 03.97'N	10° 00.10'W	425	PS114_053_01	EGS1-2	recovered
76° 32.76'N	7° 22.58'W	763	PS114_060_02	EGS2-1	recovered

Latitude	Longitude	Depth [m]	Station	Mooring	Status
77° 54.40'N	9° 59.79'W	233	PS114_051_01	EGS3-1	recovered
77° 28.98'N	10° 00.15'W	262	PS114_052_01	EGS4-1	recovered
79° 00.017'N	7° 00.041'E	1245	PS114_018_01	F4-18	deployed
79° 00.694'N	7° 02.088'E	1247	PS114_019_01	F4W-1	deployed

Tab. 3.2: Overview of the instruments recovered from moorings on PS114. The type is identified in Tab 3.4. Also given are the serial numbers of the instruments and their depths in meters from the surface according to the mooring drawings.

Mooring	Type	SN	Depth [m] drawing
F4-17	SBE37 ODO	243	150
	SBE37	13968	250
	LRADCP	23978	385
	SBE37 ODO	245	500
	AQD	12658	750
	SBE37 ODO	13966	751
	AQD	12654	1207
R1-1	SBE37 ODO	13973	65
	SBE56	6363	100
	SBE56	6364	150
	QMADCP	24069	247
	SBE37 ODO	13974	252
	SBE56	6365	349
	SBE56	6366	499
	AQD	12685	752
	SBE37 ODO	13985	752
	SBE53	436	3012
R2-1	SBE37 ODO	13979	52
	SBE56	6367	109
	SBE56	6368	148
	QMADCP	23806	253
	SBE37 ODO	13980	254
	SBE56	6369	355
	SBE56	6370	505
	AQD	12718	755
	SBE37 ODO	13981	755
	SBE37 ODO	13969	2500
R3-1	SBE37 ODO	13982	65
	SBE56	6371	109
	SBE56	6372	173

Mooring	Type	SN	Depth [m] drawing
	AZFP	23673	174
	QMADCP	23673	278
	SBE37 ODO	13986	285
	SBE56	6394	367
	SBE56	6395	517
	AQD	12745	771
	SBE37 ODO	13984	772
	Holgiphone	1477	836
	SBE53	437	2778
R5-1	SBE37 ODO	14015	78
	SBE56	6400	127
	SBE56	6401	177
	QMADCP	24071	279
	SBE37 ODO	14005	281
	SBE56	6402	308
	SBE56	6403	508
	AQD	12667	780
	SBE37 ODO	14006	781
	SBE53	438	3141
R4-1	SBE37 ODO	13978	63
	SBE56	6396	101
	SBE56	6397	149
	QMADCP	23976	251
	SBE37 ODO	13907	253
	SBE56	6398	353
	SBE56	6399	503
	AQD	12680	753
	SBE37 ODO	13987	753
EGS1-2	SBE37	14004	110
	SBE56	7061	135
	AuralM2	000722CF	138
	SBE56	7062	160
	SBE56	7063	185
	SBE37	13487	210
	SBE56	7064	235
	SBE56	7065	260
	SBE56	7066	300
	QMADCP	22388	340
	SBE37	225	342

Mooring	Type	SN	Depth [m] drawing
	SBE56	7083	417
	SBE26	227	425
EGS2-1	AQD	11328	88
	SBE37	13491	88
	SBE56	7076	118
	SBE56	7068	148
	SBE56	7069	178
	AQD	11333	208
	SBE56	7070	208
	SBE56	7071	258
	AQD	12699	308
	SBE56	7072	308
	SBE56	7073	368
	SBE37	224	428
EGS3-1	SBE37	13490	103
	AuralM2	273	106
	SBE56	7074	128
	AQD	11330	130
	SBE56	7075	153
	SBE56	7076	178
	AQD	11348	203
	SBE56	7077	203
	SBE37	230	228
	SBE53	439	233
EGS4-1	SBE37 ODO	13983	108
	SBE56	7084	132
	SBE56	7086	157
	SBE56	7087	182
	SBE56	7088	207
	SBE56	7089	232
	QMADCP	14087	253
	SBE37	226	257
79N6-1	LRADCP	3751	249
	SBE37	2927	256
79N7-1	LRADCP	3654	394
	SBE37	2921	401
79N8-1	RCM11	458	191
	SBE56	6408	202
	SBE56	6409	242

Mooring	Type	SN	Depth [m] drawing
	RCM11	314	262
	SBE37	7727	282

Tab. 3.3: Overview of the moored instruments deployed on PS114. The type is identified in Tab. 3.4. Also given are the serial numbers of the instruments and their depths in meters from the surface according to the mooring drawings.

Mooring	Type	SN	Depth [m] (drawing)
F4-18	SBE37	11419	60
	SBE37	11420	150
	SBE37	11421	250
	LRADCP	23613	380
	SBE37	10940	500
	RCM11	110	730
	SBE37	10942	731
	Develogic SonoVault	1095	800
	SBE37	2087	1202
	RCM11	109	1208
F4W-1	NGK Winch	004	155
	SBE37	9472	155
	RAS 500 watersampler	14128-07	252

Tab. 3.4: Abbreviations of the instrument types used in Tab. 3.2 and Tab. 3.3 along with the long names and the parameters measured by those instruments.

LRADCP	RDI 75 kHz ADCP	velocity profiles, temperature, pressure
QMADCP	RDI 150 kHz ADCP	velocity profiles, temperature, pressure
AQD	NORTEK Aquadopp deep water	point velocity, temperature
AuralM2	ASL Aural sound recorder	sound
Develogic SonoVault	Develogic sound recorder	sound
RCM8	Aanderaa mechanical current meter	point velocity, temperature, pressure
SBE37 ODO	SeaBird SBE37 CTD with oxygen sensor	temperature, conductivity, pressure, oxygen
SBE37	SeaBird SBE37 CTD	temperature, conductivity, pressure
SBE56	SeaBird SBE56 temperature recorder	temperature

SBE26	SeaBird SBE26 bottom pressure recorder	pressure, temperature
SBE53	SeaBird SBE53 bottom pressure recorder	pressure, temperature
AZFP	ASL Acoustic Zooplankton and Fish Profiler	zooplankton concentration
Holgiphone	Proprietary sound recorder	sound
NGK Winch	NGK profiling winch system with SeaBird SBE16plus V2 CTD	temperature, conductivity, pressure, oxygen
RAS 500 watersampler	McLane remote access sampler	water samples

Tab. 3.5: Example command file for 75kHz ADCPs.

```
>CR1
>CQ255
>CF11101
>EA0
>EB0
>ED0
>ES35
>EX00111
>EZ1111101
>WA50
>WB1
>WD111100000
>WF704
>WN70
>WP1
>WS800
>WV175
>RN23613
>TP00:07.00
>TE00:00:07.00
>TC20
>TB01:00:00.00
>TF18/07/18 13:00:00
>CK
>CS
```

Tab. 3.6: Example start protocol of Microcats (SBE37).

```
DS
SBE37SM-RS232 v4.1  SERIAL NO. 10940  18 Jul 2018 05:37:25
vMain = 13.30, vLith =  3.17
samplenumber = 1474, free = 557766
not logging, stop command
```

sample interval = 10 seconds
data format = converted engineering
transmit real-time = no
sync mode = no
pump installed = yes, minimum conductivity frequency = 3161.8
<Executed/>
SampleInterval=3600
<Executed/>
SampleNumber=0
this command will modify memory pointers
repeat the command to confirm
<Executed/>
SampleNumber=0
DS
SBE37SM-RS232 v4.1 SERIAL NO. 10940 18 Jul 2018 05:38:38
vMain = 13.24, vLith = 3.17
samplenumber = 0, free = 559240
not logging, stop command
sample interval = 3600 seconds
data format = converted engineering
transmit real-time = no
sync mode = no
pump installed = yes, minimum conductivity frequency = 3161.8
<Executed/>
StartDateTime=07192018120000
<start dateTime = 19 Jul 2018 12:00:00/>
<Executed/>
StartLater
<!--start logging at = 19 Jul 2018 12:00:00, sample interval = 3600 seconds-->
<Executed/>
DS
SBE37SM-RS232 v4.1 SERIAL NO. 10940 18 Jul 2018 05:39:11
vMain = 13.22, vLith = 3.17
samplenumber = 0, free = 559240
not logging, waiting to start at 19 Jul 2018 12:00:00
sample interval = 3600 seconds
data format = converted engineering
transmit real-time = no
sync mode = no
pump installed = yes, minimum conductivity frequency = 3161.8
<Executed/>

CTD and salinometer

Hydrographic measurements during the PS114 cruise were conducted by a CTD system. The CTD's sensors, main unit and rosette were provided by the physical oceanography group from AWI (OZE rosette). Altogether 59 CTD profiles were conducted in Fram Strait and on the Northeast Greenland continental shelf (Fig. 3.2). Water samples were mainly used for filtrations and chemical measurements.

The CTD sonde was mounted in a rosette with 24 bottles (12 liter each) for water sampling (bottles #1-24 were mounted). The CTD contained dual sensors for temperature, conductivity and oxygen, and one sensor for pressure. A fluorometer for chlorophyll fluorescence, a beam transmissometer, and a downward looking altimeter were also attached to the frame and connected to the coaxial cable. Details of the sensors with serial numbers and calibration dates can be found in Tab. 3.8 to 3.12.

There were a few events to note. Initially the CTD was equipped with two SBE43 oxygen sensors (SN 0467 and SN 1834). There were two additional sensors on board for replacement (SN 0048 and SN 1605). For SN 0048 initially no calibration data were available. Instead there was a calibration sheet for sensor SN 2292 which was not on board. For SN 1834 and SN 2292 the calibration data in the .xml files were not in agreement with the .pdf files from Seabird. The first CTD profile (004_01) showed that SN 0467 did not measure properly. Thereafter we changed the calibration for SN 0467 and used configuration 2 which did not solve the problem. We replaced the oxygen sensor with SN 0467 by SN 1605 and used configuration 3 from cast 009_01 onward. Both oxygen sensors (SN 1605 and SN 1834) were in good agreement. However, from cast 012_01 onwards sensor SN 1605 showed increasingly noisy data. Therefore, we replaced the oxygen sensor SN 1605 by SN 0048 and used configuration 4 afterwards (casts 024_01 and following). No calibration data for SN 0048 was available. Instead the calibration data from SN 2292 was used. From cast 034_01 onwards calibration data for SN 0048 was available and configuration 5 was used. Tab. 3.7 shows a list of all configurations used on cruise PS114.

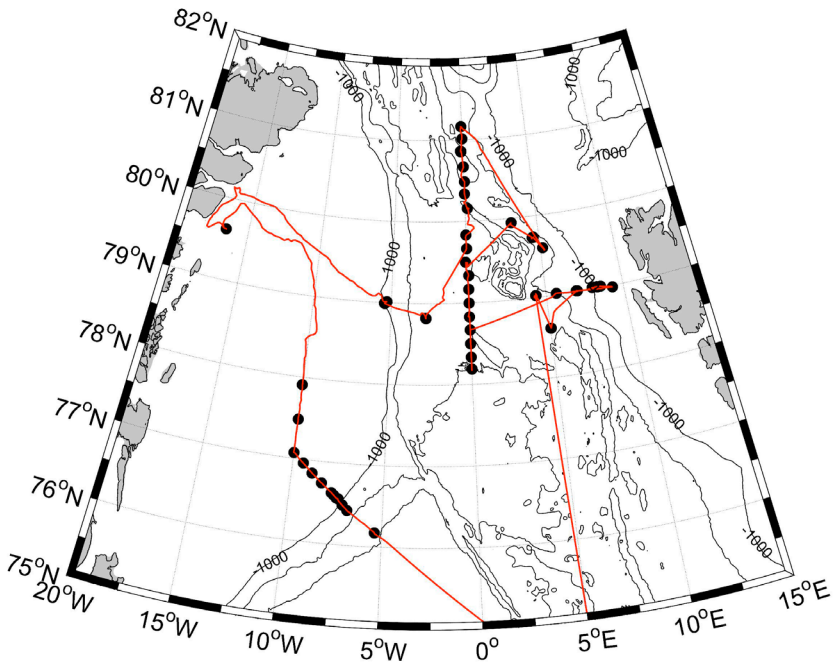

Fig. 3.2: Map of CTD stations during PS114

Tab. 3.7: List of configurations used on PS114

conf	Sensor number	SBE43	Problems
1	1	0467	Unrealistic data
	2	1834	Oxygen_SBE43_1834.xml file was used but is not in agreement with SBE 43 O1834 14Nov17.pdf
2	1	0467	Unrealistic data
	2	1834	Calibration data used from .pdf file
3	1	1605	Spiky data after cast 012_01
	2	1834	Calibration data used from .pdf file
4	1	0048	Wrong calibration data (no correct calibration data on board)
	2	1834	Calibration data used from .pdf file
5	1	0048	Correct calibration data sent by G. Rohardt and used thereafter
	2	1834	Calibration data used from .xml file

Tab. 3.8: CTD/Rosette configuration 1. Used for station 004_01

	Type	SN and calibration date
CTD	SBE911plus	
CTD-Sensors	SBE3 T0 (primary)	4127, cal.date 23-Nov-2017
	SBE4 C0 (primary)	3238, cal.date 22-Nov-2017
	SBE9plus pressure	0937, 14-Nov-2017
	SBE3 T1 (Secondary)	5101, cal.date 23-Nov-2017
	SBE4 C1 (secondary)	3290 cal.date 15-Nov-2017
Oxygen	SBE43 (primary)	0467, cal.date 30-Nov-2017
	SBE43 (secondary)	1834, cal.date 05-Dec-2017
Altimeter	Benthas PSA916	47768, cal.date 23-Mar-2009
Transmissometer	WETLabs C-Star	1198, cal.date 17-Dec-2008
Fluorometer	WETLabs ECO-AFL/FL	1853, cal.date 26-May-2010
Rosette	SBE Carousel	24 bottles á 12L
Winch	EL 32	

Tab. 3.9: CTD/Rosette configuration 2. Used for stations 004_03 to 004_06

	Type	SN and calibration date
CTD	SBE911plus	
CTD-Sensors	SBE3 T0 (primary)	4127, cal.date 23-Nov-2017
	SBE4 C0 (primary)	3238, cal.date 22-Nov-2017
	SBE9plus pressure	0937, 14-Nov-2017

	Type	SN and calibration date
	SBE3 T1 (Secondary)	5101, cal.date 23-Nov-2017
	SBE4 C1 (secondary)	3290 cal.date 15-Nov-2017
Oxygen	SBE43 (primary)	0467, cal.date 30-Nov-2017
	SBE43 (secondary)	1834, cal.date 14-Nov-2017
Altimeter	Benthas PSA916	47768, cal.date 23-Mar-2009
Transmissometer	WETLabs C-Star	1198, cal.date 17-Dec-2008
Fluorometer	WETLabs ECO-AFL/FL	1853, cal.date 26-May-2010
Rosette	SBE Carousel	24 bottles á 12L
Winch	EL 32	

Tab. 3.10: CTD/Rosette configuration 3. Used for stations 009_01 to 023_01

	Type	SN and calibration date
CTD	SBE911plus	
CTD-Sensors	SBE3 T0 (primary)	4127, cal.date 23-Nov-2017
	SBE4 C0 (primary)	3238, cal.date 22-Nov-2017
	SBE9plus pressure	0937, 14-Nov-2017
	SBE3 T1 (Secondary)	5101, cal.date 23-Nov-2017
	SBE4 C1 (secondary)	3290 cal.date 15-Nov-2017
Oxygen	SBE43 (primary)	1605, cal.date 29-Nov-2017
	SBE43 (secondary)	1834, cal.date 14-Nov-2017
Altimeter	Benthas PSA916	47768, cal.date 23-Mar-2009
Transmissometer	WETLabs C-Star	1198, cal.date 17-Dec-2008
Fluorometer	WETLabs ECO-AFL/FL	1853, cal.date 26-May-2010
Rosette	SBE Carousel	24 bottles á 12L
Winch	EL 32	

Tab. 3.11: CTD/Rosette configuration 4. Used for stations 024_01 to 032_06.

	Type	SN and calibration date
CTD	SBE911plus	
CTD-Sensors	SBE3 T0 (primary)	4127, cal.date 23-Nov-2017
	SBE4 C0 (primary)	3238, cal.date 22-Nov-2017
	SBE9plus pressure	0937, 14-Nov-2017
	SBE3 T1 (Secondary)	5101, cal.date 23-Nov-2017

	Type	SN and calibration date
	SBE4 C1 (secondary)	3290 cal.date 15-Nov-2017
Oxygen	SBE43 (primary)	0048, cal.date 02-Dec-2017
	SBE43 (secondary)	1834, cal.date 14-Nov-2017
Altimeter	Benthas PSA916	47768, cal.date 23-Mar-2009
Transmissometer	WETLabs C-Star	1198, cal.date 17-Dec-2008
Fluorometer	WETLabs ECO-AFL/FL	1853, cal.date 26-May-2010
Rosette	SBE Carousel	24 bottles á 12L
Winch	EL 32	

Tab. 3.12: CTD/Rosette configuration 5. Used for stations 034_01 onwards

	Type	SN and calibration date
CTD	SBE911plus	
CTD-Sensors	SBE3 T0 (primary)	4127, cal.date 23-Nov-2017
	SBE4 C0 (primary)	3238, cal.date 22-Nov-2017
	SBE9plus pressure	0937, 14-Nov-2017
	SBE3 T1 (Secondary)	5101, cal.date 23-Nov-2017
	SBE4 C1 (secondary)	3290 cal.date 15-Nov-2017
Oxygen	SBE43 (primary)	0048, cal.date 02-May-2017
	SBE43 (secondary)	1834, cal.date 05-Dec-2017
Altimeter	Benthas PSA916	47768, cal.date 23-Mar-2009
Transmissometer	WETLabs C-Star	1198, cal.date 17-Dec-2008
Fluorometer	WETLabs ECO-AFL/FL	1853, cal.date 26-May-2010
Rosette	SBE Carousel	24 bottles á 12L
Winch	EL 32	

The behaviour of the temperature and salinity sensors was monitored by taking differences between the values of primary and secondary sensors (secondary minus primary). In general, the sensors performed well (Fig. 3.3). No sensor drift has been detected for the temperature sensors. The difference of the temperature sensors is in a range of 0.0019°C for most stations. The salinity/conductivity differences show a shift towards higher offsets during the second half of the cruise. The difference of conductivity sensors is 0.0029 mS/cm for most stations. The difference in salinity derived from both conductivity cells is less than 0.002 PSU. All sensors show notable events at stations 014_01 and 046_01, where they differ from the ranges given above.

In order to define offset and drift of conductivity sensors, 28 salt samples were taken at 7 stations (Tab. 3.13). Conductivities were measured under temperature and pressure controlled environment using the Optimare Precision Salinometer on-board *Polarstern* (SN. 006) and standard seawater from Ocean Scientific International. The salinity measurements

with the salinometer were conducted following a guideline of Operational manual of Precision salinometer System issued on 1 May 2011. Preliminary results suggest that primary and secondary conductivity sensors have an offset of 0.0004 ± 0.001 [psu] and -0.0024 ± 0.001 [psu], respectively (Fig. 3.4). Precise calibration on the conductivity sensors will be carried out at AWI. Likewise, we collected 57 oxygen samples from 6 casts using a titration method for later calibration of the oxygen sensor.

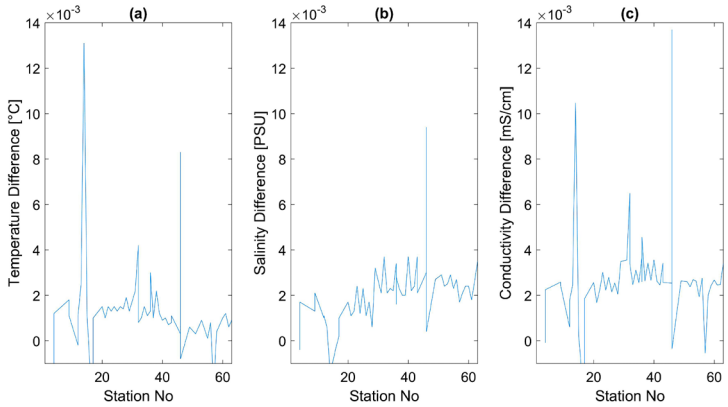

Fig. 3.3: (a) Difference in temperature sensors (secondary - primary). (b) Difference in salinity values (secondary - primary). (c) Difference in conductivity sensors (secondary - primary)

Tab. 3.13: CTD salinometer results

Date	Station	cast	depth	OSA	Standardization
24.07.2018	4	06	2030	34.9126	2018-07-24
24.07.2018	4	06	2030	34.9110	
24.07.2018	4	06	1011	34.9130	
24.07.2018	4	06	1011	34.9128	
24.07.2018	9	04	2031	34.9121	
24.07.2018	9	04	2031	34.9119	
24.07.2018	9	04	1013	34.9102	
24.07.2018	9	04	1013	34.9107	
24.07.2018	23	01	2033	34.9110	
24.07.2018	23	01	2033	34.9111	
24.07.2018	23	01	1014	34.9126	
24.07.2018	23	01	1014	34.9126	
24.07.2018	29	01	2032	34.9172	
24.07.2018	29	01	2032	34.9174	
24.07.2018	29	01	1013	34.8988	
24.07.2018	29	01	1013	34.8987	
24.07.2018	32	06	2605	34.9159	
24.07.2018	32	06	2605	34.9160	
24.07.2018	32	06	2031	34.9105	
24.07.2018	32	06	2031	34.9106	2017-07-30
30.07.2018	36	02	2031	34.9183	
30.07.2018	36	02	2031	34.9182	

Date	Station	cast	depth	OSA	Standardization
30.07.2018	36	02	1013	34.8987	
30.07.2018	36	02	1013	34.8992	
30.07.2018	43	02	2031	34.9172	
30.07.2018	43	02	2031	34.9169	
30.07.2018	43	02	1012	34.8976	
30.07.2018	43	02	1012	34.8976	2017-08-02
02.08.2018	63	01	1522	34.9121	
02.08.2018	63	01	1522	34.9122	

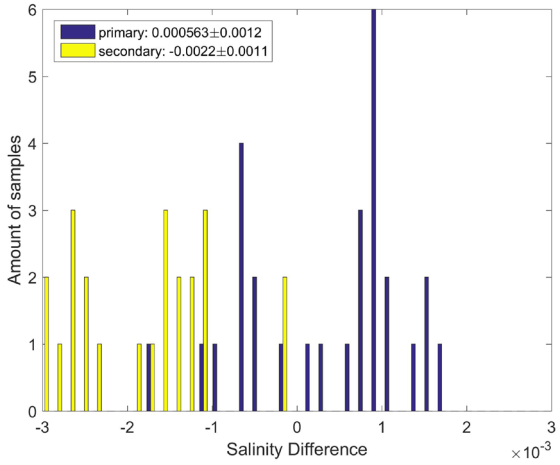

Fig. 3.4: Difference in salinity measurement as histogram. Salinity derived from primary (secondary) sensors in blue (yellow)

Vessel mounted ADCP

We measured profiles of ocean current velocity in the upper 300 m underway with a vessel-mounted Acoustic Doppler Current Profiler (VMADCP). The RDI Ocean Surveyor instrument (150 kHz) was mounted at an angle of 45 degree in the 'Kastenkiel' of *Polarstern*. The instrument was configured in narrowband mode and set to measure 80 bins with 4 m bin size (configuration file cmd_OS150NB_trigger_off.txt) covering a range from 15 m (11 m transducer depth and 4 m blanking distance below the transducer) to about 200 - 300 m depending on sea state, ice conditions, ship's speed and backscatter signals. On the continental shelf, i.e. in areas shallower 500 m water depth, the configuration was changed to narrowband mode with single-ping bottom track pings (data sets numbers 027 to 028, configuration file cmd_OS150NB_BT_trigger_off.txt). The number of bins was reduced to 50 while both the bin size and the blanking distance were increased to 8 m. We used a maximum search depth of 500 m in this configuration. The number of pings per ensemble in either configuration is one with an ensemble time (time between ensembles) of two seconds. The configuration was changed back to the first mode when we left the continental shelf and entered deeper waters on 31.07.2018, 00:43 UTC.

The velocity data might be affected by the use of other acoustic instruments on board, such as the acoustic release of the moorings.

A new record was started once per day (for data processing reasons). For unknown reasons the communication to the navigational input from the vessel's GPS system could not be established after restart on 15.07.2018 7:35 UTC for files with dataset number 06. After restarting the recording software VmDas (Teledyne RD Instruments) the record continued without any problems with dataset number 13 on 15.07.2018 at 7:47 UTC. Thus there are no file names with dataset numbers between 07 and 12. However, no data is missing.

The software VmDas was used to set up the ADCP. Finally, the Ocean Surveyor data conversion was done using Matlab routines last changed by Gerd Krahmann in January 2015 (osheader.m, osdatasip.m, osrefine.m, osbottom.m). Minor changes were made to these routines in order to adapt them for the needs of this cruise. The VMADCP data was corrected by using a misalignment angle of 0.97° and an amplitude factor of 1.02.

Preliminary (expected) results

During the cruise, the CTD and VMADCP measurements were preliminarily analyzed. The CTD section along the prime meridian (Fig. 3.2) confirmed the expected distribution of water masses (Fig. 3.5). Warm and saline Atlantic Water is present in the upper 300 m of the water column and north of 79°N it is covered by cold and fresh Polar Water. The velocity measurements indicate high meso-scale variability, which can be linked to the recirculation of Atlantic waters in Fram Strait.

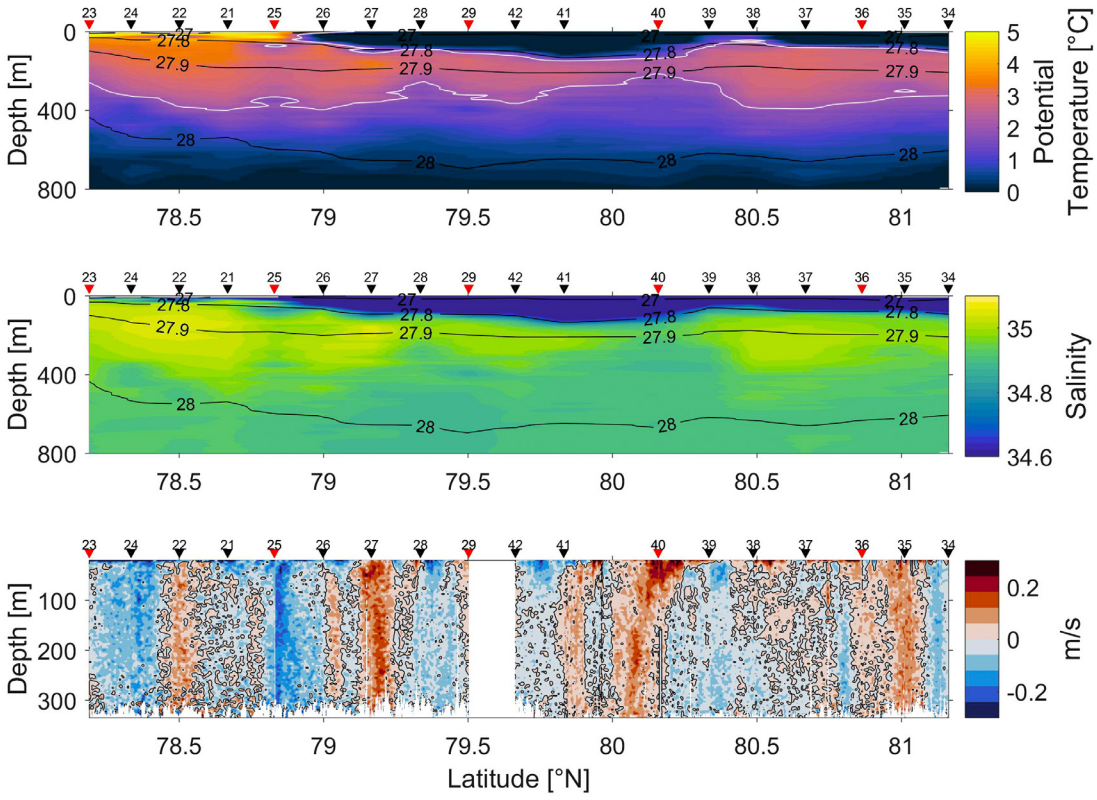

Fig. 3.5: Distribution of (a) potential temperature, (b) salinity, and (c) cross-section velocities from the vessel-mounted ADCP along the prime meridian between 78°N and 81.5°N. Triangles at the top indicate station locations; red triangles indicate mooring positions.

Data management

The data recorded by the moored instruments recovered on PS114 will be processed after the cruise at AWI and submitted to the PANGAEA data publisher. The moorings deployed on PS114 will be recovered in 2020. The data recorded on those instruments will accordingly be processed after recovery and submitted to the PANGAEA data publisher at that time. The data collected during PS114 from the CTD and the VMADCP will be processed at AWI and afterwards submitted to the PANGAEA data publisher.

References

Bersch M, I Yashayaev, and KP Koltermann (2007) Recent changes of the ther- mohaline circulation in the subpolar north atlantic, Ocean Dynamics, 57(3), 223–235, doi:10.1007/s10236-007-0104-7.

Beszczynska-Möller A, E Fahrbach, U Schauer, and E Hansen (2012) Variability in atlantic water temperature and transport at the entrance to the arctic ocean, 1997-2010, ICES Journal of Marine Science: Journal du Conseil, 69(5), 852–863, doi: 10.1093/icesjms/fss056.

Bourke R H, J L Newton, R G Paquette, and M D Tunnicliffe (1987) Circulation and water masses of the east greenland shelf, Journal of Geophysical Research: Oceans, 92(C7), 6729–6740, doi:10.1029/JC092iC07p06729.

Budeus G, and W Schneider (1995) On the hydrography of the northeast water polynya, Journal of Geophysical Research: Oceans, 100 (C3), 4287–4299, doi:10.1029/94JC02024. Budus, G, W Schneider, and G Kattner (1997), Distribution and exchange of water masses in the northeast water polynya (greenland sea), Journal of Marine Systems, 10(14), 123 – 138, doi:http://dx.doIorg/10.1016/S0924-7963(96)00074-7.

de Steur L, E Hansen, R Gerdes, M Karcher, E Fahrbach, and J Holfort (2009) Freshwater fluxes in the East Greenland Current: A decade of observations, Geophysical Research Letters, 36(23).

de Steur L, E Hansen, C Mauritzen, A Beszczynska-Möller, and E Fahrbach (2014) Impact of recirculation on the East Greenland Current in Fram Strait: Results from moored current meter measurements between 1997 and 2009, Deep Sea Research, 92, 26–40.

Dietrich R, H-G Maas, M Baessler, A Ru¨lke, A Richter, E Schwalbe, and P West- feld (2007) Jakobshavn isbræ, west greenland: Flow velocities and tidal interaction of the front area from 2004 field observations, J GeophyS ReS, 112(F03S21), doi: 10.1029/2006JF000601.

Hattermann T, P E Isachsen, W-J von Appen, J Albretsen, and A Sundfjord (2016) Where eddies drive recirculation of Atlantic Water in Fram Strait, Geophysical Research Letters, 43, 1-9.

Helm V, A Humbert, and H Miller (2014) Elevation and elevation change of greenland and antarctica derived from cryosat-2, The Cryosphere, 8 (4), 1539–1559, doi:10.5194/tc- 8-1539-2014.

Holland D M, R H Thomas, B de Young, M H Ribergaard, and B Lyberth (2008) Acceleration of jakobshavn isbrae triggered by warm subsurface ocean waters, Nature Geosci, 1(10), 659–664.

Hopkins T S (1991) The GIN seas synthesis of its physical oceanography and literature review 19721985, Earth-Science Reviews, 30(34), 175 – 318, doi: http://dx.doIorg/10.1016/0012-8252(91)90001-V

Howat I M, I Joughin, M Fahnestock, B E Smith, and T A Scambos (2008) Synchronous retreat and acceleration of southeast Greenland outlet glaciers 2000- 06: ice dynamics and coupling to climate, Journal of Glaciology, 54, 646–660, doi: 10.3189/002214308786570908.

Johnson, M, and H J Niebauer (1995) The 1992 summer circulation in the northeast water polynya from acoustic doppler current profiler measurements, Journal of Geo- physical Research: Oceans, 100(C3), 4301–4307, doi:10.1029/94JC01981.

Khan S A, K H Kjær, M Bevis, J L Bamber, J Wahr, K K Kjeldsen, A A Bjørk, N J Korsgaard, L A Stearns, M R van den Broeke, L Liu, N K Larsen, and I S Muresan (2014) Sustained mass loss of the northeast greenland ice sheet triggered by regional warming, Nature CliM Change, 4 (4), 292–299.

Mayer C, N Reeh, F Jung-Rothenhusler, P Huybrechts, and H Oerter (2000) The sub- glacial cavity and implied dynamics under nioghalvfjerdsfjorden glacier, ne-greenland, Geophysical Research Letters, 27(15), 2289–2292, doi:10.1029/2000GL011514.

Metfies K, W-J von Appen, E Kilias, A Nicolaus, and E-M N¨othig (2016) Biogeography and Photosynthetic Biomass of Arctic Marine Pico-Eukaroytes during Summer of the Record Sea Ice Minimum 2012, PLOS ONE, 11(2), doi: doi:10.1371/journaLponE0148512.

Milne G A, W R Gehrels, C W Hughes, and M E Tamisiea (2009) Identifying the causes of sea-level change, Nature Geosci, 2 (7), 471–478.

Mouginot J, E Rignot, B Scheuchl, I Fenty, A Khazendar, M Morlighem, A Buzzi, and J Paden (2015) Fast retreat of zachariæ isstrøm, northeast greenland, Science, doi:10.1126/sciencEaac7111.

Murray T, K Scharrer, T D James, S R Dye, E Hanna, A D Booth, N Selmes, A Luckman, A L C Hughes, S Cook, and P Huybrechts (2010) Ocean regulation hypothesis for glacier dynamics in southeast greenland and implications for ice sheet mass changes, Journal of Geophysical Research: Earth Surface, 115 (F3), doi: 10.1029/2009JF001522, f03026.

Nick F M, A Vieli, I M Howat, and I Joughin (2009) Large-scale changes in greenland outlet glacier dynamics triggered at the terminus, Nature Geosci, 2 (2), 110–114.

Pritchard H D, R J Arthern, D G Vaughan, and L A Edwards (2009) Extensive dynamic thinning on the margins of the greenland and antarctic ice sheets, Nature, 461(7266), 971–975.

Rignot E, and P Kanagaratnam (2006) Changes in the velocity structure of the green- land ice sheet, Science, 311 (5763), 986–990, doi:10.1126/sciencE1121381.

Rudels B, G Bjo¨rk, J Nilsson, P Winsor, I Lake, and C Nohr (2005) The interaction between waters from the Arctic Ocean and the Nordic Seas north of Fram Strait and along the East Greenland Current: results from the Arctic Ocean-02 Oden expedition, Journal of Marine Systems, 55(1), 1–30.

Schaffer J, W-J von Appen, P A Dodd, C Hofstede, C Mayer, L de Steur, and T Kanzow (2017) Warm water pathways toward Nioghalvfjerdsfjorden Glacier, Northeast Greenland, J GeophyS ReS Oceans, 122, doi:10.1002/ 2016JC012462.

Schaffer J (2017) Ocean impact on the 79 North Glacier, Northeast Greenland, PhD thesis, University of Bremen, http://nbn-resolvinGde/urn:nbn:de:gbv:46-00106281-12

Schneider W, and G Budus (1997) A note on norske ø ice barrier (northeast green- land), viewed by landsat 5, Journal of Marine Systems, 10(14), 99 – 106, doi: http://dx.doIorg/10.1016/S0924-7963(96)00076-0.

Schneider W, and G Budus (1995) On the generation of the northeast water polynya, Journal of Geophysical Research: Oceans, 100 (C3), 4269–4286, doi:10.1029/94JC02349. Stearns, L A, and G S Hamilton (2007), Rapid volume loss from two east greenland outlet glaciers quantified using repeat stereo satellite imagery, Geophysical Research Letters, 34(5), doi:10.1029/2006GL028982, l05503.

Straneo, F, G S Hamilton, D A Sutherland, L A Stearns, F Davidson, M O Hammill, G B Stenson, and A Rosing-Asvid (2010) Rapid circulation of warm subtropical waters in a major glacial fjord in east greenland, Nature Geosci, 3(3), 182–186.

Straneo F, R G Curry, D A Sutherland, G S Hamilton, C Cenedese, K Vage, and L A Stearns (2011) Impact of fjord dynamics and glacial runoff on the circulation near helheim glacier, Nature Geosci, 4 (5), 322–327. Straneo, F, D A Sutherland, D Holland, C Gladish, G S Hamilton, H L Johnson, E Rignot, Y. Xu, and M Koppes (2012-11-01T00:00:00), Characteristics of ocean waters reaching greenland's glaciers, Annals of Glaciology, 53(60), 202–210, doi: doi:10.3189/2012AoG60A059.

Thomas H R (2004) Force-perturbation analysis of recent thinning and accel- eration of Jakobshavn Isbrae, Greenland, Journal of Glaciology, 50, 57–66, doi: 10.3189/172756504781830321.

Thomsen, H H, N Reeh, O B Olesen, C E Bøggild, W Starzer, A Weidick, and A K Higgins (1997) The nioghalvfjerdsfjorden glacier project, north-east greenland: a study of ice sheet response to climatic change, Geology of Greenland Survey Bulletin, 176, 95–103.

Topp R, and M Johnson (1997) Winter intensification and water mass evolution from yearlong current meters in the northeast water polynya, Journal of Marine Systems, 10(14), 157 – 173, doi:http://dx.doIorg/10.1016/S0924-7963(96)00083-8.

Velicogna I (2009) Increasing rates of ice mass loss from the greenland and antarctic ice sheets revealed by grace, Geophysical Research Letters, 36(19), doi: 10.1029/2009GL040222, l19503.

Vieli A, and F M Nick (2011) Understanding and modelling rapid dynamic changes of tidewater outlet glaciers: Issues and implications, Surveys in Geophysics, 32(4), 437– 458, doi:10.1007/s10712-011-9132-4.

von Appen W-J, U Schauer, T Hattermann, and A Beszczynska-Möller (2016) Seasonal cycle of mesoscale instability of the West Spitsbergen Current, Journal of Physical Oceanography, 46 (4), 1231-1254, doi:10.1175/JPO-D-15-0184.1.

von Appen W-J, C Wekerle, L Hehemann, V Schourup-Kristensen, C Konrad, and M Iversen (2018) Observations of a submesoscale cyclonic filament in the marginal ice zone, Geophysical Research Letters, in press, doi:10.1029/2018GL077897

Wilson N J, and F Straneo (2015) Water exchange between the continental shelf and the cavity beneath nioghalvfjerdsbr (79 north glacier), Geophysical Research Letters, 42(18), 7648–7654, doi:10.1002/2015GL064944, 2015GL064944.

Wullf T, E Bauerfeind, and W-J von Appen (2016) Physical and ecological processes at a moving ice edge in the Fram Strait as observed with an AUV, Deep Sea Research, 115, 253-264.

4. HAUSGARTEN: IMPACT OF CLIMATE CHANGE ON ARCTIC MARINE ECOSYSTEMS

Normen Lochthofen[1], Jana Bäger[1], Freya Eckhard[1], Lennard Frommhold[1], Florian Kraußl[1], Janine Ludszuweit[1], B. Sablotny[1] (not on board), Miriam Seifert[1], Rafael Stiens[1], Lili Hufnagel[1], Christian Konrad[1], Wilken-Jon von Appen[1], M. Iversen[1] (not on board), T. Soltwedel[1] (not on board)

[1]AWI

Grant-No. AWI_PS114_01

Preface

While always fluctuating, the global climate is presently experiencing a period of rapid change, with a warming trend amplified in the Arctic region. Results of large-scale simulations of the future Earth's climate by several global climate models predict a further increase in temperatures, also leading to further reduction in ice cover. Moreover, there has been a significant thinning of the sea ice by approx. 50 % since the late 1950s.

The shift from a white cold ocean to a darker, warmer ocean will have severe impacts on the polar marine ecosystem. Thinner ice may permit better growth of ice algae, but more rapid spring melting may reduce their growing season. The timing and location of pelagic primary production will generally alter. Whether sea ice retreat generally leads to an increase in primary productivity is under debate, but biogeochemical models predict no or even negative changes in productivity and export flux. Altered algal abundance and composition will affect the zooplankton community structure and subsequently the flux of particulate organic matter to the seafloor, where the quantity and quality of this matter will impact benthic communities. Changes in the predominance of certain trophic pathways will have cascading effects propagating through the entire marine community. Generally, Arctic marine organisms will be compromised by temperature regimes approaching the limits of their thermal capacity. As a consequence, warmer waters in the Arctic will allow a northward expansion of sub-Arctic and boreal species. Besides water temperature increase, expanding ocean acidification will pose another threat to pelagic and benthic life in the Arctic Ocean.

Objectives

To detect and track the impact of large-scale environmental changes in the transition zone between the northern North Atlantic and the central Arctic Ocean, and to determine experimentally the factors controlling deep-sea biodiversity, the Alfred-Wegener-Institute Helmholtz-Zentrum für Polar-und Meeresforschung (AWI) established the LTER (Long-Term Ecological Research) observatory HAUSGARTEN. Regular sampling as well as the deployment of moorings and different free-falling systems (bottom-lander), which act as local observation platforms, has taken place since the observatory was established back in 1999. Since 2014, this observatory is successively extended within the frame of the HGF financed infrastructure project FRAM (Frontiers in Arctic marine Monitoring) and currently covers 21 permanent sampling sites on the West-Spitsbergen and East-Greenland slope at water depths between 250 and 5,500 m.

To determine the seasonal changes in nutrient concentrations in the euphotic zone, water samplers were deployed in 2017 (PS107) at approximately 20 m and 80 m depth. In total, 24 discrete samples were taken with weekly to monthly resolution (depending on season) to follow the biological drawdown of nutrients. The moorings are also equipped with a physical and biogeochemical sensor package including SBE37-SMP-ODO (temperature, salinity, oxygen), SAMI pH, SAMI pCO_2, Wetlabs PAR (photosynthetically active radiation), Wetlabs Ecotriplet (Chlorophyll and CDOM fluorescence plus scattering), SUNA Deep Nitrate, current meters, and Acoustic Doppler Current Profilers. The combination of these sensors and the water samplers, in combination with the deployment of a profiling winch facilitates the assessment of seasonal stratification and nutrient concentrations above and below the pycnocline. The nutrient drawdown enables an estimate of new production. Furthermore, the samples will be used for DNA sequencing to examine seasonal changes in bacterial community structure. The particle samplers collected and preserved filters for DNA extraction and sequencing that together with the fluorescence sensors will allow us to track the progression of phytoplankton biomass and community composition over different seasons. These efforts give us a novel year-round description of biological, chemical, and physical processes in the Fram Strait.

In addition, water samplers were deployed at ~80 m water depth in the anticipated cores of the West Spitsbergen and East Greenland Currents. Together with detailed measurements of physical parameters, these samples will be used to measure the nutrient composition of water masses flowing into and out of the Arctic Ocean through the Fram Strait.

During PS114 we conducted multidisciplinary research activities at a sub-set of stations mainly in the northern and western HAUSGARTEN area (Fig. 4.1).

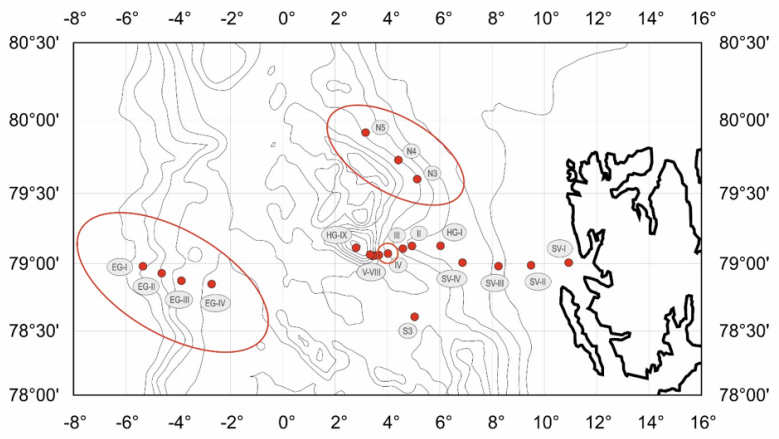

Fig. 4.1: Permanent sampling sites of the LTER Observatory HAUSGARTEN in Fram Strait; red circles indicate stations visited during PS114 except for EG-III and in addition also HG-IV, S3, SV-III and SV-II.

Work at sea

Surface water characteristics and vertical flux of particulate organic matter

At the central HAUSGARTEN site HG-IV (see Fig. 4.1), we recovered and re-deployed a special mooring with a prototype profiling winch system carrying a sensor package. This device has been developed within the BMBF funded project ICOS-D (Integrated Carbon Observation System, Germany) and shall conduct measurements within the upper 200 m of the water column at regular preprogramed intervals. At present, the sensor package consists of instruments for measuring carbon dioxide, oxygen, conductivity, temperature, pressure, and chlorophyll fluorescence.

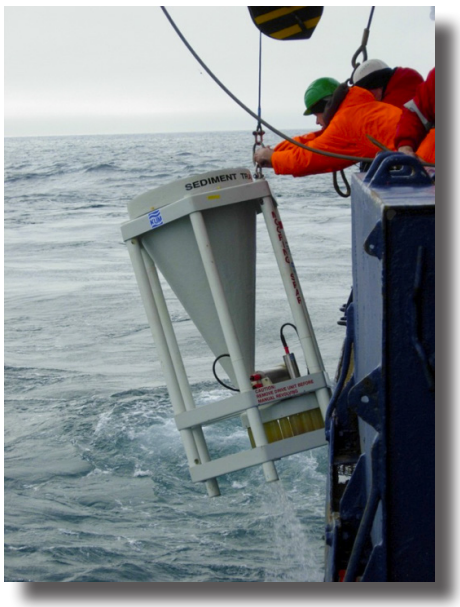

Fig. 4.2: Deployment of a sediment trap to assess particle fluxes to the seafloor

Measurements of the vertical flux of particulate matter at HAUSGARTEN have been conducted since the establishment of the observatory. By means of these measurements we are able to quantify the export of organic matter from the sea surface to the deep sea, and trace changes in these fluxes over time. The organic material which is produced in the upper water layers or introduced from land is the main food source for deep-sea organisms. Estimates of organic matter fluxes are conducted by bottom-tethered moorings carrying sediment traps (Fig. 4.2) at ~200 m and ~1,000 m below sea-surface, and about 180 m above the seafloor. In addition, the moorings carry autonomous McLane RAS 500 water samplers that are programmed to collect and preserve water samples (~0.5 L) with approximately weekly resolution, as well as particle samplers that filter and preserve ~10 L water samplers with approximately bi-weekly resolution. Besides these instruments, the moorings are equipped with Aanderaa current meters (RCM11, Seaguard) and self-recording CTDs (Seabird SBE37-ODO).

During PS114, we recovered the moorings and instruments that were deployed at the HAUSGARTEN stations HG-IV, N4, and EG-IV (see Fig. 4.1) during the expedition PS107 in 2017 and re-deployed new moorings at the same positions for another year except for the mooring in the East Greenland Current which was moved to HAUSGARTEN location EG-I (Tab. 4.1).

Tab. 4.1: Positions of the moorings deployed by the deep sea group during PS114

Mooring ID	Latitude	Longitude	Water depth [m]
FEVI-37	79° 44,484‘N	004° 31,363‘E	2.639
FEVI-38	79° 00,019‘N	004° 19,959‘E	2.540
SWIPS-2018	79° 01,391‘N	004° 24,291‘E	2.483
HG-IV-S-3	79° 01,361‘N	004° 15,714‘E	2.543
F4-S-3	79° 00,714‘N	006° 57,831‘E	1.219
HG-EGC-5	78° 59,723‘N	005° 23,642‘W	997

Sediment properties and the benthic biota

Virtually undisturbed sediment samples were taken using a video-guided multicorer (TV-MUC; Fig. 4.3). Various biogenic compounds from these sediments were analysed to estimate the input of organic matter from phytodetritus sedimentation (indicated by sediment-bound chloroplastic pigments) and to assess activities (i.e. bacterial exo-enzymatic activity). At the home lab, sediments retrieved by the TV-MUC will also be analysed for the total sediment-bound biomass (i.e. particulate proteins, phospholipids) and the smallest sediment-inhabiting organisms (size range: bacteria - meiofauna). Results will extend our time-series on ecosystem changes in the benthos of the Arctic Ocean.

Epibenthic megafauna, defined as the group of organisms ≥1 cm, considerably contribute to the continuous redistribution of organic matter, oxygen and other nutrients in surficial sediments. Megafaunal organisms create pits, mounds and traces that enhance habitat heterogeneity and thus diversity of smaller sediment-inhabiting biota in otherwise apparently homogenous environments. In this way, erect biota enhances 3D habitat complexity and provides shelter from predation.

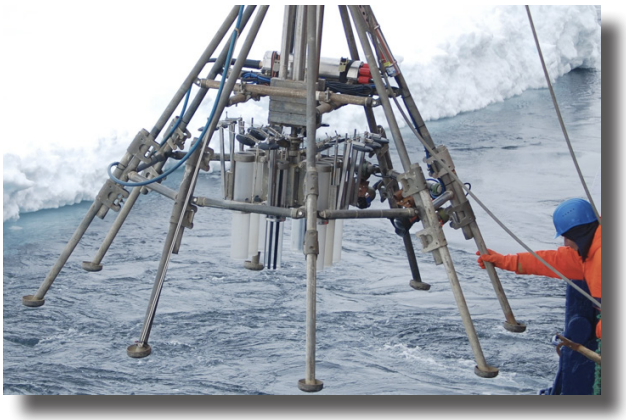

Fig. 4.3: Sediment sampling using a video-guided multicorer (TV-MUC)

Megafaunal predators control the population dynamics of their prey and therefore shape benthic food webs and community structure. Sunken organic matter that is not converted into benthic biomass and forwarded along food chains might be actively transported from the water column-sediment interface into the sediment by bioturbation. Organic matter is then degraded/recycled into nutrients and CO_2. Mega- and macrofaunal species thus actively influence biogeochemical processes at the sediment–water interface. An understanding of megafaunal dynamics is therefore vital to our understanding of the fate of carbon at the deep seafloor, Earth's greatest carbon repository.

OFOS

During PS114, we continued to study interannual dynamics of megafaunal organisms using our towed camera system (Ocean Floor Observation System, OFOS; Fig. 4.4). The OFOS was towed along two established tracks at Hausgarten stations N3 and N5. At Hausgarten station EG-IV the established track was covered with quickly moving dense sea ice. Therefore, the observations were taken along a straight line extension of the original line which happened to be in open water at the time. The new footage extends our image time series started in 2002.

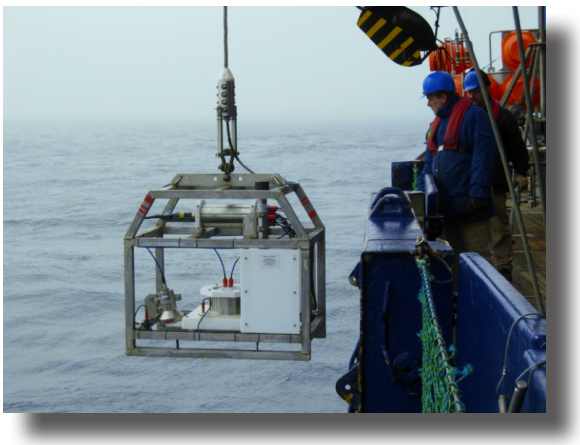

Fig. 4.4: Deployment of the Ocean Floor Observation System (OFOS)

Vertical profiles with the InSitu Camera system

System description: The InSitu Camera (ISC) consisted of an industrial camera with removed infrared filter (from Basler) with backend electronics for timing, image acquisition and storage of data and a fixed focal length lens (16 mm Edmund Optics). Furthermore, a DSPL battery (24V, 38Ah) was used to power the system (Fig. 4.5).

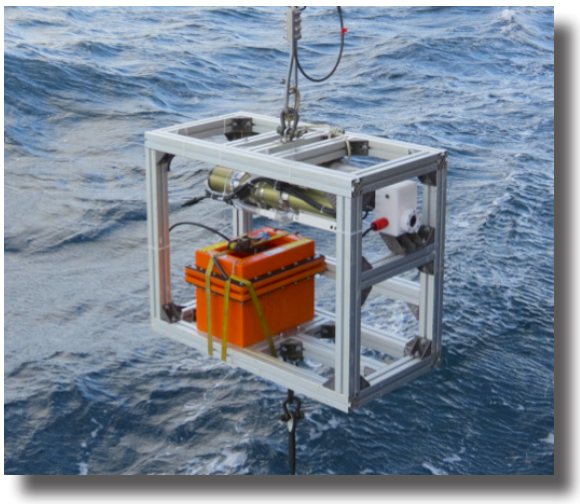

Fig. 4.5: Deployment of the InSitu Camera (ISC), consisting of an industrial camera and lens with electronics, an infrared light source, the DSPL battery and a Seabird SBE19 CTD

A single board computer was both used as the operating system for the infrared camera and to acquire the images from the camera and send them to a SSD hard drive where they were stored. The illumination was provided by a custom-made light source that consisted of infrared LEDs which were placed in an array in front of the camera. The choice of the infrared illumination was done to avoid disturbing the zooplankton that potentially would feed on the settling particles. With this geometrical arrangement of the camera and the light source we obtained shadow images of particles through the water column. We captured 2 images per second and lowered the ISC with 0.3 meters per second (lowest possible speed of winch).

Sampling: We made 4 vertical profiles with the IR-Camera. Profile 02 (just to 50 m) was used for calibration and test. On the camera frame also a Seabird SBE19 CTD was mounted. With that a better correlation of depth and images can be achieved. During the whole cruise both instruments were used in standalone mode and data was then afterwards correlated with Matlab. With that we got 3 successful profiles (1x1,000 m, 1x500 m, 1x250 m). An overview of all measured profiles can be found in Tab. 4.2.

Tab. 4.2: List of stations where the InSitu Camera (ISC) was deployed in the profiling mode

Profile No.	Station No	Date	Start Time	Lat (°)	Lon (°)	Wdepth (m)	Pdepth (m)
1	PS114_04_07	16/07/2018	22:40:24	79.0242°N	4.3308°E	2472	1000
2	PS114_004_08	17/07/2018	01:05:31	79.0230°N	4.3257°E	2482	50
3	PS114_032_07	22/07/2018	20:50:22	79.7382°N	4.6180°E	2636	500
4	PS114_049_05	28/07/2018	22:17:03	79.6165°N	16.5105°W	280	250

Recovery and deployment of the biooptical platform (BOP) - In-situ long-term monitoring of abundance, size-distribution, sinking velocity of settling aggregates

Objectives: During PS107 we deployed the BioOptical Platform (BOP) on the FEVI-36 mooring at the HG-IV station. We developed the BOP system to be able to follow aggregate dynamics at high temporal resolution at different seasons throughout a whole year. BOP uses an InSitu Camera system to determine daily size-distribution, abundance and size-specific sinking velocities of settling particles at one particular depth throughout one year (during the FEVI-36 deployment it was at app. 565 m). This is done by having a settling cylinder where particles sink through. At the bottom part of the settling cylinder we have attached a perpendicular camera system that records image sequences daily. At the bottom of the settling cylinder we

attached a rotation table with 40 collection cups so each cup could be placed under the settling column for a pre-determined collection period (Fig. 4.6). The cups are filled with a viscous gel which preserves the size and three dimensional structures of particles sinking into the gel. This makes it possible to identify and quantify different particle types as well as their compositions.

Fig 4.6: The old *BOP system deployed during PS107 and recovered during PS114 with the glass settling column and camera system (a: left image) and the rotation table with collection cups (b: right image)*

The BOP system was based on a modified sediment trap (KUM GmbH) where the collection funnel was replaced with a glass cylinder to avoid that the settling particles were sliding/rolling down the sides of the funnel, which may alter their physical structure. The glass cylinder has an inner diameter of 35 mm and functions as a settling cylinder that excludes ocean currents while the particles settle through it (Fig. 4.6). The camera system placed at the lower part of the settling cylinder consisted of an industrial camera (Basler), a fixed focal length lens (Edmund Optics) and a single board computer including a SSD hard disc and custom made power and time management circuitry. The images were illuminated by a custom made visible light source providing backlight. The whole camera system was powered by a Li-Ion battery (24V, 1670Wh, SubCTech GmbH).

Recovery of the BOP at FEVI-36, HG-IV (deployed during PS107)

During this cruise (PS114), we recovered the BOP system at the FEVI-36 mooring at station HG-IV (PS114_02_01) on 16 July 2018. The cups had all rotated through to cup 38 (according to timing) and all contained material. From this we could confirm that the BOP system was able to capture settling particles at all seasons.

The camera system had captured 28 min of images every second day from the 10 August 2017 and until 14 February 2018, which resulted in 188 days of image sequences.

Deployment of the BOP system at FEVI-38 (deployed during PS114)

We deployed a new version of the BOP system, which was equipped with two rotating tables and capable of collecting sinking particles in 40 gel-cups. The camera system was similar to that described above. We deployed the BOP system on the FEVI-38 mooring at station PS107_06-01 on the 17 July 2018 at 79°00.019'N and 04°19.985'E. We timed the cup openings according to the deep ocean sediment traps on the same mooring, but ensured that we would have several gel cups with only three days of opening period at each collection period of the deep ocean sediment traps. This was to ensure that we would not have particles falling on top

of each other, which would prevent us from doing image analyses on the particles collected in the gel traps. We programmed the camera for measurements of particle type, size-distribution, abundance, and sinking velocities to switch on daily at 00:00 (UTC) and capture one image every four seconds for 22 minutes.

Preliminary results

PS114 provided a large number of samples and data recordings from moored instruments as well as from ship-bound devices. The majority of the moored equipment worked well during the deployment of one year. Full records were obtained from all current meters, MicroCATs, water samplers and phytoplankton samplers. Two sediment traps performed not as expected, all other traps worked well. The underwater winch system has taken profiling data until the beginning of the winter 2017/2018. In addition to the obtained profiling temperature/salinity data, the deployment provided valuable information about the behaviour of the new system during long-term applications which will lead to significant improvements.

All the collected data and samples need processing and analysing at home. This applies for the images and video footage from OFOS as well as for sediment samples that were collected with the TV-MUC at selected sites, thus no preliminary results can be shown here.

Data management

Sample processing will be carried out at AWI. Data acquisition from the several types of investigations will required different amounts of time. The time periods from post processing to data provision will vary from one year maximum for sensor data, to several years for organism related datasets. Until then preliminary data will be available to the cruise participants and external users after request to the senior scientist. The finally processed data will be submitted to the PANGAEA data library. The unrestricted availability from PANGAEA will depend on the required time and effort for acquisition of individual datasets and its status of scientific publication.

5. PLANKTON ECOLOGY AND BIOGEOCHEMISTRY IN THE CHANGING ARCTIC OCEAN (PEBCAO, FRAM MICROBIAL OBSERVATORY)

Nicole Hildebrandt[1], Nicolas Goldbach[1], Julia Grosse[2], Nadine Knüppel[1], Benjamin Staufenbiel[1], Susanne Töller[1], Anabel von Jackowski[2],
not on board: K. Metfies[1], B. Niehoff[1] , E.-M. Nöthig[1], I. Peeken[1], A. Engel[2], J. Bäger[1], J. Wulf[3], C. Bienhold[1,3], B. Fuchs[3]

[1]AWI
[2]GEOMAR
[3]MPI

Grant-No. AWI_PS114_01

Objectives

The project PEBCAO (Plankton Ecology and Biogeochemistry in a Changing Arctic Ocean) focusses on the plankton community and the microbial processes relevant for biogeochemical cycles of the Arctic Ocean. This research focus acknowledges that the Arctic Ocean has gained increasing attention over the past years because of the drastic decrease in sea ice and increase in temperature, which is about twice as fast as the global mean rate. In addition, the chemical equilibrium and the elemental cycling in the surface ocean will alter due to ocean acidification. These environmental changes will have consequences for the biogeochemistry and ecology of the Arctic pelagic system. The effects of changes in the environmental conditions on the polar plankton community can only be detected through long-term observation of the species and processes. Our studies on plankton ecology have started in 1991, and since 2009 sampling has been intensified by the PEBCAO team in the Fram Strait at ~79°N. Since then, our studies are based on combining a broad set of parameters. This includes e.g. classical bulk measurements and microscopy, optical measurements and satellite observations, molecular genetic approaches, or cutting edge methods for zooplankton observations to study plankton ecology in a holistic approach.

Over the past nine years, we have compiled complementary information on annual variability in phytoplankton composition, primary production, bacterial activity and zooplankton composition (Nöthig et al., 2015). Previous assessments in the observation area indicated that the protist composition in the West Spitsbergen Current changed in the summer months. A dominance of diatoms was replaced by a dominance of *Phaeocystis pouchetii* and other small pico- and nanoplankton species. Our recent regular annual observations in Fram Strait suggest that TEP concentration in the observation area could be correlated with *P. pouchetii* abundance (Engel et al., 2017). These data were complemented by our molecular genetic investigations that provided new insights into eukaryotic microbial community composition with special emphasis on the contribution of pico-eukaryotes to plankton communities (Metfies et al., 2016).

Biogeochemistry and phytoplankton

Climate induced changes will impact the biodiversity in pelagic ecosystems. At the base of the food web, we expect small algae to gain more importance in mediating element and matter turnover as well as matter and energy fluxes in future Arctic pelagic systems. In order

to examine changes, including the smallest fractions, molecular methods are applied to complement traditional microscopy. The characterization of the communities with molecular methods is independent of cell-size and distinct morphological features. The assessment of the biodiversity and biogeography of Arctic phytoplankton will be based on the analysis of ribosomal genes with next generation sequencing technology, Automated Ribosomal Intragenic Sequence Analysis (ARISA), and quantitative PCR. Besides molecular methods, the set of parameters investigated includes classical bulk measurements (e.g. chlorophyll *a*, POC/PON, POP, biogenic silica) and microscopy.

Automated sampling for molecular analyses

Marine phytoplankton distribution displays high spatial heterogeneity or "patchiness". Therefore, comprehensive observation of marine phytoplankton requires sampling with high spatial and temporal resolution. The latter is a labor-intensive task and requires high amounts of ship time. The automated filtration system for marine microbes (AUTOFIM) has high potential to reduce the described effort related to adequate sampling of marine phytoplankton. It is coupled to the inflow of the ships pump system in ~10 m depth and allows filtration of a sampling volume of up to 5 liters. In total, 12 filters can be taken and stored in a roundel. Prior to the storage, a preservative can be applied to the filters to prevent degradation of the sample material, which can be used for molecular or biochemical analyses. The filtration can be triggered at defined regular time intervals or remote-controlled by a scientist. AUTOFIM thus provides the technical background for automated high-resolution collection of marine samples for molecular analyses (Metfies et al., 2016).

Bacterioplankton

Strong phytoplankton blooms characterize polar regions in late spring to early summer. The decay of such blooms has been well documented for the North Sea around Helgoland in recent years, but is still challenging to follow in polar regions. During PS114, we addressed the question, which microbial groups are responding to the phytoplankton bloom in Fram Strait and which are responsible for their degradation. The microbial data will be particularly correlated to algal diversity and abundance in order to reveal causal relationships between the two.

Zooplankton

Many zooplankton species are associated with a specific water mass. In Fram Strait, for example, the boreal species *Calanus finmarchicus* (Copepoda) and *Themisto abyssorum* (Amphipoda) are transported northward with the West Spitsbergen Current whereas their larger sibling species *C. hyperboreus* and *T. libellula* inhabit Arctic water masses. Rising water temperatures and altered hydrographical conditions could therefore result in a shift in the zooplankton species composition. This could have severe consequences for the ecosystem functioning. To detect the impacts of climate change on pelagic ecosystems in the Arctic, we studied the zooplankton community composition and depth distribution in Fram Strait during PS114 and will compare the results with those gained on previous cruises to the same area.

Work at sea

During PS114, we used CTD and net casts as well as AUTOFIM to take samples for a large variety of parameters, which are summarized in Tab 5.1 and 5.2.

Tab 5.1: Biogeochemical parameters sampled from CTD casts: DAA: dissolved amino acids; chl a: chlorophyll a (fractionated (10/3/0.4µm) and unfractionated)); CSP: Coomassie stained particles; DCHO: dissolved carbohydrates; DOC: dissolved organic carbon; DOP: dissolved organic phosphorus; PbSi: particulate biogenic silica; POC: particulate organic carbon; PON: particulate organic nitrogen; POP: particulate organic phosphorus; TDN: total dissolved nitrogen; TEP: transparent exopolymer particles

	Station	chl a / POC / PON / POP / PbSi	Seston	DOC / DOP / DCHO / TDN	DAA	TEP/CSP
HG-IV	PS114_4	x	x	x	x	x
S3	PS114_9	x	x	x	x	x
SV-IV	PS114_12	x	x	x	x	x
SV-III	PS114_13	x		x	x	x
SV-II	PS114_16	x		x	x	x
F5-17	PS114_20	x		x	x	x
0° transect	PS114_23	x		x	x	x
0° transect	PS114_25	x		x	x	x
0° transect	PS114_29	x		x	x	x
N5	PS114_31	x		x	x	x
N4	PS114_32	x	x	x	x	x
N3	PS114_33	x		x	x	x
0° transect	PS114_36	x		x	x	x
0° transect	PS114_40	x		x	x	x
EG-IV	PS114_43	x	x	x	x	x
EG-I	PS114_46	x	x	x	x	x
79N8-1	PS114_49			x	x	x

Tab 5.2: Biological parameters sampled from CTD casts, net casts and AUTOFIM: AUTOFIM: samples automatically collected for molecular analyses on a 0.4 µm filter; Bact: bacterial cell numbers; Bact growth: bacterial growth rates; DNA Bact: DNA of bacteria; FISH Bact: bacterial samples for analysis with the Fluorescence In-Situ Hybridisation method; Microscopy Phyto: samples for analyzing phytoplankton species composition under a light microscope; Phyto: phytoplankton cell numbers; Phyto growth: phytoplankton growth rates; RNA Euk: RNA of eukaryotes; Zoo: Zooplankton

	Station	AUTOFIM	RNA Eukaryoten	Bact/ Phyto	Micros-copy Phyto	Phyto-plankton growth rates	Bacterial growth rates	DNA Prokary-oten	FISH Prokary-oten	Zoo-plankton
HG-IV	PS114_4	x	x	x	x	x	x	x	x	x
S3	PS114_9	x	x	x	x		x	x	x	x
SV-IV	PS114_12	x	x	x	x	x	x	x	x	x
SV-III	PS114_13	x	x	x	x		x	x	x	
SV-II	PS114_16	x	x	x	x		x	x	x	
F5-17	PS114_20	x	x	x	x		x	x	x	
0° transect	PS114_23	x	x	x	x		x	x	x	x

	Station	AUTOFIM	RNA Eukaryoten	Bact/ Phyto	Micros-copy Phyto	Phyto-plankton growth rates	Bacterial growth rates	DNA Prokary-oten	FISH Prokary-oten	Zoo-plankton
0° transect	PS114_25	x	x	x	x		x	x	x	x
0° transect	PS114_29	x	x	x	x		x	x	x	x
N5	PS114_31	x	x	x	x	x	x	x	x	
N4	PS114_32	x	x	x	x		x	x	x	x
N3	PS114_33	x	x	x	x		x	x	x	
0° transect	PS114_34							x	x	
0° transect	PS114_36	x	x	x	x		x	x	x	x
0° transect	PS114_38							x	x	
0° transect	PS114_40	x	x	x	x		x	x	x	x
0° transect	PS114_41							x	x	
EG-IV	PS114_43	x	x	x	x	x	x	x	x	
EG-I	PS114_46	x	x	x	x		x	x	x	x
79N8-1	PS114_49							x	x	x

Biogeochemistry, phytoplankton and bacterioplankton

To analyze biogeochemical parameters such as chlorophyll *a*, particulate organic carbon (POC), nitrogen (PON), phosphorus (POP) and particulate biogenic silica (PbSi), seawater from 5 to 12 depths was sampled with a CTD/rosette at 16 stations in Fram Strait (HAUSGARTEN area, 0° meridian, East Greenland shelf; see Tab 5.1) and filtered on GFF or cellulose acetate filters. In addition, seston filters were taken at those stations where moorings were deployed. All filters were stored at 20°C and will be analyzed at the AWI laboratories in Bremerhaven.

Fig. 5.1: Filtering CTD water for biogeochemical analyses

To molecularly analyze the phytoplankton community composition and cellular activity in Fram Strait, CTD water samples were collected from the upper 100 m of the water column at 16 stations (Tab 5.2) and filtered for 18S meta-barcoding and meta-transcriptome analyses. Samples for 18S meta-barcoding analyses were fractionated by three filtrations on 10, 3 and 0.4 µm filters. One additional archive sample was collected from every depth by filtration on 0.2 µm filters to provide a sample for future analyses methods. All samples were preserved, refrigerated or frozen at -20°C or -80°C for storage until analyses in the home laboratories (AWI, Bremerhaven). In addition, seawater samples were preserved with formalin in order to determine phyto- and protozooplankton abundance using light microscopy.

To determine the impact of microbial processes on the cycling of organic matter, seawater from five depth layers was sampled with a CTD/rosette at 17 stations (Tab 5.1) in order to analyze dissolved biogeochemical parameters. Samples for dissolved organic carbon (DOC) / total dissolved nitrogen (TDN) and dissolved organic phosphorus (DOP) were filtered over 0.45 µm GMF syringe filters. Samples for dissolved amino acids (DAA) and carbohydrates (DCHO) were filtered over 0.45

µm Acrodisc filters. Concentrations of the dissolved substances will be determined by the use of IC and HPLC at GEOMAR in Kiel. Furthermore, samples for transparent exopolymer particles (TEP) and Coomassie-stainable particles (CSP) were taken and stored at -20°C until analysis by photometry and microscopy in the home laboratory. Bacteria and phytoplankton abundances will be determined using flow-cytometry.

Additionally, phytoplankton and bacterial growth rates were determined on board at 4 and 16 stations, respectively (Tab 5.2), using a radioactive isotope approach with 14-C sodium bicarbonate and 3-H leucine.

To characterize the diversity of microbes present in the photic zone, water samples from the CTD/rosette were taken at 20 stations (Tab 5.2). Fractionated filtrations using pore sizes of 10, 3 and 0.3 µm were then conducted for 16S rRNA gene tag sequencing and metagenomic studies. Additionally, aliquots of seawater were preserved and filtered for visualization and quantification of specific microbial groups by fluorescence *in-situ* hybridization (FISH). All filters were stored frozen at -20°C or -80°C and will be analyzed at the MPI in Bremen.

Automated sampling for molecular analyses

AUTOFIM is part of the underway sampling measurement instruments of *Polarstern*, filtering water for molecular protist community analyses. In order to evaluate to what extent the protist community composition in the AUTOFIM sample (taken from ~10 m depth) is representative for the protist community in the photic zone at the same sampling site, samples were collected with AUTOFIM at 16 stations in parallel to the CTD/rosette sampler (Tab 5.2). In addition, AUTOFIM automatically collected a sample every 24 h during our time in the working area in Fram Strait. Furthermore, it was used for underway measurements during the transit to Fram Strait and also during transit back to Tromsø. Here, the sampling interval was set to 3 hours. All samples were filtered and stored frozen at -80°C for further molecular genetic analyses in the home laboratory at AWI. During the cruise, we were able to test new functions added to the AUTOFIM software during shipyard time. The interval function now allows the operator to programme the next 12 filtrations in advance.

Zooplankton

Mesozooplankton community composition and depth distribution were investigated at 5 HAUSGARTEN stations, 5 stations along a transect at the 0° meridian from open water into ice-covered areas as well as one station close to the 79°N glacier at Greenland (Tab 5.2), using three different devices. To analyze the large-scale zooplankton distribution in the upper 1,500 m of the water column, we used a MultiNet (Fig 5.2A) that was equipped with five nets of 150 µm mesh size. The net was towed vertically at seven stations (HG-IV, S3, N4, SV-IV, EG-I, 0°, 79°N glacier) to sample five different depths layers. Standard depth layers in areas with >1,500 (or >1,000) m water depth were 1,500(or bottom)-1,000-500-200-50-0 m. In shallower regions (EG-I, 79°N glacier), the depth intervals were adjusted to obtain a higher resolution in surface waters. The samples were then immediately preserved in 4 % formalin buffered with hexamethylenetetramine for later analyses under a stereo microscope.

To analyse the small-scale distribution of zooplankton species in the upper 1,000 m of the water column, a combination of the optical plankton recorder LOKI (Lightframe On-sight Key species Investigation; Fig 5.2B) and the acoustic device AQUAscat were deployed at 11 stations. LOKI was equipped with a 150 µm plankton net and taking pictures of zooplankton organisms and particles at a rate of 18 frames per second while being towed vertically through the water column. Simultaneously, depth, temperature, conductivity, oxygen content and fluorescence were recorded to relate the zooplankton abundance to the environmental conditions. Unfortunately, at five stations a system failure occurred, so that no pictures were recorded

during the end of the casts, i.e. in surface waters. The AQUAscat was mounted to the upper part of the LOKI frame, facing sideward, and successfully recorded the acoustic backscatter at 0.5, 1, 2 and 4 MHz at five stations in order to derive mean particle size and concentration. The simultaneously taken optical images allow to attribute the backscatter characteristics across the multiple acoustic frequencies to specific (plankton) organisms. The goal is to gain more reliable biomass estimates from acoustics, which reduce the target avoidance that limits conventional methods (cooperation with M. Doble, Polar Scientific Ltd, Scotland).

Fig 5.2 (A) The MultiNet with an additional bongo net bag attached to the side; (B) The LOKI/Aquascat system during deployment

A bongo net bag (150 µm mesh size) was mounted to the side of the MultiNet frame (Fig 5.2A) to sample additional zooplankton organisms. At four stations (HG-IV, S3, EG-I, 79°N glacier), these samples were used to individually pick copepods (*Calanus finmarchicus*, *C. hyperboreus*, *C. glacialis*, *Paraeuchaeta* spp.), ostracods, amphipods (*Themisto abyssorum*, *T. libellula*, *Cyclocaris guilelmi*, Gammaridae), chaetognaths (*Parasagitta* sp., *Eukrohnia* sp.) and krill (*Thysanoessa* sp.) for microplastic analyses (cooperation with M. Bergmann, AWI). At two stations, samples were given to the PETRA group for incubation experiments (see chapter 7).

Preliminary (expected) results

All samples will be analyzed in the home laboratories at AWI in Bremerhaven (biogeochemical parameters, phytoplankton abundance and molecular biology, zooplankton community composition and distribution), at GEOMAR in Kiel (TEP, amino acids, phytoplankton/bacterial growth rates), at MPI in Bremen (bacterioplankton community) and at Polar Scientific Ltd in Scotland (zooplankton acoustics).

Data management

Analyses of samples for species identification and enumeration (phyto- and zooplankton) require tedious and time-consuming processing and, therefore, these analyses will take longer than chemical measurements. Thus, depending on the parameter as well as on the methods used for the analyses, it will take up to three years to complete our analyses. As soon as the data sets are available, other cruise participants may request and use them. When the data are to be published, they will also be submitted to the PANGAEA Data Publisher for Earth & Environmental Science and are then open for external use.

References

Engel A, Piontek J, Metfies K, Endres S, Sprong P, Peeken I, Gäbler-Schwarz S & Nöthig E-M (2017) Inter-annual variability of transparent exopolymer particles in the Arctic Ocean reveals high sensitivity to ecosystem changes Scientific Reports, 7 (4129), 1-9.

Metfies K, von Appen WJ, Kilias E, Nicolaus A & Nöthig E-M (2016) Biogeography and Photosynthetic Biomass of Arctic Marine Pico-Eukaryotes during Summer of the Record Sea Ice Minimum 2012. PLOSone, 11(2), e0148512.

Nöthig, E-M, Bracher A, Engel A, Metfies K, Niehoff B, Peeken I, Bauerfeind E, Cherkasheva A, Gäbler-Schwarz S, Hardge K, Kilias E, Kraft A, Mebrahtom Kidane Y, Lalande C, Piontek J, Thomisch K, Wurst M (2015) Summertime plankton ecology in Fram Strait - a compilation of long- and short-term observations. Polar Research, 34, doi:10.3402/polar.v34.23349.

6. TEMPORAL VARIABILITY OF NUTRIENT AND CARBON TRANSPORTS INTO AND OUT OF THE ARCTIC OCEAN

Sinhue Torres-Valdés[1], Daniel Scholz[1], Annika Morische[2], Wilken-Jon von Appen[1], Rafael Stiens[1], Jana Bäger[1], Elliott Price[3], Matthias Monsees[1], Normen Lochthofen[1], L. Wischnewski[1] not on board)

[1]AWI
[2]Uni Oldenburg
[3]Uni Liverpool

Grant-No. AWI_PS114_01

Rationale

Current gaps in knowledge concerning nutrient and carbon biogeochemical cycles at the pan-Arctic scale stem from the lack of information necessary to constrain their budgets. Available computations (MacGilchrist et al., 2014; Torres-Valdés et al., 2013, 2016) indicate the Arctic Ocean (AO) is a net exporter of phosphate, dissolved organic phosphorus, silicate, dissolved organic nitrogen and dissolved inorganic carbon (DIC). Nitrate net transports are balanced, but large nitrogen losses due to denitrification imply there are sources yet unaccounted for. With the exception of silicate, whose export appears to be driven by riverine inputs, there are still unknowns regarding nutrients and carbon sources and sinks. Moreover, temporal changes are not constrained because continuous observations are not available. Under ongoing and predicted climate change, identifying and quantifying sinks and sources becomes relevant to: *i)* generate baseline measurements against which future change can be evaluated, *ii)* assess the impact of climate change on biogeochemical processes (e.g., primary production, organic carbon export, remineralisation), *iii)* understand the complex interaction between biogeochemical and physical processes, and how such interactions affect the transport of nutrients downstream and the capacity of the Arctic Ocean to function as a sink of atmospheric CO_2, *iv)* determine whether long-term trends occur.

Available AO nutrient and carbon budgets derive from transport calculations across the main gateways (Fram Strait, the Barents Sea Opening, Bering Strait and Davis Strait). However, these calculations are mostly based on summer time measurements. It is therefore necessary to generate continuous observations to evaluate transports and budgets over seasonal and longer times scales.

We aim to generate continuous observations of nutrients and DIC in Fram Strait through the deployment of FRAM sensors and remote access samplers, targeting core (~250 m) and surface waters of the West Spitsbergen Current and the East Greenland Current. We will use these data to address the points described above and to assess the role of transports across one of the main Arctic gateways -Fram Strait- within the wider Arctic Ocean nutrient and carbon budgets.

ARISE

The ARISE project aims to identify climate induced changes to the food web in the Arctic Ocean across large spatial and temporal ranges, and to the highest resolution possible. Such changes are identified using stable isotope ratios as biomarkers that reflect environmental variability and indicate changes to trophic interactions. We therefore measure the isotope

ratios of as many food web members as possible, from high trophic level predators such as polar bears and seals, to mid-level zooplankton and elements of the lower food web such as Particulate Organic Matter, Dissolved Organic Matter and Dissolved Inorganic Nitrogen. The PS114 cruise was used as an opportunity to increase the spatial and temporal resolution of the isoscape by sampling the underway system for POM and taking seawater samples from the CTD for DIN.

Work at sea during PS114

Sensors and remote access samplers

We prepared and deployed sensors and remote access samplers (RAS) in the following moorings: EGC-5 at 70 and 239 m depth in the East Greenland Current, and F4S-3 at 27 m and F4W-1 at 260 m in the West Spitsbergen Current. Each package consists of a RAS with a SUNA nitrate, pH, pCO2 and CTD-O2 sensors attached (Fig 6.1). With additional PAR and Eco-triplet sensors in close-to-surface deployments.

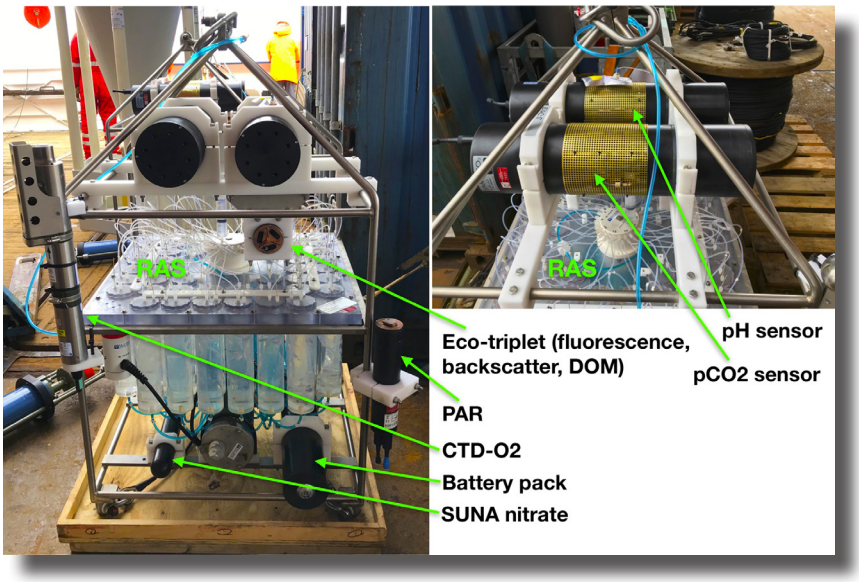

Fig 6.1: Sensor package: remote access sampler (RAS) with sensors attached to its frame. This image shows one of the packages attached to mooring EGC-5 just before deployment.

Sample collection and analysis

Samples were collected from CTD casts for the analysis of dissolved inorganic nutrients, total nitrogen and total phosphorus, and dissolved inorganic carbon (DIC). Samples for dissolved inorganic nutrients were collected in 15 mL Falcon tubes from selected depths and measured on board using a QuAAtro Seal Analytical autoanalyser. Samples for total nitrogen and total phosphorus were collected in pre-cleaned HDPE 120 mL bottles and stored frozen at -20°C for later analysis at the AWI. DIC samples were collected into 500 mL glass bottles, fixed with half saturated mercuric chloride solution (200 µL) and stored at 5°C for later analysis at the AWI.

With the exception of CTD cast PS114_049_02 for which samples were collected and stored frozen (as above), samples collected from casts PS114_004_01 to PS114_046_08 were all analysed onboard within 12 h of collection. Samples were analysed in groups of two or more stations in a single run, which minimises chemical waste and analytical uncertainty associated with run to run variability. All samples collected were measured in duplicate. Samples for total nitrogen and total phosphorus were also collected from all CTD casts up to PS114_049_02. DIC samples were only collected from stations associated with the West Spitsbergen Current and East Greenland current. Tab 6.1 lists samples and depths collected from CTD casts.

Tab 6.1: samples and depths collected from the CTD casts. x = inorganic nutrients measured onboard, ○ = samples frozen, analyses of TN and TP, D = samples collected for later analysis of DIC, P = nitrate profiles with SBE SUNA sensor. The second part of the table identifies station numbers to the incremental profile numbering used in the first part of the table.

Depth [m]	CTD_ cast														
	1	2	3	4 (P)	5	6	7	8	9 (P)	10	11	12	13	14 (P)	15 (P)
10	x ○ D		x ○ D		x ○ D		x ○		x ○ D	x ○ D	x ○	x ○	x ○	x ○	x ○
20												x ○			x ○
25									x ○ D					x ○	
30			x ○ D								x ○				
40										x ○ D	x ○		x ○		
50								x ○	x ○ D		x ○	x ○	x ○	x ○	x ○
60															
70															
75	x ○ D		x ○ D		x ○ D		x ○ D	x ○ D	x ○	x ○ D	x ○			x ○	
80												x ○	x ○		x ○
90															
100	x ○ D		x ○ D		x ○ D		x ○ D	x ○ D	x ○ D	x ○ D	x ○	x ○	x ○	x ○	x ○
150						x ○ D									
200												x ○	x ○		x ○
250	x ○ D	x ○ D	x ○ D	x ○ D	x ○ D	x ○ D	x ○ D	x ○ D	x ○ D		x ○			x ○	
300						x ○		x ○	x ○ D			x ○	x ○	x ○	x ○
350															
400						x ○ D		x ○			x ○		x ○	x ○	x ○
450															
500	x ○ D	x ○ D	x ○ D	x ○ D	x ○ D	x ○ D	x ○ D	x ○ D			x ○	x ○	x ○	x ○	x ○
550															
600												x ○	x ○		x ○
650															
700			x ○ D				x ○ D					x ○	x ○		x ○
750						x ○		x ○ D			x ○			x ○	

Depth [m]	CTD_ cast														
	1	2	3	4 (P)	5	6	7	8	9 (P)	10	11	12	13	14 (P)	15 (P)
800						x ○ D						x ○			x ○
850															
900															
950															
1000	x ○ D					x ○ D					x ○				
1200		x ○ D		x ○ D							x ○				
1500														x ○	
2000				x ○ D											
2500														x ○	
3000															
3500															
bottom		x ○ D (2507m)		x ○ (2286m)		x ○ (1200m)					x ○ (1942m)			x ○ (2990m)	

Depth [m]	CTD_cast	16 (P)	17 (P)	18	19	20	21 (P)	22 (P)	23	24	25	26 (P)	27 (P)	28 (P)	29	30	31
10		x ○	x ○	x ○	x ○	x ○	x ○	x ○		x ○	x ○	x ○	x ○	x ○	x ○	x ○	
20							x ○			x ○		x ○	x ○			x ○	
25		x ○		x ○	x ○	x ○					x ○			x ○	x ○		x ○
30													x ○				
40													x ○				
50				x ○	x ○						x ○	x ○	x ○	x ○	x ○	x ○	x ○
60						x ○											
70						x ○											
75		x ○					x ○	x ○		x ○			x ○	x ○			x ○
80				x ○	x ○						x ○	x ○			x	x ○	
90																	
100		x ○				x ○	x ○	x ○		x ○	x ○		x ○	x ○	x ○		x ○
150				x ○	x ○							x ○			x	x ○	
200			x ○	x ○	x ○							x ○		x ○	x ○		
250		x ○				x ○	x ○	x ○	x ○	x ○					x		x ○
300		x ○	x ○			x ○					x ○	x ○	x ○		x ○		x
350				x ○											x		
400		x ○		x ○	x ○							x ○	x ○		x	x	x
450																	
500		x ○	x ○	x ○	x ○	x ○	x ○	x ○	x ○	x ○	x ○	x ○	x ○	x ○	x ○	x ○	x ○
550																	
600			x ○	x ○	x ○						x ○	x ○			x	x	
650														x	x		
700			x ○	x ○	x ○		x ○	x ○		x ○	x ○	x ○			x	x	
750		x ○				x ○			x ○				x ○	x ○			x ○
800			x ○								x ○	x ○			x ○	x ○	
850																	
900																	
950																	

Depth [m]	CTD_cast															
	16 (P)	17 (P)	18	19	20	21 (P)	22 (P)	23	24	25	26 (P)	27 (P)	28 (P)	29	30	31
1000	x ○				x ○			x ○				x ○				x ○
1200								x ○								x ○
1500	x ○											x ○				x ○
2000	x ○				x ○			x ○				x ○				
2500	x ○				x ○							x ○				x ○
3000												x ○				
3500																
bottom	x ○ (2573m)				x ○ (2759m)			x ○ (2561m)				x ○ (3127m)				

Depth [m]	CTD_cast						
	32	33	34 (P)	35 (P)	36	37 (P)	38 (P)
10	x ○	x ○					x
20							
25		x ○					x
30	x ○	x ○					
40				x ○ D			
50	x ○	x ○					x
60							
70							x
75		x ○		x ○ D		x ○ D	
80							x
90							x
100	x ○	x ○		x ○ D		x ○ D	x
150		x ○					x
200	x ○	x ○					x
250			x ○ D	x ○ D	x ○ D		x
300		x ○					
350							
400	x ○	x			x ○ D		
450							
500	x		x ○ D	x ○ D	x ○ D		
550		x ○					
600	x ○						
650		x ○					
700	x ○	x ○	x ○ D	x ○ D			
750					x ○ D		
800	x ○	x ○					
850							
900							
950							
1000			x ○ D				
1200			x ○ D				
1500							
2000			x ○ D				
2500							
3000							
3500							
bottom		x ○ (3074m)	x ○ D (2531m)		x ○ D (959 m)		x (271 m)

CTD_ cast	
1	PS114_004-01
2	PS114_004-06
3	PS114_009-01
4	PS114_009-04
5	PS114_012-01
6	PS114_012-04
7	PS114_013-02
8	PS114_014-01
9	PS114_015-01
10	PS114_016-01
11	PS114_020-01
12	PS114_021-01
13	PS114_022-01
14	PS114_023-01
15	PS114_024-01
16	PS114_025-02
17	PS114_026-01
18	PS114_027-01
19	PS114_028-01
20	PS114_029-01
21	PS114_031-01
22	PS114_032-02
23	PS114_032-06
24	PS114_033-01
25	PS114_034-01
26	PS114_035-01
27	PS114_036-02
28	PS114_037-01
29	PS114_038-01
30	PS114_039-01
31	PS114_040-03
32	PS114_041-01
33	PS114_042-01
34	PS114_043-02
35	PS114_043-04
36	PS114_046-01
37	PS114_046-08
38	PS114_049-02

Calibrants

Calibration standards were prepared using 1000 mg/L NO_3^-, NO_2^{2-}, PO_4^{3-}, Si and NH_4^+ MERC solutions. First, intermediate standards were prepared in Milli-Q water using 50 mL volumetric flasks. Then, calibration standards were prepared in artificial seawater (35 g NaCl/L) using 1 L or 100 mL volumetric flasks. Tab 6.2 shows target concentrations -which are concentrations aimed for when preparing the standards- and actual concentrations –which have been obtained given the molarity of stock/ intermediate solutions.

Tab 6.2: Set of calibration standards (Std) used for dissolved inorganic nutrient analysis. Concentration units are mmol L^{-1}. Target concentrations are shown in bold characters. Actual concentrations as calculated from the molarity of the stock/ intermediate solutions are shown in normal characters. Concentrations for NO_3^- are the sum of NO_3^- and NO_2^-, hence NO_3^-+NO_2^-.

	Si		**PO_4^{3-}**		**NO_2^-**		**NO_3^-**		**NH_4^+**	
Std 1	**1.25**	1.25	**0.125**	0.126	**0.125**	0.125	**0.50**	0.62	**0.50**	0.50
Std 2	**2.50**	2.54	**0.250**	0.253	**0.250**	0.250	**2.50**	2.75	**1.00**	1.00
Std 3	**5.00**	5.03	**0.500**	0.500	**0.500**	0.500	**5.00**	5.50	**1.50**	1.50
Std 4	**10.00**	10.02	**1.000**	1.001	**1.000**	1.000	**10.00**	11.00	**2.00**	2.00
Std 5	**20.00**	20.04	**2.000**	2.001	**2.000**	2.000	**20.00**	22.00	**3.00**	3.00

Quality Controls (QCs)

Reference materials for the analysis of nutrients in seawater (RMNS): In order to test the accuracy and precision of the analyses, RMNS from KANSO Japan Co., were measured in triplicates following the measurement of calibrants and in duplicates after samples every run (15 runs for inorganic nutrients). For PS114 bottles of lot CD and lot CJ were used; certified concentrations of these are shown in Tab 6.3.

Tab 6.3: Certified values of measured reference materials

RMNS	**Si**	**PO_4^{3-}**	**NO_3^-**	**NO_2^-**
Certified conc.				
CD (mmol kg^{-1}**)**	13.93±0.09	0.446±0.008	5.498±0.05	0.018±004
(mmol L^{-1}**)**	14.26±0.10	0.457±0.008	5.62±0.05	0.018±005
CJ (mmol kg^{-1}**)**	38.5±0.40	1.19±0.02	16.20±0.20	0.031±007
(mmol L^{-1}**)**	39.41±0.41	1.21±0.02	16.58±0.20	0.032±007

Problems were encountered during the analysis. In particular the PO4 and NH4 channels of the analyser, which were producing anomalous peaks, with noise in the former and drifts in the latter. Test were done to pin down the problems, which occurred due to the sample to reagent ratio in the former and was solved by increasing sample volume in the PO4 channel. In the latter case, the drift was avoided by attaching a line to the fluorometer waste tube, thereby stabilising the flow of sample through the fluorometer cell.

The consistency and stability of measurements were monitored by continuously plotting calibrant and reference materials output. These data were also used to assess analytical uncertainty at different concentration levels. Tab 6.4 shows the precision of

measurements at different concentration levels, as determined from calibrant measurements throughout the expedition. Fig 6.2 and 6.3 show examples of NO_3+NO_2 calibrants and RMNS time series.

Tab 6.4: Mean, standard deviation and precision of all standards measured as calibrants. These are the results of the regression the AACE software fits from the input of 'target' calibrants and the signal produced by the analysis.

	$Si(OH)_4$	Prec. (%)	PO_4^{3-}	Prec.	NO_3^-+NO_2^{2-}	Prec.	NO_2^-	Prec.	NH_4^+	Prec.
Std 1	1.21±0.05	4.4	0.129±0.009	6.8	0.60±0.06 11.1		0.57±0.04	7.2	0.479±0.010	2.0
Std 2	2.48±0.05	2.0	0.257±0.006	2.5	2.72±0.04 1.6		4.91±0.05	1.0	1.017±0.008	0.7
Std 3	5.09±0.09	1.8	0.500±0.003	0.7	5.55±0.11 2.0		9.76±0.06	0.6	1.519±0.025	1.7
Std 4	10.10±0.08	0.8	0.992±0.022	2.2	11.01±0.11 1.1		19.53±0.1	0.5	1.991±0.027	1.3
Std 5	19.98±0.06	0.3	2.003±0.008	0.4	21.98±0.06 0.3		39.18±0.1	0.3	2.993±0.008	0.3

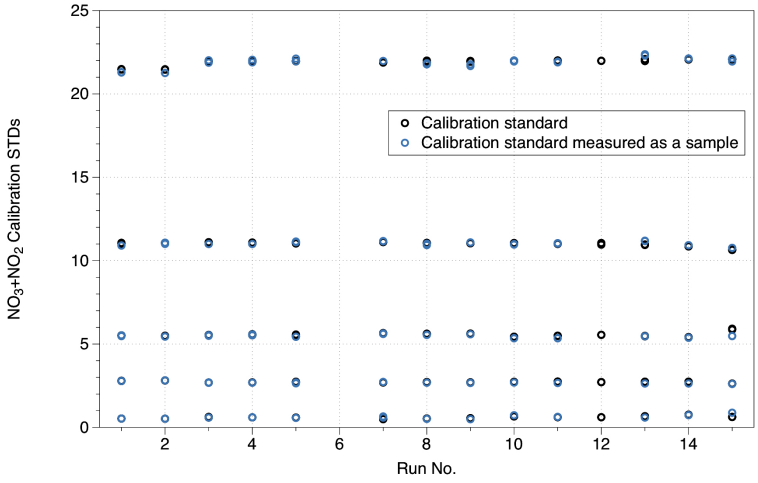

Fig 6.2: Example of calibration standards time series throughout the expedition. Black symbols represent calibrants set up as such within the analyser software, while blue symbols show calibrants measured as unknowns (i.e., as if these were samples). Overall, this time series shows the analytical variability from run to run was small and represents -as shown in Tab 6.4- the cruise global analyses uncertainty at different concentration levels. All samples were analysed in 15 analysis runs.

Additionally, the SUNA sensor deployed in mooring EGC-5 was used, prior to deployment, to generate high resolution profiles in all CTD casts shallower than 800 m. Our aims were to: 1) optimise sampling frequency, 2) generate code to process SUNA data, for which temperature (T) and salinity (S) data from the CTD is required, 3) to calibrate/adjust SUNA data with discrete sample measurements, and 4) simultaneously, to compare high vertical resolution data against discrete sample measurements. Fig 6.4 shows an example of a SUNA-nitrate profile with ancillary CTD data. Note the detailed vertical structure shown in the nutrient profile is *i)* consistent with the structure shown in the O_2 profile and temperature profile, and *ii)* not well represented by discrete measurements. The sensor was measuring at 2 Hz obtaining a dark measurement every 10 seconds for baseline correction. With the CTD's descending speed of about 1 m/s a

resolution of two data points per meter was achieved and averaged in following processing. A linear fit expressing the correlation between SUNA data and discrete measurements was used to eliminate a remaining offset in TS corrected SUNA profiles (Sakamoto et al 2009). The strong gradient in surface water salinity has an impact on the discrete analysis and needs to be considered when measuring backup samples at AWI. For this reason, the upper most discrete sample were not considered in the linear fit.

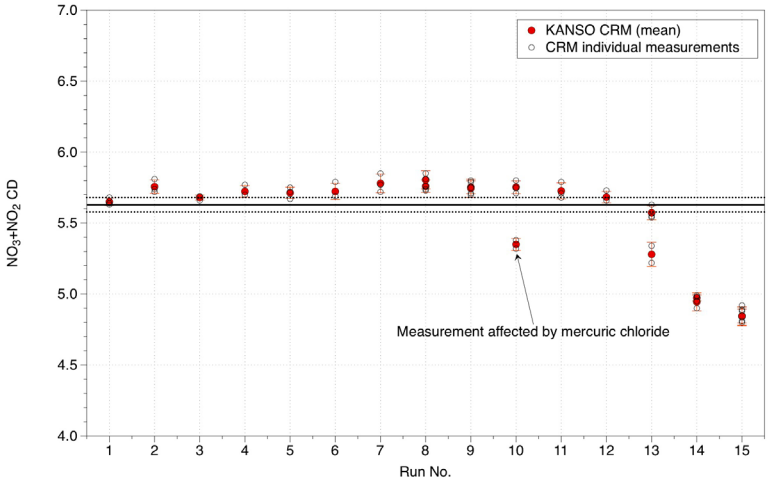

Fig 6.3: Time series of NO_3+NO_2 RMNS, Lot CD. The black thick line represents the certified NO_3+NO_2 concentration, with the dashed lines showing the uncertainty bounds of the certified concentration. Red symbols are the mean of triplicate or duplicate (beginning and end of a given run, respectively) measurements, with error bars showing the standard deviation/difference. Empty symbols show individual measurements. What this type of plot is useful for, is to assess the accuracy of individual methods. Here we can see that in most runs, concentrations were slightly overestimated, while in some, the concentrations were underestimated. The latter case was particularly true for analyses of samples from remote access samplers, where the mercuric chloride used to fix samples affects the reduction efficiency of the Cd coil in the NO_3+NO_2 autoanalyser channel. Results from the RMNS will be later evaluated in more detail to determine correction factors for the data generated.

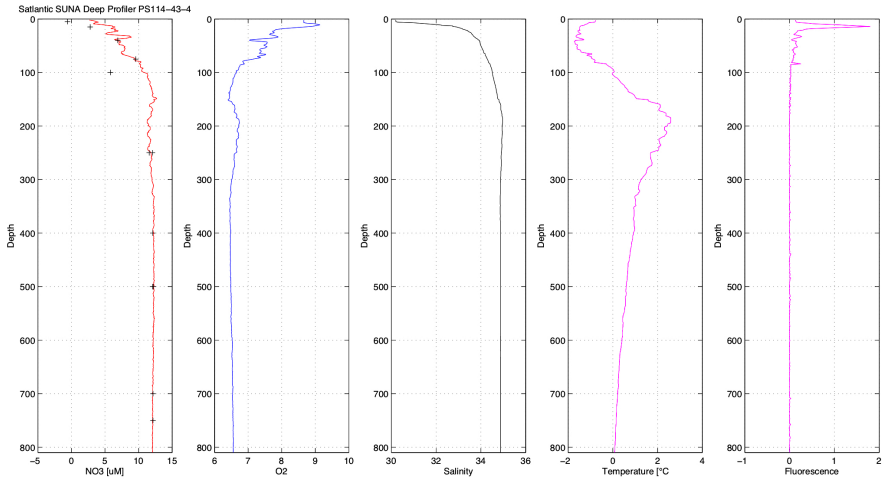

Fig 6.4: SUNA-nitrate profile adjusted via a linear fit with discrete measurements (crosses) and ancillary CTD-O2 data (dissolved oxygen, salinity, temperature and fluorescence-chlorophyll) from cast PS114_043_04. Temperature and salinity data are used by the SUNA data processing algorithm (Sakamoto et al., 2009) to calculate nitrate concentrations.

POM Sampling

Sampling from the underway system began on the 12/07/2018 at 61.5°N and 4.2°E. From this point, samples were taken every 6 hours when the ship was in transit, and once at each station. 2 x 5 litre plastic carboys were filled with seawater from the underway system. These were then filtered through 25 mm (diameter), 0.45 um (mesh) glass fibre filters using a vacuum pump. Filtering was deemed completed when there was sufficient colour on the filters. Depending on the amount of POM in the water, the amount of litres filtered for each sample ranged from 1 L to 10 L. A total of 84 samples were taken (Fig 6.5) and stored in a Styrofoam box in -20°C.

Significant issues were encountered involving the 10 L vacuum bottle that collects the filtered water. The bottle was not able to withstand the pressure of the vacuum and was subsequently sucked in on itself, meaning that it was not possible to create a pressure that was high enough to filter the water in a reasonable amount of time. The original sampling protocol stated that at each sampling location two filters were to be taken, each acting as a duplicate sample. However, with the vacuum bottle issue this was not feasible, therefore water was filtered through three filters at a time, and those three were accumulated as one sample. This was then repeated so that another three filters made up the second duplicate sample. This made it possible to filter the same amount of water in a reasonable time as would be possible with a vacuum-strengthened vacuum bottle.

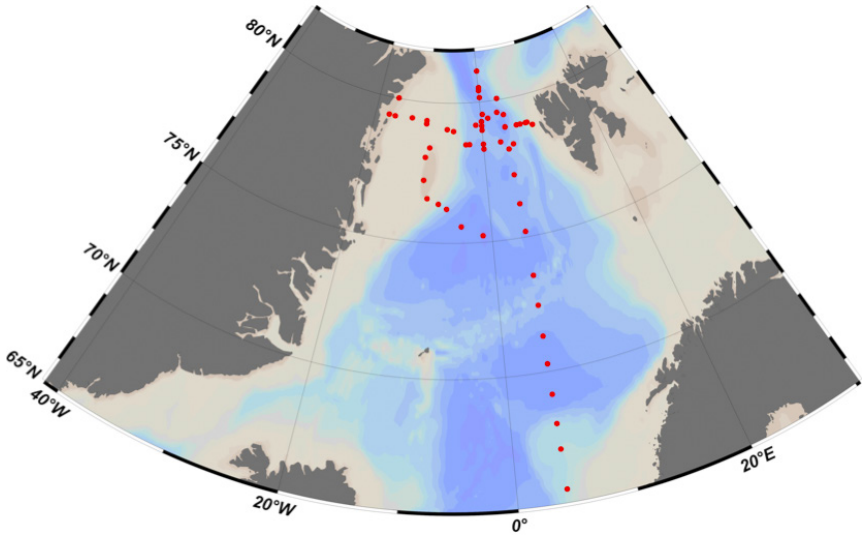

Fig 6.5: The 84 locations where the underway system was sampled for Particulate Organic Matter (POM) in the Nordic Seas and Fram Strait

Dissolved Inorganic Nitrogen Sampling

CTD sampling from different depths was carried out depending on the hydrographic properties of the station to get a diverse range of hydrographic properties contained within the sample set. The depth profiles were sampled in order to get a higher resolution in the top 200 m, with increasing distances between depths at greater depths. The standard depth profile taken for a typical full depth station (of which there were 8) was; Surface (10 m), Above Chlorophyll a

max, Chlorophyll a max, Below Chlorophyll a max, 50 m, 75 m, 100 m, 250 m, 500 m, 750 m, 1,000 m, 1,500 m, 2,000 m, Bottom. Stations where only a shallow CTD was cast (up to 800 m) were sampled 7 times (Fig 6.6).

The seawater was filtered through an Acropak filtration system directly from the Niskin bottle into acid-washed HDPE bottles. Prior to taking the sample, at each Niskin bottle the Acropak filter was attached and water was allowed to flow through the filter and tubing for 30 seconds to ensure there was no contamination from the previous sample. All bottles were immediately stored in the -20°C container.

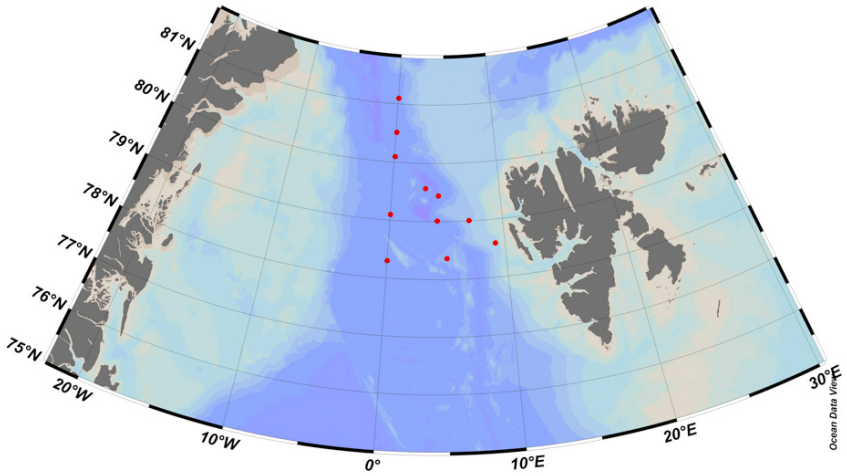

Fig 6.6: Stations where Dissolved Inorganic Nitrogen samples were taken from the CTD

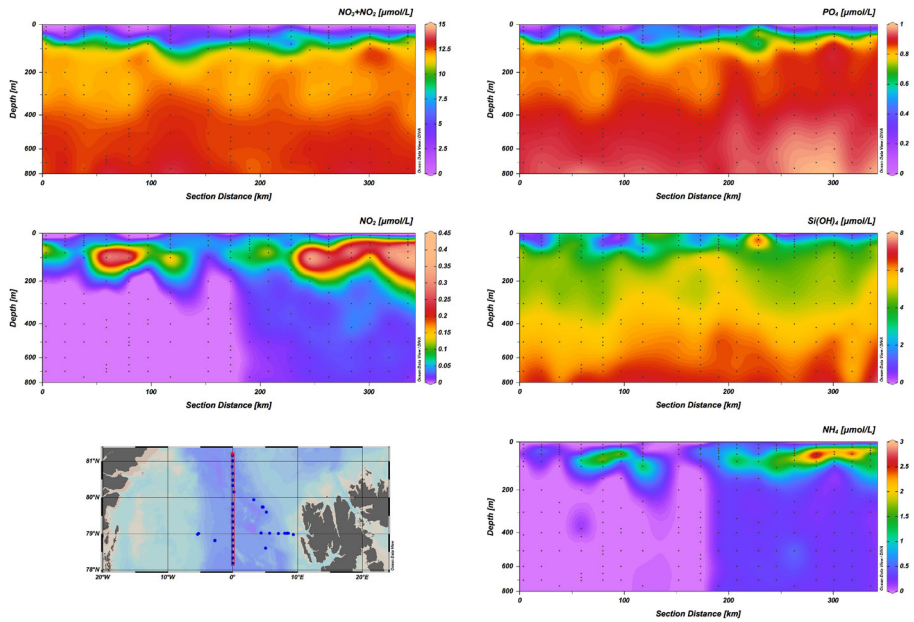

Fig 6.7: Nutrient sections along the prime meridian, from 78.188°N to 81.162°N. Overall, the NO_3+NO_2, PO_4 and $Si(OH)_4$ field show strong vertical gradients between ~50 and ~100 m depth. The vertical structure is remarkable, revealing features most likely resulting from eddies/recirculation in the area. We aim to collaborate with the physical oceanography team and combine these data with CTD data and velocity fields to assess the effect of recirculation on the nutrient distribution at Fram Strait. NO2 and NH4, which are by-products of biological activity, reveal a thick layer of more than 100 m where these nutrients occur.

Preliminary (expected) results

Samples collected for later analysis (TN/TP and DIC) will be retrieved from *Polarstern* once she is back in Bremerhaven (October). Analyses will then be carried out within 6 months. The data that has been generated during the cruise will be further quality controlled through the evaluation of RMNS, calibrants and Cd coil reduction efficiency tests. Once this is done, corrections will be applied if deemed necessary. The final version of the data will also be used to calibrate the SUNA-Nitrate data. We envisage a final data set from the analysis onboard and from the SUNA profiles will be available within 6 months following the end of the expedition. Processing and availability of data from recovered mooring sensors, will most likely take longer (6 to 12 months).

In Fig 6.7 we show examples of results from CTD casts along a prime meridian section. We also present results from the analyses of RAS-collected samples (Fig 6.8), deployed at 23 m in mooring F4-S2 (79° 00.701' N, 006° 57.860' E), programmed to take two samples at 12:00 and 13:00, roughly every two weeks (starting on 16.08.2017).

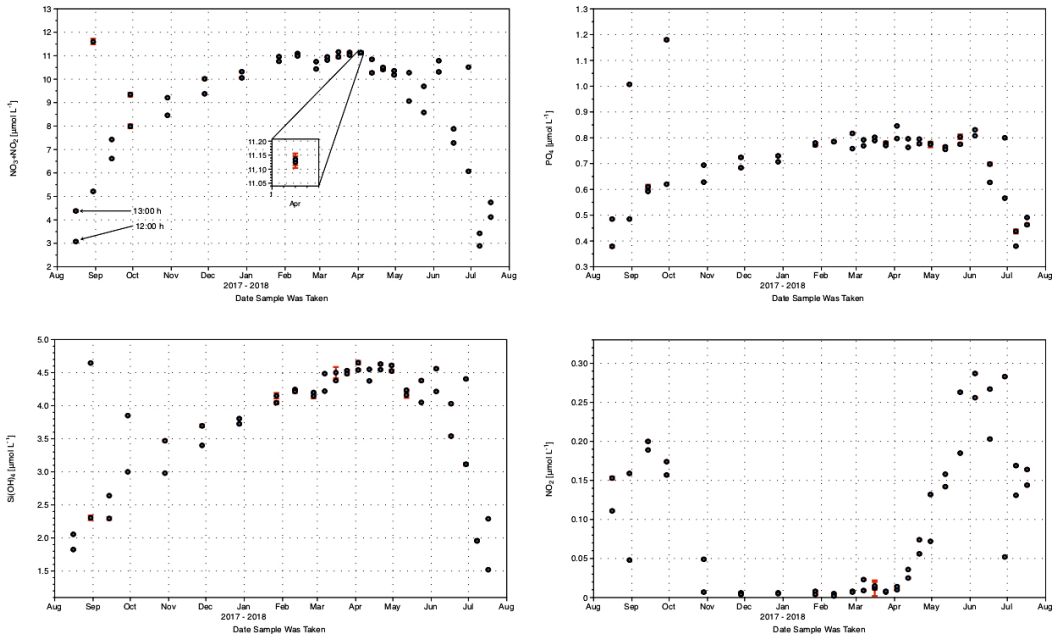

Fig 6.8: Nutrients measured from RAS (mooring F4-S2; 79° 00.701' N, 006° 57.860' E) collected samples. The plots reveal the seasonal cycle of surface nutrients; nitrate+nitrite, phosphate, and silicate show low concentrations at the end of the productive season in August 2017, which are replenished as winter develops. Towards April-May the productive season begins again, drawing nutrients quickly from the surface layers. In contrast, nitrite, a by-product of biological production shows relatively high concentrations by the end of the productive season. Concentration are then undetectable during the winter months (polar night), increasing rapidly as soon as the productive season in 2018 starts. Samples were taken approximately every two weeks at 12:00 and 13:00 h. There are clear differences in nutrient content between the two sampling times. This is probably the result of the RAS drawing sample from different depths as the mooring gets knocked down by currents. These differences diminished during the winter season possibly due to the water column being well mixed.

Data management

For instrumentation deployed during PS114, our aim is to compile data from the different devices in a single file once individual data sets have been retrieved, quality controlled and analysed. Data will then be submitted to PANGAEA.

Data generated during PS114 and from samples collected for later analysis will be submitted to PANGAEA once final data sets are completed (approximately within 6 months from the end of the expedition).

All data produced by ARISE from samples collected during this cruise PS114 will be stored in the PANGAEA database.

References

MacGilchrist GA, Naveira-Garabato AC, Tsubouchi T, Bacon S, Torres-Valdés S, Azetsu-Scott K (2014) The Arctic Ocean carbon sink. Deep Sea Research I, 86, 39-55, doi: 10.1016/j.dsr.2014.01.002.

Sakamoto CM, Johnson KS, Coletti LJ (2009) Improved algorithm for the computation of nitrate concentrations in seawater using an in situ ultraviolet spectrophotometer, Limnology & Oceanography: Methods 7, 132-143.

Torres-Valdés S, Tsubouchi T, Bacon S, Naveira-Garabato AC, Sanders R, McLaughlin FA, Petrie B, Kattner G, Azetsu-Scott K, Whitledge TE (2013) Export of nutrients from the Arctic Ocean. Journal of Geophysical Research: Oceans, 118(4), 1625-1644, doi: 10.1002/jgrc.20063.

Torres-Valdés S, Tsubouchi T, Davey E, Yashayaev I, Bacon S (2016) Relevance of dissolved organic nutrients for the Arctic Ocean nutrient budget. Geophysical Research Letters, 43(12), 6418-6426.

7. PATHWAYS AND EMISSIONS OF CLIMATE-RELEVANT TRACE GASES IN A CHANGING ARCTIC OCEAN - PETRA

Damian Arévalo-Martínez[1], Moritz Baumann[1], Ian Brown[2], Hanna Campen[1], Jacqueline Maud[2], Glen Tarran[2], not on board: H. Bange[1], A. Rees, C.R. Löscher[3]

[1]GEOMAR
[2]PML
[3]Nordcee

Grant-No. AWI_PS114_02

Background and objectives

The Arctic Ocean is exceptionally susceptible to climate change. Recent studies have shown that surface seawater is warming faster than in other oceans, atmospheric CO_2 dissolution in seawater is causing Ocean Acidification (OA), and the documented retreat of sea-ice will increase light penetration, including UV. These environmental parameters are highly likely to act as stressors and alter the Arctic Ocean ecosystem structure and function, which in turn will feedback on climate. One of the key feedbacks is derived from the cycling of climatically active trace gases whose production and consumption pathways are closely associated with several physical and biological processes. Thus, investigating the effect of the above-mentioned stressors (warming, OA, increase in light availability) in trace gases production in the Arctic is necessary if potential responses to future climate change are to be accurately assessed. The major goal during PETRA is to investigate the role of multiple stressors for future cycling of the trace gases nitrous oxide (N_2O), methane (CH_4), dimethylsulphide (DMS) and carbon monoxide (CO) in the Arctic Ocean.

Work at sea

In order to fulfill the overarching goal of PETRA, we combined several approaches for underway and discrete measurements of trace gases, and carried out four incubation experiments at selected locations.

Continuous surface measurements

Underway measurements of dissolved N_2O, CO_2 and CH_4 in seawater were carried out by means of an autonomous equilibrator headspace setup coupled to a trace gas cavity ringdown spectroscopy analyzer (CRDS; Picarro Inc., USA). The combined setup is shown in Fig 7.1. Seawater was drawn from about 11 m depth into the system by using the ship's continuous supply. Control measurements and calibration procedures were performed every 24 h by means of two standard gas mixtures (Deuste Steininger GmbH, Germany) bracketing the expected concentrations in this area.

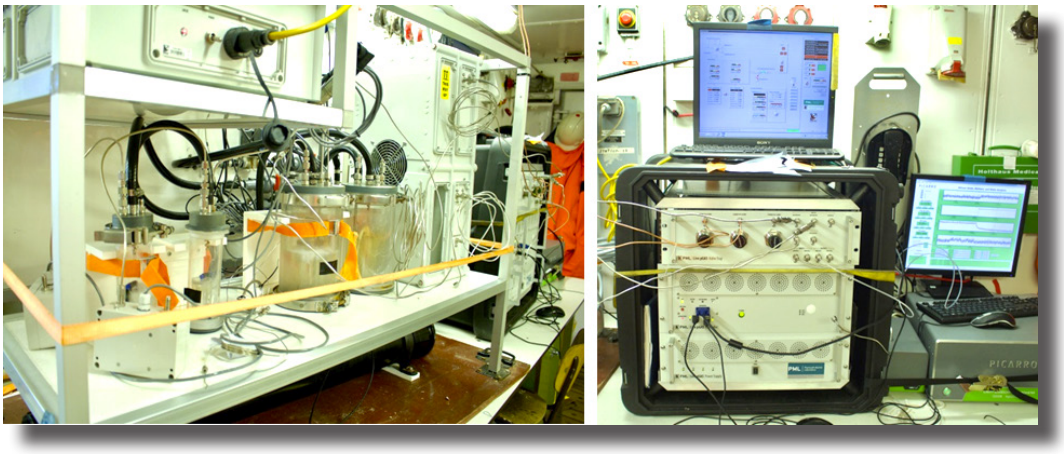

Fig 7.1: System for continuous monitoring of trace gases during PS114. The left panel shows the equilibration chambers, in which continuously flowing surface waters are equilibrated with a fixed amount of air in order to measure the amount of dissolved gas along the cruise track. The right panel shows the spectroscopic analyzer and its control unit (photo credit: Moritz Baumann).

Discrete sampling

In order to decipher the depth distribution and cycling of N_2O in this area, seawater samples were collected during several CTD stations. Whenever the ice conditions did not allow for deep sampling, surface sampling from the ship's underway supply system (~11 m depth) was carried out (this was particularly frequent in the western part of the working area, off the coast of Greenland). For N_2O, bubble-free triplicate samples were collected and immediately sealed by means of butyl stoppers and aluminum crimps. Subsequently 50 µL of a saturated mercuric chloride ($HgCl_2$) solution were added. The samples will be analyzed by means of a headspace equilibrium method and gas chromatographic analysis at the chemical oceanography department of GEOMAR. In order to determine the presence and abundance of functional gene markers of nitrogen cycling, samples were collected at selected locations and the same depths at which inorganic nutrients (see Chapter 6) and N_2O samples were collected. Sample processing consisted of filtering water from selected depths into Durapore® membrane filters (0.22 µm) which were immediately frozen at -80°C. In all stations with molecular work, samples for flow cytometry analysis were also taken. The molecular analysis will be carried out by Carolin Löscher at the biology department of the University of Southern Denmark. An overview of the sampling locations is shown in Fig 7.2.

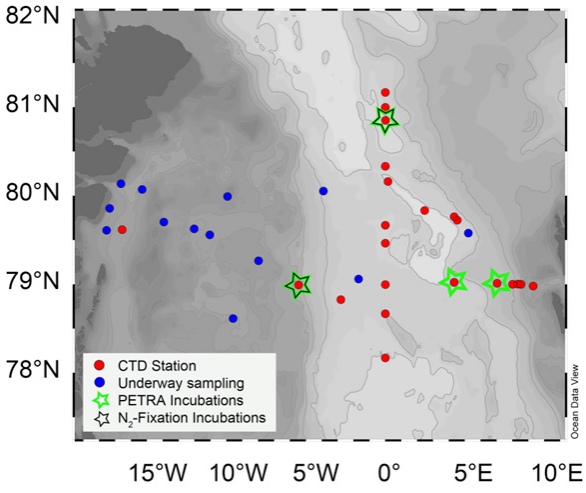

Fig 7.2: Sampling and experiment locations for trace gases during PS114. The red dots indicate stations where samples for depth profiles of N_2O and functional gene markers were collected, whereas the blue dots indicate the same sampling but for surface waters only. Stars show the sampling locations in which large volumes of water were gathered for incubation experiments.

Since characterizing the physical and biogeochemical environment which influences the production/consumption pathways of trace gases in the Arctic is a key aspect of PETRA, sampling for the determination of the depth distribution of a range of additional parameters was carried out at selected locations during the cruise. Tab 7.1 shows an overview of these parameters.

Tab 7.1: List of additional parameters for which water sampling from the CTD/Rosette was carried out during PS114

Station	Parameter							
	Ammonium	DIC/ Alkalinity	POC	DNA	Primary Production	Pigments	Flow Cytometry	CDOM
PS114_04_03	X	X	X	X	X	X	X	
PS114_16_01								X
PS114_17_01	X	X	X	X	X	X	X	
PS114_23_01								X
PS114_26_01								X
PS114_31_01								X
PS114_32_01								X
PS114_34_01								X
PS114_35_01								X
PS114_36_04	X	X	X	X	X	X	X	
PS114_37_01								X
PS114_39_01								X
PS114_41_01								
PS114_43_03	X	X	X	X	X	X	X	X

Incubation experiments

In order to assess the impact of ocean warming, ocean acidification and increased light availability in the production/consumption of N_2O, CH_4, DMS and CO in the Arctic, experimental manipulations of temperature, pH and irradiance were performed in four selected locations during PS114 (c.f. Fig 7.2). Incubations were carried out at ambient temperature and ambient plus 2°C, pH was changed by adding 1M hydrochloric acid and 1M bicarbonate solutions. For CO light and dark incubations were carried out by storing light-transmitting incubation bottles (DURAN®, borosilicate glass) in special incubators on deck simulating light conditions at the surface. Light incubators had transparent plexiglass side walls and no lid. This allowed the full natural sunlight spectrum (including UVB and UVA) to penetrate the enclosures from above and photosynthetically active radiation from all sides through the plexiglass. Black and covered water chambers served as dark incubators and excluded any incoming light. Light penetration was measured with a RAMSES ACC-Vis Hyperspectral radiometer (TriOS, Oldenburg, Germany).

For all experiments large volumes of water were drawn from the CTD/Rosette and after amendment were incubated in experimental enclosures for up to 48 h (DMS, CO) or 96 h (N_2O, CH_4). Incubations from water depths below the surface, as well as those which implied temperature manipulation were conducted in temperature-controlled laboratory containers, whereas those simulating surface ocean conditions were performed in “on-deck” chambers with a constant water supply from about 11 m depth (Fig 7.3). Furthermore, two light sensor

(RAMSES ACC-Vis) profiles were done at the stations of incubation experiments 3 and 4 (PS114_36_04 and PS114_43_03 respectively) in order to learn about the light penetration of different spectral bands (320 nm to 800 nm) over depth.

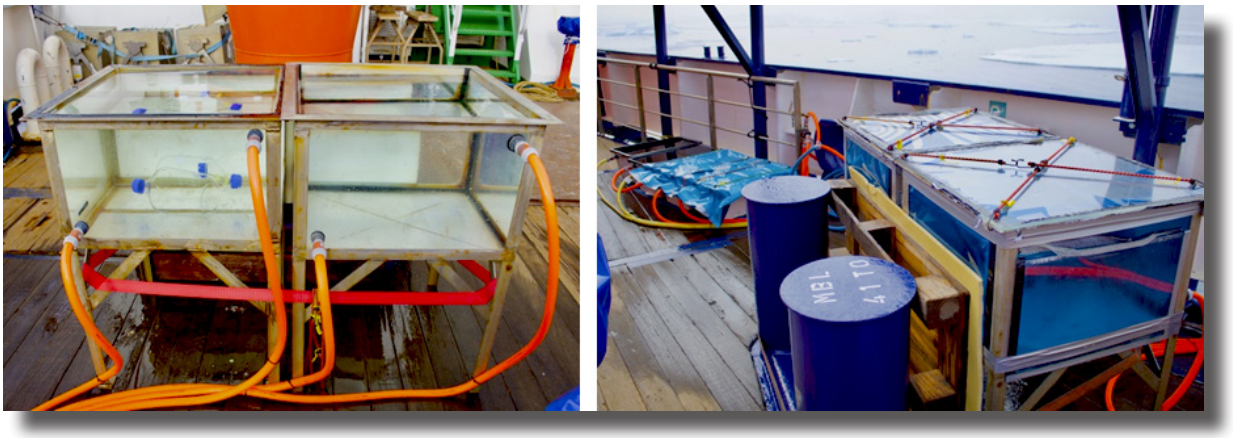

Fig 7.3: On-deck incubation chambers used during the experiments. The incubators simulated natural variability in light conditions, whereas other enclosures for pH and temperature manipulations were located in temperature-controlled containers (photo credit: Moritz Baumann).

In addition to the work done within the framework of PETRA, measurements for functional gene markers of nitrogen fixation (*nifH*) as well as incubation experiments to determine nitrogen and carbon fixation rates were carried out during PS114. Experimental manipulations with bicarbonate and glucose were done in order to establish the occurrence and relative importance of heterotrophic diazotrophs. In conjunction with the depth profiles and surface distribution of gene markers (see above), these experiments are expected to provide insights on the role of nitrogen fixation in polar waters. The experiments were carried out with surface waters (10 m depth) collected with the CTD/Rosette and the incubation took place in on-deck incubators equipped with a blue foil which simulates decreased light intensity at that depth. Filtered samples were either frozen (DNA analysis and flow cytometry) or oven-dried (N/C isotopic analysis) and will be measured at the biology department of the University of Southern Denmark by Carolin Löscher.

Expected results

The field work conducted during the PS114 cruise will provide:

a) High resolution measurements of trace gases (N_2O, CO_2 and CH_4) in Arctic surface waters, thereby leading to a regional estimate of the rate of transfer between ocean and atmosphere and its overall importance.

b) Comprehensive view of the large-scale water column distribution of N_2O, which in combination with hydrographic and chemical information collected by other groups will help elucidating its transport pathways towards and from the Arctic, and its main production/consumption processes.

c) Crucial insights on the effect(s) of single and/or multiple stressors (temperature, OA and light) in the cycling of trace gases in the Arctic.

d) Novel data on the occurrence, distribution and relevance of nitrogen fixation in polar waters.

Data management

Data generated during the PETRA project will form four basic types: 1) Environmental data, 2) Bio- and chemical-assay type experimental data, 3) Molecular biology/Genetic information on microbial populations and 4) Model code.

1) Environmental data on the concentrations of N_2O, CH_4, DMS and CO will be lodged with BODC, BADC and PANGAEA, MEMENTO (-> N2O, CH4 concentration data) and the PMEL DMS database (-> DMS concentration data) as appropriate.

2) Bio- and chemical-assay data generated in PETRA on the concentrations of N_2O, CH_4, DMS and CO will be lodged with BODC.

3) Molecular data originated by PETRA's collaborator Bess Ward (Princeton) will be deposited at Gene Expression Omnibus (http://www.ncbi.nlm.nih.gov/projects/geo/).

4) Model code developed in PETRA will be made publicly available through the ERSEM webpage (www.ersem.com) and connected code repository under GNU General Public License v. 3.

Throughout the project, a project-specific website will be set up, which will be maintained by GEOMAR and PML. All the data mentioned above will be also duplicated and deposited to this project website, which will be made available to the scientific community and the general public. It is anticipated that all data will be publicly available within 6-12 months upon completion of PETRA in 2021, or as soon as the publication of the results in scientific journals.

8. INVESTIGATION OF EMERGING ORGANIC CONTAMINANTS IN THE NORTH ATLANTIC AND THE ARCTIC

Zhiyong Xie, Hanna Joerss HZG

Grant-No. AWI_PS114_03

Objectives

Along with the rapid increasing of the world pollutions and the fast developments of the economy and industry, many kinds of chemical pollutants have been and continue to be poured into the environment in considerable amounts. Therefore, analysis and evaluation of these contaminants in the marine environment is a critical issue nowadays. Besides the notorious Persistent Organic Pollutants (POPs), the emerging organic contaminants (EOCs), although not on the list of POPs under scrutiny by Stockholm Convention currently, are attracting more and more concerns on their occurrence and transport behaviours from the local sources to the remote regions. Additionally, climate change may significantly influence the transport and environmental fate of EOCs in the polar regions.

The investigation of ionic legacy and emerging PFASs in this project aims at a better understanding of the substances' distribution and fate including the involved transportation pathways. Having a higher water solubility and a lower vapor pressure than neutral PFASs, ionic PFASs are considered to be significantly transported via the aqueous pathway. For legacy PFASs like PFOS and PFOA it is known that they reach remote areas and accumulate there. Experimental data on potential long-range transport of emerging PFASs is still very limited. Modeling data suggest that the ether-based alternatives and their common predecessors have comparable physicochemical properties, as well as similar long-range transport potential indicators. The compounds have been detected in different environmental matrices in Europe, China and North America already. Together with the first findings in Arctic biota, these data indicate that ether-based replacements can be globally distributed and reach remote areas.

For the 2018 cruise PS114, this project is focused on studies of the distribution and atmospheric transport of emerging organic contaminants (EOCs), e.g. halogenated flame retardants (HFRs) including brominated flame retardants (BFRs), Dechlorane Plus (DP) and organophosphate esters (OPEs), phthalate esters (PEs) and per- and polyfluoroalkyl substances (PFASs) in the Atlantic and the Arctic. The aims of the project are: (1) characterization of the concentrations of EOCs in the atmosphere, sea water and snow pack in the Arctic; (2) evaluation of the air–water and air-snow exchange process intervening in the transport of EOCs in the Arctic; (3) modelling the input of EOCs into the Arctic via atmospheric dry and wet deposition. The results will contribute to the filling of data gaps regarding fluorinated alternatives. The data will be used to estimate the transport path of EOCs from high concentrated region (European continent, Asian and American Arctic) to relatively low contaminated region (European Arctic), and discover the flow of persistent organic pollutants via air-water or air-snow interaction in the Arctic summer.

Work at sea

Air samples were collected using a high-volume air sampler equipped with a PUF/XAD-2 column for gas-phase compounds and a quartz fiber filter (QFF) (Pore size: 1 µm) for atmospheric particles, respectively. The ship-borne air samplers were mounted on the upper deck of the research vessel. Field blanks were prepared by espousing the PUF/XAD-2 column shortly to the sampling site. Air samples were collected from 57°N to 81°N and the spatial distribution of air samples is shown in Fig 8.1. Field blanks are prepared by shortly espousing the columns to the sampling site. Air samples were stored at 0°C in a cooling room.

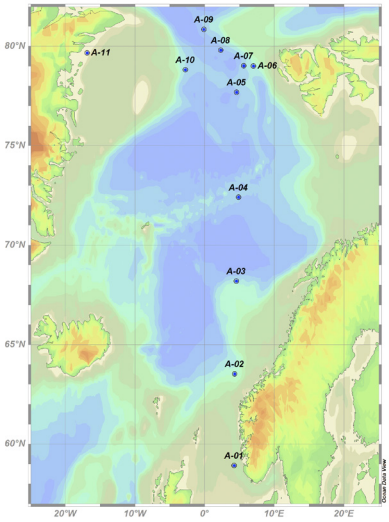

Fig 8.1: Average sampling positions of high-volume air samples during PS114

Seawater samples were collected through the ship's seawater intake system from 12 m depth (stainless steel pipe) at regular intervals along the route. A glass cartridge packed with PAD-3 is used to enrich the analytes in the dissolved phase, and a glass fibre filter (GF/C, pore size 1.2 µm) is used to collect suspended particular matters (SPMs). Each sample continually ran for ~5 to 20 hours to achieve a sample volume of 200 -600 L. Sample columns were stored at 0°C in a cooling container. Spatial distribution of the high-volume seawater samples is shown in Fig 8.2.

Fig 8.2: Sampling positions of high-volume seawater samples during PS114

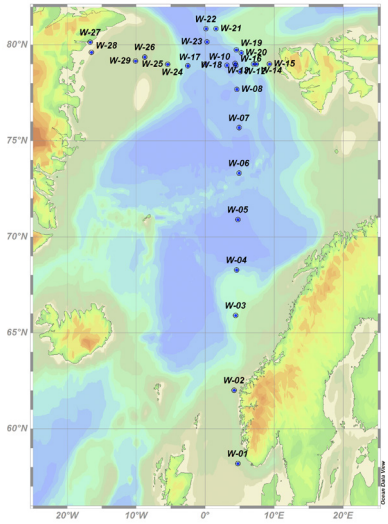

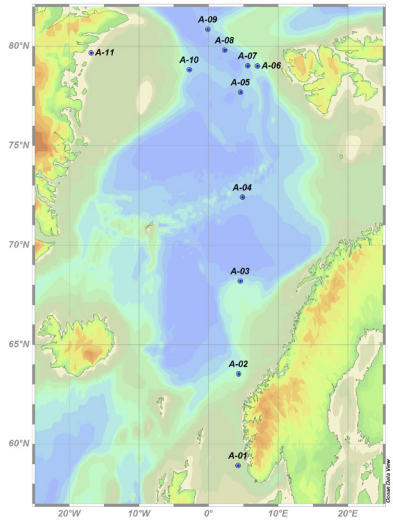

Fig 8.3: Sampling positions of 1-L seawater samples for PFAS analysis during PS114

Moreover, fifty-four 1-L seawater samples were collected in PP bottles for the determination of alternative PFASs across the North Atlantic and the Arctic (Fig 8.3). Seawater samples were spiked with 400 pg mass-labelled internal standards and loaded onto preconditioned solid phase extraction cartridges (Waters Oasis WAX; 6cc, 500 mg, 60 µm) on board. Further sample handling will be performed in a clean lab at Helmholtz-Zentrum Geesthacht (HZG).

Twelve snow samples have been collected on the Arctic sea-ice using 10-L stainless steel barrels with helicopter, boat and Mummy Chair. Eight surface sediments were sampled with a multi-core sampler roughly along 79°N. Snow and sediment samples were stored at -20°C in a cooling container. The positions of sediment and snow samples are shown in Fig 8.4.

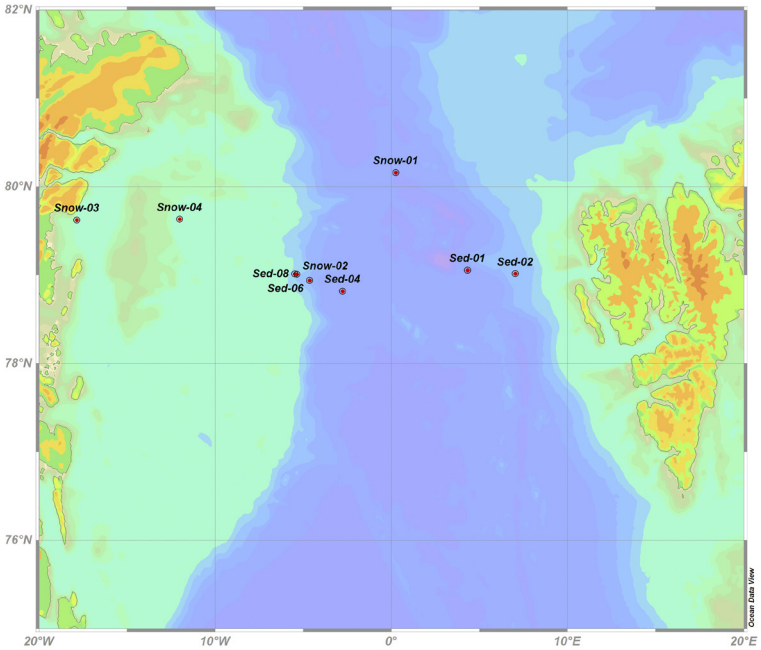

Fig 8.4: Sampling positions of snow and sediment samples during PS114

In addition, sampling for organic contaminants was also part of the CTD water budget (Tab 8.1). Seawater from 5 to 9 depths was sampled from the bottom up to the surface, which may give a primary vertical profile and provide evidence for discharge of organic contaminants from melting snow and ice. The vertical profiles can give information for the mixing of organic contaminants in different water masses.

Tab 8.1: Seawater samples collected from CTD casts during PS114

Station and Cast	Date	Longitude	Latitude	Profile depth	Sample number
PS114_004_06	16.07.2018	79°01.374'N	4°19.914'E	2507 m	5
PS114_009_01	17.07.2018	78°36.354'N	5°02.174'E	700 m	7
PS114_009_04	17.07.2018	78°36.444'N	5°02.880'E	2286 m	2
PS114_012_01	18.07.2018	79°00.722'N	7°02.133'E	1238 m	6
PS114_012_04	18.07.2018	79°00.697'N	7°02.066'E	1239 m	2
PS114_025_02	20.07.2018	78°49.756'N	0°00.658'W	2573 m	8
PS114_036_02	24.07.2018	80°50.175'N	0°08.026'W	3117 m	8
PS114_043_02	26.07.2018	78°49.367'N	2°47.462'W	2600 m	6
PS114_043_04	26.07.2018	78°49.078'N	2°46.088'W	700 m	7
PS114_046_01	27.07.2018	78°59.576'N	5°26.730'W	959 m	3
PS114_046_08	27.07.2018	79°00.739'N	5°17.230'W	100 m	5
PS114_049_02	28.07.2018	79°36.928'N	16°31.516'W	271 m	5

Preliminary (expected) results

The samples will further be handled in a clean-lab at HZG. Melt snow water samples are liquid-liquid extracted using dichloromethane. Sediment samples, PUF/XAD-2, PAD-3 columns and GF/QF filters are spiked with an internal standard mixture as surrogates, and extracted with MX-Soxhlet for 16 h using DCM. All extracts are concentrated to 2 mL by rotary evaporation, and then down to 150 µl with nitrogen evaporator (Barkey gmbH, Germany). The samples are further cleaned on a silica gel column for the determination of neutral PFASs, PEs, BFRs, CUPs, OPEs and chlorinated paraffins. Qualification and quantitation are performed with gas chromatography coupled to mass spectrometry (GC-MS).

For analysis of PFASs, after the elution of the target compounds, eluates will be reduced to 150 µL under nitrogen and [13C8]-PFOA will be added as injection standard. Instrumental analysis will be performed by liquid chromatography-mass spectrometry (HPLC-MS/MS). The analytical method includes 26 legacy PFASs as well as 10 emerging PFASs, such as per- and polyfluoroether carboxylic and sulfonic acids (PFECAs and PFESAs).

Analytical results will show the occurrence and distribution of EOCs in surface waters along potential transport pathways from Europe to the Arctic. Samples taken along a transect from 57°N to 79°N will be used to discuss differences in pollution levels going from the European continent as an emission area to the remote Arctic region. In the working area of the Alfred Wegener Institute, a zonal transect along 79/80 °N is expected to show the influence of the different water masses carried by the West Spitsbergen Current, the recirculation of Atlantic Water and the East Greenland Current as well as processes on the East Greenland shelf. Vertical profiles deriving from CTD samples may reveal further information on sources and transport of EOCs in this area.

By combining integrated atmospheric samples and the collections of reprehensive seawater as well as snow samples across different regions of the Arctic, findings are sought as to determine air-water/snow exchange and setting flux of these organic pollutants. Data and feedback from this project may improve models to predict the environmental progression and assess the effect of climate change on the long-range transport and the fate of the EOCs in the marine and Arctic ecosystem.

Data management

The finally processed data will be submitted to the PANGAEA data library. The unrestricted availability from PANGAEA will depend on the required time and effort for achievement of individual datasets and its status of scientific publication.

APPENDIX

A.1 TEILNEHMENDE INSTITUTE / PARTICIPATING INSTITUTIONS

A.2 FAHRTTEILNEHMER / CRUISE PARTICIPANTS

A.3 SCHIFFSBESATZUNG / SHIP'S CREW

A.1 TEILNEHMENDE INSTITUTE / PARTICIPATING INSTITUTIONS

	Address
AWI	Alfred-Wegener-Institut Helmholtz-Zentrum für Polar- und Meeresforschung Postfach 120161 27515 Bremerhaven Germany
DWD	Deutscher Wetterdienst Geschäftsbereich Wettervorhersage Seeschifffahrtsberatung Bernhard Nocht Str. 76 20359 Hamburg Germany
GEOMAR	GEOMAR Helmholtz Zentrum für Ozeanforschung Wischhofstraße 1-3 24148 Germany
HeliService	Heli Service International GmbH Gorch-Fock-Straße 105 26721 Emden Germany
HZG	Helmholtz Zentrum Geesthacht Max-Planck-Straße 1 21502 Geesthacht Germany
MPI	Max Planck Institut für Marine Mikobiologie Celsiusstraße 1 28359 Bremen Germany
PML	Plymouth Marine Laboratory Prospect Place Plymouth PL1 3DH United Kingdom
Uni Liverpool	University of Liverpool Liverpool L69 3BX United Kingdom
Uni Oldenburg	Carl von Ossietzky Universität zu Oldenburg Ammerländer Heerstraße 114-118 26129 Oldenburg Germany

A.2 FAHRTTEILNEHMER / CRUISE PARTICIPANTS

Name	Vorname/ First name	Institut/ Institute	Beruf/ Profession	Fachbereich/ Discipline
Arevalo-Martinez	Damian	GEOMAR	Scientist	Chemical oceanography
Bäger	Jana	AWI	Technician	Deep sea ecology
Baumann	Moritz	GEOMAR	Scientist	Chemical oceanography
Behrendt	Axel	AWI	Scientist	Physical oceanography
Brown	Ian	PML	Scientist	Chemical oceanography
Campen	Hanna	GEOMAR	Scientist	Chemical oceanography
Eckhardt	Freya	AWI	Technician	Deep sea ecology
Frommhold	Lennard	AWI	Engineer	Deep sea ecology
Garcia	Alberto	HeliService	Heli technician	
Gischler	Michael	HeliService	Pilot	
Goldbach	Nicolas	AWI	Student	Plankton ecology
Große	Julia	GEOMAR	Scientist	Plankton ecology
Hildebrandt	Nicole	AWI	Scientist	Plankton ecology
Hofmann	Zerlina	AWI	Student	Physical oceanography
Hufnagel	Lili	AWI	Student	Deep sea ecology
Joerss	Hanna	HZG	Student	Air chemistry
Kendzia	Jan	HeliService	Pilot	
Knüppel	Nadine	AWI	Technician	Plankton ecology
Konrad	Christian	AWI	Engineer	Deep sea ecology
Krauß	Florian	AWI	Student	Deep sea ecology
Kuhlmey	David	AWI	Technician	Physical oceanography
Lochthofen	Normen	AWI	Engineer	Deep sea ecology
Ludszuweit	Janine	AWI	Technician	Deep sea ecology
Maud	Jacqueline	PML	Scientist	Chemical oceanography
Monsees	Matthias	AWI	Technician	Physical oceanography
Morische	Annika	Uni Oldenburg	Student	Chemical oceanography
Price	Elliott	Uni Liverpool	PhD student	Chemical oceanography
Raeke	Andreas	DWD	Meteorologist	
Rentsch	Harald	DWD	Meteorologist	
Richter	Maren	AWI	Student	Physical oceanography
Richter	Roland	HeliService	Heli technician	
Rohleder	Christian	DWD	Meteorologist	
Schaffer	Janin	AWI	Scientist	Physical oceanography
Schmidt	Carl	AWI	Student	Physical oceanography
Scholz	Daniel	AWI	Engineer	Chemical oceanography
Seifert	Miriam	AWI	PhD student	Deep sea ecology
Specht	Mia Sophie	AWI	Student	Physical oceanography

Name	Vorname/ First name	Institut/ Institute	Beruf/ Profession	Fachbereich/ Discipline
Staufenbiel	Benjamin	GEOMAR	Student	Plankton ecology
Stiens	Rafael	AWI	Technician	Deep sea ecology
Tarran	Glen	PML	Scientist	Chemical oceanography
Töller	Susanne	AWI	PhD student	Plankton ecology
Torres Valdes	Sinhue	AWI	Scientist	Chemical oceanography
Vernaleken	Jutta	AWI	Technician	Physical oceanography
von Appen	Wilken-Jon	AWI	Scientist	Physical oceanography
von Jackowski	Anabel	AWI	Student	Plankton ecology
Wulf	Jörg	MPI	Technician	Plankton ecology
Xie	Zhiyong	HZG	Scientist	Air chemistry

A.3 SCHIFFSBESATZUNG / SHIP'S CREW

	Name	First Name	Rank
1	Schwarze	Stefan	Master
2	Langhinrichs	Moritz	Chiefmate
e	Kentges	Felix	1st Mate
4	Fallei	Holger	2nd Mate
5	Neumann	Ralph Peter	2nd Mate
6	Farysch	Bernd	Chief
7	Grate	Jens	2nd Eng.
8	Haack	Michael Detlev	2nd Eng.
9	Krinfeld	Oleksandr	2nd Eng.
10	Redmer	Jens	E-Eng.
11	Christian	Boris	Chief ELO
12	Ganter	Armin	ELO
13	Himmel	Frank	ELO
14	Hüttebräucker	Olaf	ELO
15	Nasis	Ilias	ELO
16	Rudde-Teufel	Claus Friedrich ...	Ships doc
17	Loidl	Reiner	Bosun
18	Reise	Lutz	Carpen.
19	Brück	Sebastian	MP Rat.
20	Klee	Philipp	MP Rat.
21	Möller	Falko	MP Rat.
22	Neubauer	Werner	MP Rat.
23	Bäcker	Andreas	AB
24	Hans	Stefan	AB
25	Scheel	Sebastian	AB
26	Wende	Uwe	AB
27	Preußner	Jörg	Storek.
28	Gebhardt	Norman	MP Rat
29	Lamm	Gerd	MP Rat
30	Schwarz	Uwe	MP Rat
31	Teichert	Uwe	MP Rat
32	Möller	Wolfgang Hans He„	Cook
33	Martens	Michael	Cooksm.
34	Silinski	Frank	Cooksm.
35	Czyborra	Bärbel	Chief Stew.
36	Wöckener	Martina	Nurse
37	Arendt	Rene	2nd Stew.
38	Chen	Dansheng	2nd Stew.
39	Dibenau	Torsten	2nd Stew.
40	Golla	Gerald	2nd Stew.
41	Hu	Guoyong	2nd Stew.
42	Silinski	Carmen	2nd Stew.

A.4 STATIONSLISTE / STATION LIST

Station	Date	Time	Latitude	Longitude	Depth [m]	Gear	Action	Comment
PS114_0_Underway-1	2018-07-10	06:00	53.56681	8.55505	NA	WST	profile start	
PS114_0_Underway-2	2018-07-11	08:26	56.95065	5.53887	46	ADCP_150	profile start	
PS114_0_Underway-2	2018-08-02	11:01	71.62816	14.91220	193	ADCP_150	profile end	
PS114_0_Underway-3	2018-07-12	09:49	61.73438	4.19111	222	FBOX	profile start	
PS114_0_Underway-3	2018-08-01	11:10	73.99038	5.01289	3090	FBOX	profile end	
PS114_0_Underway-4	2018-07-12	09:49	61.73653	4.19129	218	PCO2_GO	profile start	
PS114_0_Underway-4	2018-07-20	07:23	78.18307	-0.00039	3055	PCO2_GO	profile end	
PS114_0_Underway-5	2018-07-12	09:49	61.73522	4.19117	219	PCO2_SUB	profile start	
PS114_0_Underway-5	2018-08-01	11:09	73.99235	5.00384	2743	PCO2_SUB	profile end	
PS114_0_Underway-6	2018-07-11	15:03	58.12284	4.77190	NA	SVP	profile start	
PS114_0_Underway-6	2018-07-12	05:24	60.85319	4.16985	9	SVP	profile end	
PS114_0_Underway-6	2018-07-12	09:49	61.73438	4.19111	222	SVP	profile start	
PS114_0_Underway-6	2018-08-03	04:49	69.80087	19.36522	189	SVP	profile end	
PS114_0_Underway-7	2018-07-11	15:00	58.11196	4.77860	NA	TSG_KEEL	profile start	
PS114_0_Underway-7	2018-07-12	05:24	60.85319	4.16985	9	TSG_KEEL	profile end	
PS114_0_Underway-7	2018-07-12	09:49	61.73438	4.19111	222	TSG_KEEL	profile start	
PS114_0_Underway-7	2018-08-02	13:15	71.40439	15.79685	1275	TSG_KEEL	profile end	
PS114_0_Underway-8	2018-07-11	15:00	58.11186	4.77866	NA	TSG_KEEL_2	profile start	
PS114_0_Underway-8	2018-07-12	05:24	60.85319	4.16985	9	TSG_KEEL_2	profile end	
PS114_0_Underway-8	2018-07-12	09:49	61.73438	4.19111	222	TSG_KEEL_2	profile start	
PS114_0_Underway-8	2018-08-02	13:14	71.40522	15.79357	1275	TSG_KEEL_2	profile end	
PS114_0_Underway-9	2018-07-12	09:49	61.73438	4.19111	222	AFIM	profile start	
PS114_0_Underway-9	2018-08-03	04:49	69.80021	19.35712	198	AFIM	profile end	
PS114_0_Underway-10	2018-07-12	09:49	61.73438	4.19111	222	HVAIR	profile start	
PS114_0_Underway-10	2018-08-01	11:10	73.99038	5.01289	3090	HVAIR	profile end	
PS114_1-1	2018-07-16	03:18	79.01969	4.24412	2521	MOOR	retrieval start	HG-IV-S-2
PS114_1-1	2018-07-16	05:40	79.00990	4.22575	2547	MOOR	retrieval end	HG-IV-S-2
PS114_2-1	2018-07-16	06:09	78.99757	4.32961	2528	MOOR	retrieval start	HG-IV-FEVI-36
PS114_2-1	2018-07-16	08:21	78.97839	4.30709	2569	MOOR	retrieval end	HG-IV-FEVI-36
PS114_3-1	2018-07-16	10:05	79.02285	4.40069	2452	MOOR	retrieval start	HG-IV-SWIPS-2017
PS114_3-1	2018-07-16	12:12	79.01582	4.34218	2494	MOOR	retrieval end	HG-IV-SWIPS-2017
PS114_4-1	2018-07-16	12:39	79.02356	4.33284	2476	CTDOZE	station start	
PS114_4-1	2018-07-16	12:58	79.02359	4.33352	2476	CTDOZE	at depth	
PS114_4-1	2018-07-16	13:29	79.02371	4.33221	2476	CTDOZE	station end	
PS114_4-2	2018-07-16	13:43	79.02309	4.33194	2479	LOKI	station start	
PS114_4-2	2018-07-16	14:24	79.02305	4.33174	2479	LOKI	at depth	
PS114_4-2	2018-07-16	15:05	79.02371	4.32922	2478	LOKI	station end	
PS114_4-3	2018-07-16	15:25	79.02351	4.33297	2477	CTDOZE	station start	
PS114_4-3	2018-07-16	15:38	79.02336	4.33042	2479	CTDOZE	at depth	
PS114_4-3	2018-07-16	15:57	79.02356	4.33462	2475	CTDOZE	station end	
PS114_4-4	2018-07-16	17:07	79.02360	4.33423	2475	CTDOZE	station start	
PS114_4-4	2018-07-16	17:12	79.02377	4.33511	2474	CTDOZE	at depth	

Station	Date	Time	Latitude	Longitude	Depth [m]	Gear	Action	Comment
PS114_4-4	2018-07-16	17:21	79.02322	4.33323	2477	CTDOZE	station end	
PS114_4-5	2018-07-16	17:30	79.02336	4.33124	2478	MN_S5	station start	
PS114_4-5	2018-07-16	18:34	79.02333	4.33368	2476	MN_S5	at depth	
PS114_4-5	2018-07-16	19:43	79.02328	4.33244	2477	MN_S5	station end	
PS114_4-6	2018-07-16	20:01	79.02316	4.33306	2477	CTDOZE	station start	
PS114_4-6	2018-07-16	21:00	79.02341	4.33127	2477	CTDOZE	at depth	
PS114_4-6	2018-07-16	22:26	79.02407	4.33413	2473	CTDOZE	station end	
PS114_4-7	2018-07-16	22:40	79.02415	4.33089	2474	ISPC	station start	
PS114_4-7	2018-07-16	23:41	79.02458	4.32886	2474	ISPC	at depth	
PS114_4-7	2018-07-17	00:22	79.02500	4.32602	2474	ISPC	station end	
PS114_5-1	2018-07-17	04:00	79.02314	4.26254	2512	MOOR	deployment start	HG-IV-S-3
PS114_5-1	2018-07-17	05:43	79.02266	4.26179	2513	MOOR	deployment end	HG-IV-S-3
PS114_6-1	2018-07-17	07:00	79.00021	4.33340	2522	MOOR	deployment start	HG-IV-FEVI-38
PS114_6-1	2018-07-17	09:15	79.00034	4.33229	2522	MOOR	deployment end	HG-IV-FEVI-38
PS114_7-1	2018-07-17	11:00	79.02305	4.40332	2450	MOOR	deployment start	HG-IV-SWIPS-2018
PS114_7-1	2018-07-17	12:30	79.02333	4.40560	2460	MOOR	deployment end	HG-IV-SWIPS-2018
PS114_8-1	2018-07-17	13:31	79.05019	4.33256	2451	TVMUC	station start	
PS114_8-1	2018-07-17	14:44	79.05002	4.33298	2452	TVMUC	at depth	
PS114_8-1	2018-07-17	15:34	79.05073	4.33291	2449	TVMUC	station end	
PS114_9-1	2018-07-17	18:32	78.60577	5.03458	2350	CTDOZE	station start	
PS114_9-1	2018-07-17	18:53	78.60667	5.04132	2347	CTDOZE	at depth	
PS114_9-1	2018-07-17	19:22	78.60751	5.04655	2344	CTDOZE	station end	
PS114_9-2	2018-07-17	19:35	78.60728	5.04553	2345	LOKI	station start	
PS114_9-2	2018-07-17	20:13	78.60747	5.04503	2345	LOKI	at depth	
PS114_9-2	2018-07-17	20:55	78.60732	5.04562	2345	LOKI	station end	
PS114_9-3	2018-07-17	21:12	78.60751	5.04552	2345	MN_S5	station start	
PS114_9-3	2018-07-17	22:10	78.60738	5.04842	2343	MN_S5	at depth	
PS114_9-3	2018-07-17	23:32	78.60755	5.04405	2345	MN_S5	station end	
PS114_9-4	2018-07-17	23:44	78.60738	5.04802	2344	CTDOZE	station start	
PS114_9-4	2018-07-18	00:37	78.60735	5.04698	2344	CTDOZE	at depth	
PS114_9-4	2018-07-18	01:43	78.60704	5.04929	2344	CTDOZE	station end	
PS114_10-1	2018-07-18	06:13	79.01363	6.95728	1264	MOOR	retrieval start	F4-S-2
PS114_10-1	2018-07-18	06:57	79.02098	6.94522	1277	MOOR	retrieval end	F4-S-2
PS114_11-1	2018-07-18	07:45	79.00274	6.99258	1249	MOOR	retrieval start	F4-17
PS114_11-1	2018-07-18	08:30	79.00824	6.98637	1261	MOOR	retrieval end	F4-17
PS114_11-2	2018-07-18	08:42	79.00931	6.98582	1263	TVMUC	station start	
PS114_11-2	2018-07-18	09:13	79.00937	6.98598	1262	TVMUC	at depth	
PS114_11-2	2018-07-18	09:43	79.00933	6.98605	1262	TVMUC	station end	
PS114_12-1	2018-07-18	10:11	79.01215	7.03545	1277	CTDOZE	station start	
PS114_12-1	2018-07-18	10:41	79.01174	7.03459	1277	CTDOZE	at depth	
PS114_12-1	2018-07-18	11:20	79.01181	7.03510	1277	CTDOZE	station end	

Station	Date	Time	Latitude	Longitude	Depth [m]	Gear	Action	Comment
PS114_12-2	2018-07-18	11:32	79.01211	7.03308	1277	LOKI	station start	
PS114_12-2	2018-07-18	12:12	79.01193	7.03394	1277	LOKI	at depth	
PS114_12-2	2018-07-18	12:53	79.01198	7.03305	1277	LOKI	station end	
PS114_12-3	2018-07-18	13:06	79.01174	7.03538	1277	MN_S5	station start	
PS114_12-3	2018-07-18	13:51	79.01183	7.03451	1277	MN_S5	at depth	
PS114_12-3	2018-07-18	14:49	79.01196	7.03510	1278	MN_S5	station end	
PS114_12-4	2018-07-18	15:04	79.01159	7.03477	1278	CTDOZE	station start	
PS114_12-4	2018-07-18	15:35	79.01160	7.03310	1277	CTDOZE	at depth	
PS114_12-4	2018-07-18	16:10	79.01202	7.03427	1278	CTDOZE	station end	
PS114_13-1	2018-07-18	17:44	79.01824	8.00377	1101	OFOS	station start	
PS114_13-1	2018-07-18	18:11	79.01851	8.01073	1097	OFOS	at depth	
PS114_13-1	2018-07-18	18:42	79.01981	8.02262	1091	OFOS	station end	
PS114_13-2	2018-07-18	18:57	79.01930	8.00708	1100	CTDOZE	station start	
PS114_13-2	2018-07-18	19:25	79.01915	8.00755	1099	CTDOZE	at depth	
PS114_13-2	2018-07-18	20:00	79.01903	8.00784	1099	CTDOZE	station end	
PS114_14-1	2018-07-18	20:52	79.01783	8.32711	827	CTDOZE	station start	
PS114_14-1	2018-07-18	21:14	79.01796	8.32657	827	CTDOZE	at depth	
PS114_14-1	2018-07-18	21:46	79.01800	8.32738	826	CTDOZE	station end	
PS114_15-1	2018-07-18	22:39	79.01833	8.54183	395	CTDOZE	station start	
PS114_15-1	2018-07-18	22:53	79.01845	8.54220	393	CTDOZE	at depth	
PS114_15-1	2018-07-18	23:11	79.01813	8.54091	397	CTDOZE	station end	
PS114_16-1	2018-07-19	00:17	78.98023	9.30124	217	CTDOZE	station start	
PS114_16-1	2018-07-19	00:28	78.98044	9.30060	218	CTDOZE	at depth	
PS114_16-1	2018-07-19	00:45	78.98028	9.29900	218	CTDOZE	station end	
PS114_17-1	2018-07-19	03:35	79.01147	6.95761	1259	CTDOZE	station start	
PS114_17-1	2018-07-19	03:43	79.01132	6.95989	1260	CTDOZE	at depth	
PS114_17-1	2018-07-19	04:00	79.01187	6.96160	1262	CTDOZE	station end	
PS114_17-2	2018-07-19	04:59	79.01278	6.96040	1264	CTDOZE	station start	
PS114_17-2	2018-07-19	05:24	79.01214	6.96302	1263	CTDOZE	at depth	
PS114_17-2	2018-07-19	05:35	79.01245	6.96172	1263	CTDOZE	station end	
PS114_17-3	2018-07-19	06:02	79.01189	6.96432	1263	MOOR	deployment start	F4-S-3
PS114_17-3	2018-07-19	07:32	79.01185	6.96391	1262	MOOR	deployment end	F4-S-3
PS114_18-1	2018-07-19	08:14	79.00027	7.00123	1246	MOOR	deployment start	F4-18
PS114_18-1	2018-07-19	09:28	79.00038	7.00061	1245	MOOR	deployment end	F4-18
PS114_19-1	2018-07-19	11:01	79.01164	7.03585	1277	MOOR	deployment start	F4-W-1
PS114_19-1	2018-07-19	12:17	79.01154	7.03524	1277	MOOR	deployment end	F4-W-1
PS114_20-1	2018-07-19	14:11	79.01886	5.65670	1999	CTDOZE	station start	
PS114_20-1	2018-07-19	14:56	79.02060	5.64828	1987	CTDOZE	at depth	
PS114_20-1	2018-07-19	15:52	79.02444	5.62540	1982	CTDOZE	station end	
PS114_21-1	2018-07-19	21:05	78.66836	0.01160	1834	CTDOZE	station start	
PS114_21-1	2018-07-19	21:27	78.66832	0.01122	1833	CTDOZE	at depth	

Station	Date	Time	Latitude	Longitude	Depth [m]	Gear	Action	Comment
PS114_21-1	2018-07-19	21:59	78.66857	0.01099	1835	CTDOZE	station end	
PS114_22-1	2018-07-19	23:18	78.50071	-0.00286	2778	CTDOZE	station start	
PS114_22-1	2018-07-19	23:54	78.50070	-0.00148	2777	CTDOZE	at depth	
PS114_22-1	2018-07-20	00:28	78.50095	-0.00036	2777	CTDOZE	station end	
PS114_23-1	2018-07-20	02:43	78.18921	0.00095	3053	CTDOZE	station start	
PS114_23-1	2018-07-20	03:48	78.18773	0.00391	3054	CTDOZE	at depth	
PS114_23-1	2018-07-20	05:12	78.18739	-0.00795	3055	CTDOZE	station end	
PS114_23-2	2018-07-20	05:59	78.16925	-0.00451	3060	MOOR	retrieval start	R1-1
PS114_23-2	2018-07-20	07:17	78.18234	0.00015	3055	MOOR	retrieval end	R1-1
PS114_23-3	2018-07-20	07:37	78.18346	-0.00135	3055	LOKI	station start	
PS114_23-3	2018-07-20	08:06	78.18348	-0.00018	3055	LOKI	at depth	
PS114_23-3	2018-07-20	08:32	78.18316	-0.00116	3055	LOKI	station end	
PS114_24-1	2018-07-20	09:59	78.33324	-0.00620	3009	CTDOZE	station start	
PS114_24-1	2018-07-20	10:16	78.33328	-0.00821	3009	CTDOZE	at depth	
PS114_24-1	2018-07-20	10:45	78.33301	-0.00793	3009	CTDOZE	station end	
PS114_25-1	2018-07-20	13:09	78.83315	0.00157	2639	MOOR	retrieval start	R2-1
PS114_25-1	2018-07-20	14:40	78.82862	-0.00355	2636	MOOR	retrieval end	R2-1
PS114_25-2	2018-07-20	14:57	78.82921	-0.01040	2636	CTDOZE	station start	
PS114_25-2	2018-07-20	15:53	78.82974	-0.02524	2636	CTDOZE	at depth	
PS114_25-2	2018-07-20	17:08	78.83127	-0.05449	2633	CTDOZE	station end	
PS114_25-3	2018-07-20	17:18	78.83126	-0.05712	2633	LOKI	station start	
PS114_25-3	2018-07-20	17:48	78.83124	-0.06704	2630	LOKI	at depth	
PS114_25-3	2018-07-20	18:21	78.83074	-0.08379	2627	LOKI	station end	
PS114_26-1	2018-07-20	19:41	78.99865	0.00087	2595	CTDOZE	station start	
PS114_26-1	2018-07-20	20:00	78.99886	-0.00028	2596	CTDOZE	at depth	
PS114_26-1	2018-07-20	20:28	78.99946	-0.00029	2596	CTDOZE	station end	
PS114_27-1	2018-07-20	22:15	79.16496	0.00964	2725	CTDOZE	station start	
PS114_27-1	2018-07-20	22:34	79.16552	0.00627	2725	CTDOZE	at depth	
PS114_27-1	2018-07-20	23:03	79.16575	0.00249	2725	CTDOZE	station end	
PS114_28-1	2018-07-21	01:07	79.33579	0.05698	2892	CTDOZE	station start	
PS114_28-1	2018-07-21	01:26	79.33485	0.04743	2893	CTDOZE	at depth	
PS114_28-1	2018-07-21	01:56	79.33457	0.03458	2898	CTDOZE	station end	
PS114_29-1	2018-07-21	04:02	79.50246	-0.10954	2820	CTDOZE	station start	
PS114_29-1	2018-07-21	05:03	79.49474	-0.10009	2824	CTDOZE	at depth	
PS114_29-1	2018-07-21	06:20	79.48865	-0.10631	2827	CTDOZE	station end	
PS114_29-2	2018-07-21	07:35	79.49589	-0.00055	2824	MOOR	retrieval start	R3-1
PS114_29-2	2018-07-21	10:00	79.47120	0.01159	2841	MOOR	retrieval end	R3-1
PS114_29-3	2018-07-21	10:13	79.46948	0.00962	2842	LOKI	station start	
PS114_29-3	2018-07-21	10:43	79.46498	0.00968	2845	LOKI	at depth	
PS114_29-3	2018-07-21	11:17	79.46021	-0.00387	2849	LOKI	station end	
PS114_29-4	2018-07-21	12:02	79.45136	0.00153	2858	TVMUC	station start	
PS114_29-4	2018-07-21	12:56	79.44566	-0.01766	2864	TVMUC	at depth	
PS114_29-4	2018-07-21	13:47	79.43911	-0.02956	2870	TVMUC	station end	
PS114_30-1	2018-07-21	20:08	79.92624	3.06556	2598	OFOS	station start	

Station	Date	Time	Latitude	Longitude	Depth [m]	Gear	Action	Comment
PS114_30-1	2018-07-21	21:00	79.92706	3.09311	2586	OFOS	at depth	
PS114_30-1	2018-07-21	21:05	79.92739	3.09460	2586	OFOS	profile start	OFOS HG-N5 transect
PS114_30-1	2018-07-21	22:34	79.93459	3.13614	2537	OFOS	profile end	
PS114_30-1	2018-07-21	22:34	79.93460	3.13621	2569	OFOS	profile start	track continued
PS114_30-1	2018-07-22	00:30	79.94466	3.19467	2534	OFOS	profile end	
PS114_30-1	2018-07-22	01:14	79.94520	3.19782	2532	OFOS	station end	
PS114_31-1	2018-07-22	01:33	79.94513	3.19795	2532	CTDOZE	station start	
PS114_31-1	2018-07-22	01:52	79.94514	3.19870	2532	CTDOZE	at depth	
PS114_31-1	2018-07-22	02:30	79.94519	3.20057	2532	CTDOZE	station end	
PS114_31-2	2018-07-22	04:06	79.92708	3.09338	2586	TVMUC	station start	
PS114_31-2	2018-07-22	04:58	79.92714	3.09431	2586	TVMUC	at depth	
PS114_31-2	2018-07-22	05:55	79.92987	3.08595	2588	TVMUC	station end	
PS114_32-1	2018-07-22	08:18	79.73565	4.50244	2737	MOOR	retrieval start	HG-N-FEVI-35
PS114_32-1	2018-07-22	09:31	79.72571	4.48895	2747	MOOR	retrieval end	HG-N-FEVI-35
PS114_32-2	2018-07-22	09:36	79.72447	4.48508	2748	CTDOZE	station start	
PS114_32-2	2018-07-22	10:26	79.73950	4.52573	2718	CTDOZE	at depth	
PS114_32-2	2018-07-22	10:51	79.74100	4.52256	2693	CTDOZE	station end	
PS114_32-3	2018-07-22	11:02	79.74102	4.52069	2698	MOOR	deployment start	HG-N-FEVI-37
PS114_32-3	2018-07-22	13:17	79.74143	4.52276	2688	MOOR	deployment end	HG-N-FEVI-37
PS114_32-4	2018-07-22	13:45	79.72152	4.52906	2796	LOKI	station start	
PS114_32-4	2018-07-22	15:14	79.73272	4.55127	2768	LOKI	station end	
PS114_32-5	2018-07-22	15:34	79.72853	4.60696	2691	MN_S5	station start	
PS114_32-5	2018-07-22	16:36	79.73060	4.61878	2681	MN_S5	at depth	
PS114_32-5	2018-07-22	17:47	79.73471	4.63445	2648	MN_S5	station end	
PS114_32-6	2018-07-22	18:00	79.73809	4.62633	2631	CTDOZE	station start	
PS114_32-6	2018-07-22	18:55	79.73905	4.65020	2619	CTDOZE	at depth	
PS114_32-6	2018-07-22	20:20	79.73884	4.65951	2619	CTDOZE	station end	
PS114_32-7	2018-07-22	20:50	79.73820	4.61799	2636	ISPC	station start	
PS114_32-7	2018-07-22	21:25	79.73800	4.61824	2638	ISPC	at depth	
PS114_32-7	2018-07-22	21:48	79.73810	4.61796	2637	ISPC	station end	
PS114_32-8	2018-07-22	22:04	79.73757	4.61883	2640	TVMUC	station start	
PS114_32-8	2018-07-22	22:54	79.73759	4.61863	2640	TVMUC	at depth	
PS114_32-8	2018-07-22	23:53	79.73872	4.61097	2636	TVMUC	station end	
PS114_33-1	2018-07-23	01:05	79.59937	5.16467	2789	CTDOZE	station start	
PS114_33-1	2018-07-23	01:25	79.59882	5.16590	2788	CTDOZE	at depth	
PS114_33-1	2018-07-23	01:56	79.59858	5.16620	2788	CTDOZE	station end	
PS114_33-2	2018-07-23	02:08	79.59897	5.16649	2788	TVMUC	station start	
PS114_33-2	2018-07-23	03:00	79.59892	5.16659	2787	TVMUC	at depth	
PS114_33-2	2018-07-23	04:02	79.59821	5.16743	2787	TVMUC	station end	
PS114_33-3	2018-07-23	04:53	79.59815	5.16680	2787	OFOS	station start	
PS114_33-3	2018-07-23	05:48	79.59810	5.16888	2786	OFOS	at depth	
PS114_33-3	2018-07-23	05:49	79.59821	5.16875	2786	OFOS	profile start	
PS114_33-3	2018-07-23	09:13	79.56779	5.25628	2658	OFOS	profile end	

Station	Date	Time	Latitude	Longitude	Depth [m]	Gear	Action	Comment
PS114_33-3	2018-07-23	10:06	79.56288	5.26943	2651	OFOS	station end	
PS114_34-1	2018-07-23	23:57	81.16270	-0.06595	2717	CTDOZE	station start	
PS114_34-1	2018-07-24	00:16	81.16233	-0.06996	2718	CTDOZE	at depth	
PS114_34-1	2018-07-24	00:44	81.16126	-0.07900	2720	CTDOZE	station end	
PS114_35-1	2018-07-24	03:41	81.01071	0.00167	2769	CTDOZE	station start	
PS114_35-1	2018-07-24	04:01	81.01192	-0.00749	2772	CTDOZE	at depth	
PS114_35-1	2018-07-24	04:32	81.01345	-0.01398	2775	CTDOZE	station end	
PS114_36-1	2018-07-24	10:09	80.85286	-0.12266	3176	MOOR	retrieval start	R5-1
PS114_36-1	2018-07-24	11:19	80.85368	-0.14885	3184	MOOR	retrieval end	R5-1
PS114_36-2	2018-07-24	11:45	80.85266	-0.13071	3178	CTDOZE	station start	
PS114_36-2	2018-07-24	12:48	80.85517	-0.14020	3181	CTDOZE	at depth	
PS114_36-2	2018-07-24	14:31	80.85619	-0.14264	3181	CTDOZE	station end	
PS114_36-3	2018-07-24	14:40	80.85623	-0.14167	3181	LOKI	station start	
PS114_36-3	2018-07-24	15:12	80.85688	-0.14519	3182	LOKI	at depth	
PS114_36-3	2018-07-24	15:44	80.85999	-0.15345	3183	LOKI	station end	
PS114_36-4	2018-07-24	15:59	80.86034	-0.15073	3181	CTDOZE	station start	
PS114_36-4	2018-07-24	16:10	80.86067	-0.15724	3183	CTDOZE	at depth	
PS114_36-4	2018-07-24	16:30	80.86114	-0.15885	3184	CTDOZE	station end	
PS114_36-5	2018-07-24	17:33	80.86299	-0.12787	3169	CTDOZE	station start	
PS114_36-5	2018-07-24	17:54	80.86339	-0.12763	3169	CTDOZE	at depth	
PS114_36-5	2018-07-24	18:07	80.86352	-0.12730	3169	CTDOZE	station end	
PS114_36-6	2018-07-24	18:27	80.86339	-0.12791	3169	MN_S5	station start	
PS114_36-6	2018-07-24	19:01	80.86350	-0.12722	3169	MN_S5	at depth	
PS114_36-6	2018-07-24	19:51	80.86468	-0.12454	3168	MN_S5	station end	
PS114_37-1	2018-07-24	21:44	80.66881	0.02064	3251	CTDOZE	station start	
PS114_37-1	2018-07-24	22:05	80.66742	0.01374	3251	CTDOZE	at depth	
PS114_37-1	2018-07-24	22:42	80.66381	0.01379	3251	CTDOZE	station end	
PS114_38-1	2018-07-25	00:41	80.48768	0.04481	3221	CTDOZE	station start	
PS114_38-1	2018-07-25	01:00	80.48761	0.04423	3221	CTDOZE	at depth	
PS114_38-1	2018-07-25	01:35	80.48909	0.03861	3222	CTDOZE	station end	
PS114_39-1	2018-07-25	03:17	80.33443	0.00059	2465	CTDOZE	station start	
PS114_39-1	2018-07-25	03:36	80.33449	0.00727	2474	CTDOZE	at depth	
PS114_39-1	2018-07-25	04:10	80.33860	0.01542	2516	CTDOZE	station end	
PS114_40-1	2018-07-25	09:31	80.15486	0.26581	3031	LOKI	station start	
PS114_40-1	2018-07-25	10:00	80.15231	0.28573	3033	LOKI	at depth	
PS114_40-1	2018-07-25	10:31	80.14844	0.30472	3049	LOKI	station end	
PS114_40-2	2018-07-25	12:48	80.16488	0.16128	3076	MOOR	retrieval start	R4-1
PS114_40-2	2018-07-25	14:31	80.15754	0.15544	3097	MOOR	retrieval end	R4-1
PS114_40-3	2018-07-25	14:43	80.15785	0.15343	3096	CTDOZE	station start	
PS114_40-3	2018-07-25	15:46	80.15918	0.13866	3105	CTDOZE	at depth	
PS114_40-3	2018-07-25	17:05	80.16040	0.14877	3087	CTDOZE	station end	
PS114_41-1	2018-07-25	21:35	79.83179	-0.00722	2786	CTDOZE	station start	
PS114_41-1	2018-07-25	21:55	79.83128	-0.00911	2786	CTDOZE	at depth	
PS114_41-1	2018-07-25	22:25	79.83055	-0.01000	2787	CTDOZE	station end	

Station	Date	Time	Latitude	Longitude	Depth [m]	Gear	Action	Comment
PS114_42-1	2018-07-26	00:12	79.66330	-0.01894	2819	CTDOZE	station start	
PS114_42-1	2018-07-26	00:31	79.66450	-0.01840	2819	CTDOZE	at depth	
PS114_42-1	2018-07-26	01:06	79.66778	-0.01550	2817	CTDOZE	station end	
PS114_43-1	2018-07-26	12:25	78.82832	-2.79569	2592	MOOR	retrieval start	HG-EGC-4
PS114_43-1	2018-07-26	13:26	78.82419	-2.79069	2593	MOOR	retrieval end	HG-EGC-4
PS114_43-2	2018-07-26	13:38	78.82325	-2.79264	2593	CTDOZE	station start	
PS114_43-2	2018-07-26	14:32	78.81984	-2.77895	2595	CTDOZE	at depth	
PS114_43-2	2018-07-26	16:05	78.81730	-2.77539	2596	CTDOZE	station end	
PS114_43-3	2018-07-26	16:16	78.81703	-2.77456	2596	TVMUC	station start	
PS114_43-3	2018-07-26	17:03	78.81506	-2.76543	2599	TVMUC	at depth	
PS114_43-3	2018-07-26	17:56	78.81338	-2.76347	2600	TVMUC	station end	
PS114_43-4	2018-07-26	18:12	78.81798	-2.76866	2598	CTDOZE	station start	
PS114_43-4	2018-07-26	18:32	78.81758	-2.76917	2598	CTDOZE	at depth	
PS114_43-4	2018-07-26	19:05	78.81699	-2.76948	2598	CTDOZE	station end	
PS114_44-1	2018-07-26	20:20	78.88582	-3.04520	2513	OFOS	station start	
PS114_44-1	2018-07-26	21:09	78.88501	-3.04946	2512	OFOS	at depth	
PS114_44-1	2018-07-26	21:09	78.88496	-3.04972	2511	OFOS	profile start	OFOS HG-EGC transect
PS114_44-1	2018-07-27	00:26	78.86247	-3.12284	2501	OFOS	profile end	
PS114_44-1	2018-07-27	01:09	78.85938	-3.13857	2496	OFOS	station end	
PS114_45-1	2018-07-27	03:39	78.93368	-4.64509	1551	TVMUC	station start	
PS114_45-1	2018-07-27	04:11	78.93399	-4.64298	1553	TVMUC	at depth	
PS114_45-1	2018-07-27	04:44	78.93545	-4.63195	1562	TVMUC	station end	
PS114_46-1	2018-07-27	06:52	78.99286	-5.44538	990	CTDOZE	station start	
PS114_46-1	2018-07-27	07:16	78.99264	-5.43596	997	CTDOZE	at depth	
PS114_46-1	2018-07-27	07:43	78.99338	-5.41911	1009	CTDOZE	station end	
PS114_46-2	2018-07-27	07:54	78.99541	-5.41371	1018	LOKI	station start	
PS114_46-2	2018-07-27	08:29	78.99943	-5.39929	1037	LOKI	at depth	
PS114_46-2	2018-07-27	09:10	79.00328	-5.38504	1054	LOKI	station end	
PS114_46-3	2018-07-27	09:54	78.98953	-5.42076	1003	CTDOZE	station start	
PS114_46-3	2018-07-27	10:01	78.99013	-5.41778	1005	CTDOZE	at depth	
PS114_46-3	2018-07-27	10:11	78.99148	-5.41292	1010	CTDOZE	station end	
PS114_46-4	2018-07-27	11:08	78.99957	-5.38643	1046	CTDOZE	station start	
PS114_46-4	2018-07-27	11:28	79.00324	-5.37036	1065	CTDOZE	at depth	
PS114_46-4	2018-07-27	11:37	79.00464	-5.36179	1073	CTDOZE	station end	
PS114_46-5	2018-07-27	11:52	79.00450	-5.35328	1079	ICE	station start	
PS114_46-5	2018-07-27	12:04	79.00621	-5.34447	1087	ICE	station end	
PS114_46-6	2018-07-27	12:31	78.98924	-5.43770	992	MOOR	deployment start	HG-EGC-5
PS114_46-6	2018-07-27	13:36	78.99554	-5.39240	1032	MOOR	deployment end	HG-EGC-5
PS114_46-7	2018-07-27	14:01	79.00868	-5.35002	1085	MN_S5	station start	
PS114_46-7	2018-07-27	14:42	79.01177	-5.32439	1108	MN_S5	at depth	
PS114_46-7	2018-07-27	15:30	79.01251	-5.29335	1132	MN_S5	station end	
PS114_46-8	2018-07-27	15:39	79.01227	-5.28788	1136	CTDOZE	station start	
PS114_46-8	2018-07-27	15:45	79.01244	-5.28514	1139	CTDOZE	at depth	

Station	Date	Time	Latitude	Longitude	Depth [m]	Gear	Action	Comment
PS114_46-8	2018-07-27	15:57	79.01299	-5.28143	1142	CTDOZE	station end	
PS114_46-9	2018-07-27	16:28	79.00674	-5.47996	995	TVMUC	station start	
PS114_46-9	2018-07-27	16:51	79.00780	-5.46967	1003	TVMUC	at depth	
PS114_46-9	2018-07-27	17:14	79.00886	-5.46013	1012	TVMUC	station end	
PS114_47-1	2018-07-28	13:23	79.72009	-17.67222	535	MOOR	retrieval start	79N7-1
PS114_47-1	2018-07-28	13:48	79.71903	-17.67290	467	MOOR	retrieval end	79N7-1
PS114_48-1	2018-07-28	17:47	79.66958	-16.89366	264	MOOR	retrieval start	79N6-1
PS114_48-1	2018-07-28	18:08	79.66835	-16.89015	264	MOOR	retrieval end	79N6-1
PS114_49-1	2018-07-28	19:52	79.61829	-16.54212	279	MOOR	retrieval start	79N8-1
PS114_49-1	2018-07-28	20:00	79.61822	-16.53833	281	MOOR	retrieval end	79N8-1
PS114_49-2	2018-07-28	20:22	79.61543	-16.52544	280	CTDOZE	station start	
PS114_49-2	2018-07-28	20:34	79.61543	-16.52516	281	CTDOZE	at depth	
PS114_49-2	2018-07-28	20:55	79.61543	-16.52546	279	CTDOZE	station end	
PS114_49-3	2018-07-28	21:05	79.61558	-16.52539	279	LOKI	station start	
PS114_49-3	2018-07-28	21:14	79.61545	-16.52502	281	LOKI	at depth	
PS114_49-3	2018-07-28	21:27	79.61556	-16.52343	282	LOKI	station end	
PS114_49-4	2018-07-28	21:39	79.61548	-16.52173	282	MN_S5	station start	
PS114_49-4	2018-07-28	21:50	79.61549	-16.51976	280	MN_S5	at depth	
PS114_49-4	2018-07-28	22:08	79.61547	-16.51579	279	MN_S5	station end	
PS114_49-5	2018-07-28	22:17	79.61627	-16.51145	279	ISPC	station start	
PS114_49-5	2018-07-28	22:36	79.61688	-16.50762	278	ISPC	at depth	
PS114_49-5	2018-07-28	22:52	79.61698	-16.50246	278	ISPC	station end	
PS114_50-1	2018-07-29	10:28	79.62781	-11.99859	244	ICE	station start	
PS114_50-1	2018-07-29	10:35	79.62776	-12.00360	247	ICE	station end	
PS114_51-1	2018-07-30	04:02	77.90630	-10.00513	229	MOOR	retrieval start	EGS3-1
PS114_51-1	2018-07-30	04:15	77.90600	-10.01098	228	MOOR	retrieval end	EGS3-1
PS114_51-2	2018-07-30	04:24	77.90551	-10.01285	228	CTDOZE	station start	
PS114_51-2	2018-07-30	04:36	77.90555	-10.01694	241	CTDOZE	at depth	
PS114_51-2	2018-07-30	04:44	77.90557	-10.01796	203	CTDOZE	station end	
PS114_52-1	2018-07-30	08:57	77.48285	-10.00311	219	MOOR	retrieval start	EGS4-1
PS114_52-1	2018-07-30	09:06	77.48308	-10.00325	219	MOOR	retrieval end	EGS4-1
PS114_52-2	2018-07-30	09:15	77.48304	-10.00480	220	CTDOZE	station start	
PS114_52-2	2018-07-30	09:29	77.48348	-10.00292	224	CTDOZE	at depth	
PS114_52-2	2018-07-30	09:38	77.48385	-10.00139	221	CTDOZE	station end	
PS114_53-1	2018-07-30	13:37	77.06644	-9.99898	437	MOOR	retrieval start	EGS1-2
PS114_53-1	2018-07-30	14:05	77.06789	-9.99432	440	MOOR	retrieval end	EGS1-2
PS114_53-2	2018-07-30	14:13	77.06776	-9.99059	436	CTDOZE	station start	
PS114_53-2	2018-07-30	14:27	77.06786	-9.98360	436	CTDOZE	at depth	
PS114_53-2	2018-07-30	14:38	77.06768	-9.97887	438	CTDOZE	station end	
PS114_54-1	2018-07-30	16:18	76.95617	-9.42122	381	CTDOZE	station start	
PS114_54-1	2018-07-30	16:31	76.95535	-9.42228	382	CTDOZE	at depth	
PS114_54-1	2018-07-30	16:43	76.95500	-9.42294	383	CTDOZE	station end	
PS114_55-1	2018-07-30	18:32	76.84480	-8.88602	369	CTDOZE	station start	
PS114_55-1	2018-07-30	18:46	76.84624	-8.88887	366	CTDOZE	at depth	

Station	Date	Time	Latitude	Longitude	Depth [m]	Gear	Action	Comment
PS114_55-1	2018-07-30	19:01	76.84788	-8.88989	365	CTDOZE	station end	
PS114_56-1	2018-07-30	20:44	76.73811	-8.33152	359	CTDOZE	station start	
PS114_56-1	2018-07-30	20:58	76.73874	-8.32976	358	CTDOZE	at depth	
PS114_56-1	2018-07-30	21:09	76.73916	-8.32671	357	CTDOZE	station end	
PS114_57-1	2018-07-30	22:47	76.63116	-7.75509	338	CTDOZE	station start	
PS114_57-1	2018-07-30	23:00	76.63075	-7.75586	336	CTDOZE	at depth	
PS114_57-1	2018-07-30	23:08	76.63064	-7.75579	336	CTDOZE	station end	
PS114_58-1	2018-07-30	23:40	76.60428	-7.63246	341	CTDOZE	station start	
PS114_58-1	2018-07-30	23:54	76.60415	-7.63320	340	CTDOZE	at depth	
PS114_58-1	2018-07-31	00:03	76.60401	-7.63420	340	CTDOZE	station end	
PS114_59-1	2018-07-31	00:42	76.57338	-7.48974	555	CTDOZE	station start	
PS114_59-1	2018-07-31	00:59	76.57358	-7.49212	550	CTDOZE	at depth	
PS114_59-1	2018-07-31	01:12	76.57313	-7.49861	544	CTDOZE	station end	
PS114_60-1	2018-07-31	01:37	76.55972	-7.37982	740	CTDOZE	station start	
PS114_60-1	2018-07-31	01:57	76.55994	-7.38147	738	CTDOZE	at depth	
PS114_60-1	2018-07-31	02:13	76.56060	-7.38101	735	CTDOZE	station end	
PS114_60-2	2018-07-31	04:22	76.54608	-7.37869	784	MOOR	retrieval start	EGS2-1
PS114_60-2	2018-07-31	04:52	76.54544	-7.37489	790	MOOR	retrieval end	EGS2-1
PS114_61-1	2018-07-31	05:47	76.48844	-7.14293	184	CTDOZE	station start	
PS114_61-1	2018-07-31	06:17	76.48880	-7.14243	984	CTDOZE	at depth	
PS114_61-1	2018-07-31	06:42	76.48879	-7.14124	1190	CTDOZE	station end	
PS114_62-1	2018-07-31	07:24	76.42780	-6.86379	124	CTDOZE	station start	
PS114_62-1	2018-07-31	07:47	76.42786	-6.86696	1627	CTDOZE	at depth	
PS114_62-1	2018-07-31	08:12	76.42656	-6.86795	1631	CTDOZE	station end	
PS114_63-1	2018-07-31	11:29	76.17558	-5.37415	2793	CTDOZE	station start	
PS114_63-1	2018-07-31	12:26	76.17595	-5.37578	2792	CTDOZE	at depth	
PS114_63-1	2018-07-31	13:37	76.17539	-5.37679	2790	CTDOZE	station end	

Gear abbreviations	Gear
ADCP_150	ADCP 150kHz
AFIM	AutoFim
CTDOZE	CTD AWI-OZE
FBOX	FerryBox
HVAIR	High Volume Air Sampler
ICE	Ice Station
ISPC	In-Situ Particle Camera
LOKI	Light Frame On-sight Keyspecies Investigation Measuring system
MN_S5	Multinet Small 5 Nets
MOOR	Mooring
OFOS	Ocean Floor Observation System
PCO2_GO	pCO2 GO
PCO2_SUB	pCO2 Subctech
SVP	Sound Velocity Profiler
TSG_KEEL	Thermosalinograph Keel
TSG_KEEL_2	Thermosalinograph Keel 2
TVMUC	Video Multi Corer
WST	Weatherstation

Die **Berichte zur Polar- und Meeresforschung** (ISSN 1866-3192) werden beginnend mit dem Band 569 (2008) als Open-Access-Publikation herausgegeben. Ein Verzeichnis aller Bände einschließlich der Druckausgaben (ISSN 1618-3193, Band 377-568, von 2000 bis 2008) sowie der früheren **Berichte zur Polarforschung** (ISSN 0176-5027, Band 1-376, von 1981 bis 2000) befindet sich im electronic Publication Information Center **(ePIC)** des Alfred-Wegener-Instituts, Helmholtz-Zentrum für Polar- und Meeresforschung (AWI); see http://epic.awi.de. Durch Auswahl “Reports on Polar- and Marine Research“ (via “browse”/”type”) wird eine Liste der Publikationen, sortiert nach Bandnummer, innerhalb der absteigenden chronologischen Reihenfolge der Jahrgänge mit Verweis auf das jeweilige pdf-Symbol zum Herunterladen angezeigt.

The **Reports on Polar and Marine Research** (ISSN 1866-3192) are available as open access publications since 2008. A table of all volumes including the printed issues (ISSN 1618-3193, Vol. 377-568, from 2000 until 2008), as well as the earlier **Reports on Polar Research** (ISSN 0176-5027, Vol. 1-376, from 1981 until 2000) is provided by the electronic Publication Information Center **(ePIC)** of the Alfred Wegener Institute, Helmholtz Centre for Polar and Marine Research (AWI); see URL http://epic.awi.de. To generate a list of all Reports, use the URL http://epic.awi.de and select “browse”/ ”type” to browse ”Reports on Polar and Marine Research”. A chronological list in declining order will be presented, and pdf-icons displayed for downloading.

Zuletzt erschienene Ausgaben:

Recently published issues:

723 (2018) The Expedition PS114 of the Research Vessel POLARSTERN to the Fram Strait in 2018, edited by Wilken-Jon von Appen

722 (2018) The Expedition PS112 of the Research Vessel POLARSTERN to the Antarctic Peninsula Region in 2018, edited by Bettina Meyer and Wiebke Weßels

721 (2018) Alfred Wegener im 1. Weltkrieg. Ein Polarforscher und die „Urkatastrophe des 20. Jahrhunderts“, by Christian R. Salewski

720 (2018) The Expedition PS98 of the Research Vessel POLARSTERN to the Atlantic Ocean in 2016, edited by Bernhard Pospichal

719 (2018) The Expeditions PS106/1 and 2 of the Research Vessel POLARSTERN to the Arctic Ocean in 2017, edited by Andreas Macke and Hauke Flores

718 (2018) The Expedition PS111 of the Research Vessel POLARSTERN to the southern Weddell Sea in 2018, edited by Michael Schröder

717 (2018) The Expedition PS107 of the Research Vessel POLARSTERN to the Fram Strait and the AWI-HAUSGARTEN in 2017, edited by Ingo Schewe

716 (2018) Polar Systems under Pressure, 27th International Polar Conference, Rostock, 25 - 29 March 2018, German Society for Polar Research, edited by H. Kassens, D. Damaske, B. Diekmann, D. Fütterer, G. Heinemann, U. Karsten, E.M. Pfeiffer, J. Regnery, M. Scheinert, J. Thiede, R. Tiedemann & D. Wagner

715 (2018) The Expedition PS109 of the Research Vessel POLARSTERN to the Nordic Seas in 2017, edited by Torsten Kanzow

714 (2017) The Expedition SO258/2 of the Research Vessel SONNE to the central Indian Ocean in 2017, edited by Wolfram Geissler

713 (2017) The Expedition PS102 of the Research Vessel POLARSTERN to the Atlantic Ocean in 2016, edited by Karen Wiltshire, Eva-Maria Brodte, Annette Wilson and Peter Lemke

ALFRED-WEGENER-INSTITUT
HELMHOLTZ-ZENTRUM FÜR POLAR-
UND MEERESFORSCHUNG

BREMERHAVEN

Am Handelshafen 12
27570 Bremerhaven
Telefon 0471 4831-0
Telefax 0471 4831-1149
www.awi.de

HELMHOLTZ
GEMEINSCHAFT